mTORC1 CONTRIBUTES TO ER STRESS INDUCED CELL DEATH

Justin Thomas Babcock

Submitted to the faculty of the University Graduate School
in partial fulfillment of the requirements
for the degree
Doctor of Philosophy
in the Department of Biochemistry and Molecular Biology
Indiana University

December 2012

Accepted by the Faculty of Indiana University, in partial
fulfillment of the requirements for the degree of Doctor of Philosophy.

Lawrence A. Quilliam, Ph.D., Chair

Doctoral Committee

Simon J. Atkinson, Ph.D.

October 25, 2012

Harikrishna Nakshatri, Ph.D.

Ronald C. Wek, Ph.D.

© 2012

Justin Thomas Babcock

ALL RIGHTS RESERVED

DEDICATION

I dedicate this dissertation to my parents Tom and Phyllis Babcock, and Hoa Nguyen. Without their love and support I would never have reached this point.

ACKNOWLEDGMENTS

I would like to thank my mentor Dr. Lawrence Quilliam for his continual support and motivation during my dissertation work. The scientific and organizational skills I have learned from Lawrence made it possible for me to complete this work. I would also like to thank all the members of the Quilliam lab that I have worked with in my time here: Dr. Sirisha Asuri, Dr. Jingliang Yan, Hoa Nguyen, and Yujun He.

I would like to thank my committee members Dr. Simon Atkinson, Dr. Harikrishna Nakshatri, and Dr. Ronald Wek for their guidance during my dissertation work. Many thanks to Dr. Clark Wells for microscope usage and lots of advice. I would also like to thank members of the Wek lab including Souvik Dey, Reddy Palam, Tom Baird, and Brian Teske for help with regents and advice. I would also like to thank the faculty and staff of the Department of Biochemistry and Molecular Biology, in particular Sandy McClain, Sheila Reynolds, Melissa Pearcy, Jack Arthur, Patty Dilworth, Jamie Schroeder, and Darlene Lambert. Thank you to Dr. Ann Roman and Dr. Harikrishna Nakshatri of the Cancer Biology Training Program (CBPT) for advice and my DeVault Gift Estate predoctoral fellowship. Lastly, I would like to thank the LAM foundation for funding my project and making science toward understanding and curing lymphangioleiomyomatosis possible.

I would also like to thank my Mom, Dad, my sister Allison, and all my family and friends. Finally, I would like to thank my girlfriend and my best friend, Hoa, who has been a continual source of support and encouragement during my dissertation work.

ABSTRACT

Justin Thomas Babcock

mTORC1 CONTRIBUTES TO ER STRESS INDUCED CELL DEATH

Patients with the genetic disorder tuberous sclerosis complex (TSC) suffer from neoplastic growths in multiple organ systems. These growths are the result of inactivating mutations in either the *TSC1* or *TSC2* tumor suppressor genes, which negatively regulate the activity of mammalian target of rapamycin complex 1(mTORC1). There is currently no cure for this disease; however, my research has found that cells harboring TSC2-inactivating mutations derived from a rat model of TSC are sensitive to apoptosis induced by the clinically approved proteasome inhibitor, bortezomib, in a manner dependent on their high levels of mTORC1 activation. We see that bortezomib induces the unfolded protein response (UPR) in our cell model of TSC, resulting in cell death via apoptosis. The UPR is induced by accumulation of unfolded protein in the endoplasmic reticulum (ER) which activates the three branches of this pathway: Activating transcription factor 6 (ATF6) cleavage, phosphorylation of eukaryotic initiation factor 2α (eIF2α), and the splicing of X-box binding protein1 (XBP1) mRNA. Phosphorylation of eIF2α leads to global inhibition of protein synthesis, preventing more unfolded protein from accumulating in the ER. This phosphorylation also induces the transcription and translation of ATF4 and CCAAT-enhancer binding protein homologous protein (CHOP). Blocking mTORC1 activity in these cells using the mTORC1 inhibitor, rapamycin, prevented the expression of ATF4 and CHOP at both the mRNA and protein level during bortezomib treatment. Rapamycin treatment also reduced apoptosis induced by bortezomib; however, it did not affect bortezomib-induced eIF2α phosphorylation or ATF6 cleavage. These data indicate that rapamycin can repress the induction of UPR-dependent apoptosis by suppressing the transcription of ATF4 and CHOP mRNAs. In addition to these findings, we find that a TSC2-null angiomyolipoma cell line forms vacuoles when treated with the proteasome inhibitor MG-132. We found these vacuoles to be derived from the ER and that rapamycin blocked their formation. Rapamycin also enhanced expansion of the ER during MG-132 stress and restored its degradation by autophagy. Taken together these findings suggest that bortezomib might be used to treat neoplastic growths associated with TSC. However, they also caution against combining specific cell death inducing agents with rapamycin during chemotherapy.

Lawrence A. Quilliam, Ph.D., Chair

TABLE OF CONTENTS

LIST OF FIGURES x

LIST OF ABBREVIATIONS xi

CHAPTER 1. INTRODUCTION 1

1.1 Introduction to Tuberous Sclerosis Complex and Lymphangioleiomyomatosis (LAM) 2
1.2 mTOR complex-1 vs. mTOR complex-2 (mTORC1 vs. mTORC2) 2
1.3 Tuberin and Harmartin 4
1.4 Regulation via ubiquitination and acetylation 7
1.5 Amino acid, glucose, and oxygen control of mTORC1 7
1.6 mTORC1 integration of growth and metabolism to control protein synthesis 9
1.7 Autophagy 12
1.8 Lipid synthesis 15
1.9 Mitochondrial metabolism and biogenesis 15
1.10 Cell cycle 16
1.11 mTORC1 and mTORC2 in cancer 17
1.12 Directly targeting mTOR kinase activity 17
1.13 Targeting Rheb 18
1.14 Genotoxic stress 20
1.15 Nutrient depletion 21
1.16 Endoplasmic Reticulum Stress 22
1.17 mTORC1 control of c-MYC 25
1.18 Summary 26

CHAPTER 2. MATERIALS AND METHODS 27

2.1 Elt3 Cell culture 28
2.2 621-101 Cell culture 28
2.3 Nuclear lysates 28
2.4 Western blotting and antibodies 29
2.5 qRT-PCR 29
2.6 Trypan blue cell viability assays 30
2.7 Chromatin immunoprecipitation 30
2.8 Cloning and lentiviral production 30
2.9 Generation of c-MYC and empty vector stable cell lines 31
2.10 Imaging and measuring ER volume 32
2.11 Florescent live cell imaging 32
2.12 shRNA sequences and 293T shRNA knockdowns 32
2.13 Luciferase Assays 33
2.14 Statistical Analysis 33

CHAPTER 3. mTORC1 ENHANCES BORTEZOMIB-INDUCED DEATH IN TSC-NULL CELLS BY A C-MYC-DEPENDENT INDUCTION OF THE UNFOLDED PROTEIN RESPONSE 34

3.1 Introduction 35

3.2 Bortezomib induced cell death is reduced by rapamycin and by inhibition of the unfolded protein response 37
3.3 Early UPR markers are induced by bortezomib but unaffected by rapamycin in Elt3 cells 40
3.4 ATF4 and CHOP protein and mRNA levels are induced by bortezomib in a rapamycin-dependent manner 42
3.5 Bortezomib-induced expression of ATF4 and CHOP requires new mRNA and protein synthesis 44
3.6 c-MYC is upregulated by ER stressing agents at the transcriptional level in Elt3 cells 47
3.7 Rapamycin inhibits bortezomib-induced c-MYC expression and binding to the ATF4 gene promoter 53
3.8 c-MYC overexpression rescues rapamycin-mediated suppression of bortezomib-induced ATF4 and CHOP expression 56
3.9 c-MYC overexpression rescues rapamycin-mediated suppression of bortezomib-induced Elt3 cell apoptosis 61
3.10 Discussion 64

CHAPTER 4. PROTEASOME INHIBITION-INDUCED ER VACUOLATION REQUIRES mTORC1 ACTIVATION 69

4.1 Introduction 70
4.2 MG-132 induces vacuolation and cell death in a rapamycin-sensitive manner 72
4.3 Cell death and vacuolation is not associated with caspase-dependent apoptosis 79
4.4 Rapamycin pretreatment enhances basal autophagic processes 81
4.5 Autophagy may play a role in ER expansion during MG-132 treatment 85
4.6 Vacuoles may represent failed autophagosomal degradation of ER 89
4.7 PI3P fails to accumulate in the ER in the absence of rapamycin 91
4.8 JNK activation is required for omegasome formation during UPR induced autophagy 94
4.9.1 Discussion 96
4.9.2 Unifying Model Linking Autophagy and the UPR 96
4.9.3 Parallels may exist between Mitophagy and Reticulophagy 99
4.9.4 Reticuluophagy must have unique aspects from other cargo specific forms of autophagy 100
4.9.5 The ER as a coordinator of autophagy 101
4.9.6 ER expansion, autophagy, and human health 102

APPENDIX 1: qRT-PCR AND CHIP PRIMERS 104
APPENDIX 2: shRNA SEQUENCES 105

REFERENCES 106

CURRICULUM VITAE

LIST OF FIGURES

Figure 1-1 The mTOR kinase participates in two complexes with distinct composition, substrates, and upstream regulation ... 6
Figure 1-2 Cap-dependent translation tightly controls translational initiation ... 11
Figure 1-3 mTORC1 and the ER participate in the regulation of autophagosome formation ... 14
Figure 1-4 The Unfolded Protein Response ... 24
Figure 3-1 Elt3 cells undergo rapamycin-sensitive apoptosis when treated with bortezomib ... 39
Figure 3-2 Early UPR markers are induced by bortezomib but unaffected by rapamycin in Elt3 cells ... 41
Figure 3-3 Rapamycin prevents induction of downstream UPR markers at the mRNA level ... 43
Figure 3-4 Increased levels of ATF4 and CHOP proteins in response to bortezomib treatment require the synthesis of new mRNA and protein ... 46
Figure 3-5 Bortezomib and other ER stressors induce expression and activity of c-MYC in a rapamycin-sensitive manner ... 49
Figure 3-6 eIF4E knockdown reduces c-MYC and ATF4 expression ... 51
Figure 3-7 c-MYC binds to and stimulates the ATF4 promoter ... 54
Figure 3-8 Overexpression of c-MYC rescued bortezomib-induced ATF4 and CHOP expression following pretreatment with rapamycin ... 58
Figure 3-9 c-MYC knockdown blocks bortezomib-induced induction of ATF4 ... 60
Figure 3-10 Overexpression of c-MYC restores bortezomib-induced apoptosis ... 62
Figure 3-11 mTORC1/c-MYC play a role in inducing the ER stress response ... 65
Figure 4-1 Rapamycin decreases ER stress markers ... 74
Figure 4-2 Rapamycin treatment prevents vacuolation and cell death induced by MG-132 ... 76
Figure 4-3 Vacuoles induced by proteasome inhibition contain ER ... 78
Figure 4-4 Caspase activation is not required for MG-132-induced cell death or ER vacuolation ... 80
Figure 4-5 Fluorescent proteins used to measure cellular pH ... 82
Figure 4-6 Rapamycin treatment restores autophagic processes ... 84
Figure 4-7 mTORC1 inhibition is required for ER expansion ... 86
Figure 4-8 Autophagy inhibitors reverse rapamycin-associated ER expansion ... 88
Figure 4-9 Vacuoles derived from the ER do not acidify in the absence of rapamycin ... 90
Figure 4-10 Measuring PI3P specifically in the ER ... 92
Figure 4-11 mTORC1 activation inhibits accumulation of PI3P in the ER ... 93
Figure 4-12 mTORC1 inhibition and JNK activation are required for accumulation of PI3P in the ER ... 95
Figure 4-13 ER vacuole accumulation model ... 98

LIST OF ABBREVIATIONS

2-DG	2-Deoxy-D-glucose
3-MA	3-Methyladenine
4EBP	4E-binding protein
AF488	Alexa fluor 488
AMPK	5' adenosine monophosphate-activated protein kinase
ARD1	Arrest-defective protein 1
ATF4	Activating transcription factor 4
ATF6	Activating transcription factor 6
ATG5	Autophagy related 5
ATG7	Autophagy related 7
ATG8	Autophagy related 8
ATG13	Autophagy related 13
ATG32	Autophagy related 32
ATM	Ataxia telangiectasia mutated
ATP	Adenosine-5'-triphosphate
ATR	Ataxia telangiectasia and Rad3 related
Bax	Bcl2–associated X protein
Bcl2	B-cell lymphoma 2
Bcl-XL	B-cell lymphoma-extra large
BFA	Brefeldin A
BNIP3	BCL2/adenovirus E1B 19 kDa protein-interacting protein 3
C/EBP1α	CCAAT/enhancer-binding protein α
C/EBP1δ	CCAAT/enhancer-binding protein δ
CDK2	Cyclin-dependent kinase 2
ChIP	Chromatin Immunoprecipitation
CHOP	C/EBP homologous protein
c-MYC	V-myc myelocytomatosis viral oncogene homolog (avian)
DAPI	4',6-diamidino-2-phenylindole
DEPTOR	DEP domain containing MTOR-interacting protein
DNA	Deoxyribonucleic acid
DTT	Dithiothreitol
E6AP	E6 associated protein
EDTA	Ethylenediaminetetraacetic acid
eEF2K	Eukaryotic elongation factor-2 kinase
EGF	Epidermal growth factor
eIF2α	Eukaryotic Initiation Factor 2α
eIF4A	Eukaryotic Initiation Factor 4A
eIF4B	Eukaryotic Initiation Factor 4B
eIF4E	Eukaryotic Initiation Factor 4E
eIF4F	Eukaryotic Initiation Factor 4F
eIF4G	Eukaryotic Initiation Factor 4G
ER	Endoplasmic reticulum
ERAD	Endoplasmic-reticulum-associated protein degradation
ERK	Extracellular signal-regulated kinase
FBXW7	F-box/WD repeat-containing protein 7
FIP200	Focal adhesion kinase family interacting protein of 200 kD
FTI	Farnesyltransferase inhibitors
GAP	GTPase-Activating Protein
GAPDH	Glyceraldehyde 3-phosphate dehydrogenase

GCN2	General control nonrepressed 2
GDP	Guanosine diphosphate
GEF	Guanine nucleotide exchange factor
Grb10	Growth factor receptor-bound protein 10
GSK3	Glycogen synthase kinase 3
GTP	Guanosine-5'-triphosphate
HEPES	4-(2-hydroxyethyl)-1-piperazineethanesulfonic acid
HIF1α	Hypoxia-inducible factor 1α
HMG-CoA	3-hydroxy-3-methyl-glutaryl-CoA
HPV	Human papillomavirus
hVPS34	Human vacuolar protein sorting 34
ICMT	Protein-S-isoprenylcysteine O-methyltransferase
IGF	Insulin-like growth factor
IKKβ	IκB kinase β
IRE1	Inositol-requiring enzyme-1
JNK	c-Jun N-terminal kinase
LAM	Lymphangioleiomyomatosis
LC3	Microtubule-associated protein light chain 3
LKB1	Liver kinase B1
LRS	Leucyl-tRNA synthetase
MAPK	Mitogen-activated protein kinases
MAPKSP1	MAPK scaffold protein 1
MDM2	Murine double minute 2
MEF	Mouse embryonic fibroblast
mLST8	Mammalian lethal with Sec13 protein 8
mRNA	Messenger ribonucleic acid
mSIN1	Mammalian SAPK interacting protein 1
mTOR	Mammalian target of rapamycin
mTORC1	Mammalian target of rapamycin complex 1
mTORC2	Mammalian target of rapamycin complex 2
NFκB	Nuclear factor kappa-light-chain-enhancer of activated B cells
NF1	Neurofibromatosis 1
PAGE	Polyacrylamide gel electrophoresis
PAM	Protein associated with MYC
PBS	Phosphate Buffer Saline
PDCD4	Programmed cell death protein 4
PDGF	Platelet-derived growth factor
PERK	Protein kinase like-ER kinase
PFA	Paraformaldehyde
PGC-1α	Peroxisome proliferator-activated receptor gamma co-activator 1-alpha
PI3K	Phosphatidylinositol 3-kinase
PI3P	Phosphatidylinositol 3-phosphate
PIKK	phosphoinositide-3-kinase-related protein kinase
PKC	Protein kinase C
PML	Promyelocytic leukaemia tumor suppressor
PPARα	Peroxisome proliferator-activated receptor α
PPARδ	Peroxisome proliferator-activated receptor δ
PRAS40	40 kDa proline-rich AKT substrate
PROTOR-1	Protein observed with Rictor-1
PTEN	Phosphatase and tensin homolog
PUMA	p53 upregulated modulator of apoptosis

Rag	Ras-related GTP binding
Raptor	Regulatory associated protein of mTOR
RAS	Rat sarcoma viral oncogene homologue
RCC	Renal cell carcinoma
RCE1	CAAX prenyl protease 2
REDD1	Regulated in development and DNA damage responses 1
Rheb	Ras homolog enriched in brain
RhoA	Ras homolog gene family, member A
Rictor	RAPTOR independent companion of mTOR
S6K	Ribosomal S6 kinase
SDS	Sodium dodecyl sulfate
SGK	Serum/glucocorticoid regulated kinase 1
shRNA	Small hairpin ribonucleic acid
SKAR	S6K1 Aly/REF-like substrate
SQSTM1	Sequestosome 1
SREBP1	Sterol Regulatory Element-Binding Protein 1
TM	Transmembrane
TNFα	Tumor necrosis factor α
TSC	Tuberous sclerosis
TX-100	Triton X-100
U1snRNP70	U1 small nuclear ribonuclear protein 70
ULK1	Unc-51-like kinase 1
UPR	Unfolded protein Response
WGA	Wheat germ agglutinin
XBP1	X-box binding protein 1
YY1	Yin-yang 1

CHAPTER 1. INTRODUCTION

1.1 Introduction to Tuberous Sclerosis Complex and Lymphangioleiomyomatosis (LAM)

Two diseases are associated with loss-of-function mutations to the *TSC1* or *TSC2* tumor suppressor genes: tuberous sclerosis complex (TSC) and lymphangioleiomyomatosis (LAM). TSC is an autosomal dominant genetic disorder present in approximately 7 to 12 of every 100,000 live births (1). Patients suffering from TSC experience neoplastic growths in multiple organs systems including the brain which may result in mental retardation, autism, and seizers. TSC patients present with drastically different degrees of disease penetrance (1). Some patients suffer from life threating symptoms including renal disease, brain tumors, and bronchopneumonia while others experience only minor skin growths (1). Patients suffering from TSC may also suffer from a rare cystic lung disease known as LAM which may also occur sporadically in the general population (2). Currently, there is not a treatment or cure that effectively manages TSC or LAM; although, many strategies are being explored, including inhibitors specific to mTOR kinase or drugs targeting pathways that cells with high mTORC1 activity may rely on to survive (2).

1.2 mTOR complex-1 vs. mTOR complex-2 (mTORC1 vs. mTORC2)

As shown in figure 1-1, mTOR exists in two distinct functional complexes: The rapamycin-sensitive mTOR complex 1 (mTORC1), and mTOR complex 2 (mTORC2) which is insensitive to the direct effects of this drug. mTORC1 and mTORC2 differ in their composition and substrate specificity (3). The mTORC1 complex is made up of mTOR, PRAS40 (40 kDa proline-rich AKT substrate), DEPTOR, mLST8 (mammalian lethal with Sec13 protein 8), and Raptor (regulatory-associated protein of mTOR). PRAS40 is an inhibitory protein that blocks mTORC1 from binding substrates (4). This is overcome by Akt-mediated phosphorylation of PRAS40 at threonine 246 (5, 6). The most characterized substrates of mTORC1 are initiation factor 4E-binding protein (4E-BP) and p70-S6 kinase (S6K) (3).

The mTORC2 complex is made up of mTOR, mLST8, Rictor (rapamycin-insensitive companion of mTOR), Protor-1 (protein observed with Rictor-1), and mSIN1 (mammalian stress-activated protein kinase interacting protein 1) (3). Although mLST8 appears to bind both mTOR complexes, it is only essential for the stability of mTORC2 (7). Regulation of mTORC2 is less characterized than that of mTORC1; however, mTORC2 activity seems to be stimulated by growth factors via the PI3 kinase pathway. Known mTORC2 substrates include Akt, SGK and all conventional forms of protein kinase C (8-10).

The activities of mTORC1 and mTORC2 appear to be interconnected at some level, however, the complexity of this connection is only just beginning to be understood. Recently, mTORC1 was shown to phosphorylate Grb10 leading to its stabilization and inhibition of PI3 kinase activation through a mechanism that has yet to be characterized in detail. This inhibition of PI3 kinase reduced mTORC2's phosphorylation of Akt during stimulation with insulin or IGF (11, 12). Rapamycin treatment has been shown to relieve this inhibition leading to mTORC2 activation in multiple cancer cell lines (13). Despite this major breakthrough in the understanding of this feedback loop, many questions remain. For example, mTORC1 has been shown to inhibit both PDGF and EGF receptor signaling but Grb10 has not been shown to have an effect on these signaling pathways.

The effects mTORC2 has on mTORC1 are less understood. mTORC2 is one of two kinases required for the complete activation of Akt, an upstream regulator of mTORC1. However, both shRNA and genetic knockout of the mTORC2 component Rictor fail to reduce the activity of mTORC1 or several other well-characterized Akt substrates (7). Recently, a link in the regulation of the two complexes was established when the DEP-domain-containing mTOR-interacting protein (DEPTOR) was identified. DEPTOR binds both mTOR complexes, and shRNA-targeted knockdown of DEPTOR activated both mTORC1 and mTORC2 suggesting that it is an inhibitor of both complexes (14). However, inhibition of mTORC1 by DEPTOR overexpression unexpectedly activated mTORC2 by removing mTORC1's negative feedback loop on mTORC2 (14). Adding to this complex interplay, both complexes decrease DEPTOR transcription and enhance its degradation (14). Therefore, it is possible for DEPTOR to inhibit both mTORC1 and mTORC2 or activate mTORC2 while inhibiting mTORC1. This is determined by DEPTOR's expression level, which is controlled by both complexes.

1.3 Tuberin and Harmartin

The most characterized upstream negative regulators of mTORC1 are the tuberous sclerosis complex (TSC) 1 and 2 gene products, hamartin and tuberin, respectively. Indeed, many of the environmental signals that regulate mTOR activity are funneled through this complex. Mutations resulting in the loss of expression of either TSC1 or TSC2 cause hyperactivation of mTORC1 and severe inhibition of mTORC2 (15-21). Hamartin binds to tuberin and stabilizes its expression; therefore, loss of hamartin expression is functionally equivalent to loss of tuberin (22). Tuberin serves as a GTPase activating protein or GAP that inhibits the small GTPases Rheb1 and Rheb2 (Ras homologs enriched in brain) (23-26). Like other Ras proteins, Rhebs exist in two functional conformations: a GTP bound active state and a GDP bound inactive state. Rhebs bind to and activate mTORC1 only in their GTP bound state. Tuberin binds to active GTP-loaded Rheb and catalyzes GTP hydrolysis and the resulting transition to the inactive state.

In addition to suppressing Rheb-mediated mTORC1 activation, the hamartin-tuberin complex may play a distinct role in regulating mTORC2: It has been shown that the TS complex associates with and is required for the activity of mTORC2 (27, 28). This activity is independent of tuberin's GAP activity towards Rheb and unique to the mTORC2 complex due to an interaction with the mTORC2-specific subunit, Rictor (27, 28).

The harmartin-tuberin complex is regulated both positively and negatively by multiple protein kinases and is therefore a major node of regulation of the mTOR pathway. Growth factor activation of the PI 3-kinase and MAP kinase pathways has been shown to relieve tuberin's inhibition of Rheb activation of mTORC1, via Akt and Erk phosphorylation of tuberin, respectively (17, 29, 30). Additionally, IKKβ has been shown to phosphorylate hamartin following TNFα treatment leading to increased mTORC1 activation (31). In contrast, phosphorylation of tuberin by AMP-activated protein kinase (AMPK) increases its Rheb GAP activity leading to mTORC1 inhibition (32, 33). This phosphorylation event acts dominantly over Akt or Erk. AMPK activation of tuberin is further enhanced by GSK3 (34).

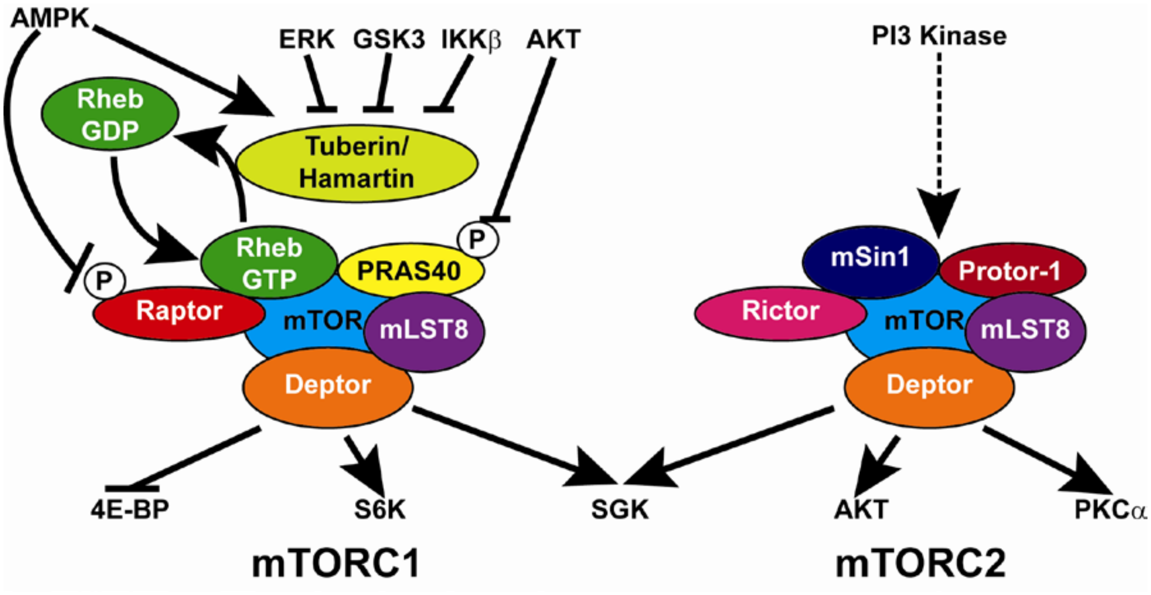
AMPK
ERK
GSK3
IKKβ
AKT
PI3 Kinase
Rheb GDP
Tuberin/ Hamartin
Rheb GTP
PRAS40
P
P
Raptor
mTOR
mLST8
Deptor
mSin1
Protor-1
Rictor
mTOR
mLST8
Deptor
4E-BP
S6K
SGK
AKT
PKCα
mTORC1
mTORC2

Figure 1-1. The mTOR kinase participates in two complexes with distinct composition, substrates, and upstream regulation

1.4 Regulation via ubiquitination and acetylation

In addition to regulation by phosphorylation, both the mTOR and TSC complexes are post-translationally modified by ubiquitination. The major ubiquitin ligase that targets mTOR for degradation via the 26S proteasome is the tumor suppressor, FBXW7/CDC4 (35). Loss of FBXW7 has been reported in breast cancer samples but typically not from patients that also lack PTEN suggesting that these genes both work to suppress mTOR-dependent growth and survival (35). Several other ubiquitin ligases have been found to target the hamartin-tuberin complex for degradation. Protein associated with Myc (PAM) and the FBW5-DDB1-Cul4-Roc1 complex oppose hamartin's stabilization of tuberin (36, 37). Additionally, following infection with high-risk human papilloma virus, the HPV16 E6 protein couples the E6AP ubiquitin ligase to tuberin (38). This targets it for degradation and results in mTORC1 activation. Tuberin degradation is also regulated by the arrest-defective protein 1 (ARD1) which promotes the stabilization of tuberin protein by acetylation (39). Like FBXW7, ARD1 expression appears to be lost in multiple types of cancer including those of breast, lung, pancreas, and ovaries (39).

1.5 Amino acid, glucose, and oxygen control of mTORC1

In addition to control by growth factor signaling or protein degradation, mTORC1 activity is regulated by the availability of glucose and amino acids through mechanisms that have only recently come to light. One of the major nutrient-mediated inputs to mTORC1 is via the class III phosphatidyl inositol (PI) 3-kinase hVPS34. It has been shown that addition of amino acids to starved cells stimulates the release of intracellular calcium leading to activation of hVPS34 through calmodulin binding (40). The activation of hVPS34 leads to the activation of Rheb and the stimulation of mTORC1. Previous studies have shown that hVPS34 is required for the production of PI3P-rich vesicles that may be required for Rheb signaling to mTOR (41, 42). Interestingly, the mTORC1 complex has recently been shown to interact with the Rag family of

GTPases that recruit mTORC1 to Rab7/Rheb containing lysosomal vesicles in the presence of amino acids (43, 44).

There are four Rag GTPases: A, B, C, and D. Rag A and B are most similar to yeast GTR1p; whereas, Rag C and D are most similar to yeast GTR2p. Rag A or Rag B can participate in a dimer with Rag C or Rag D (45). Of these dimers, those containing Rag D behave uniquely in a manner that allows them to be regulated by Leucine-tRNA synthase (LRS). Rag A-C or B-C dimers when loaded with GTP activate mTORC1; however, dimers containing Rag D bound to GTP act as a dominant negative and block stimulation of mTORC1 by amino acids. In the presence of leucine, LRS acts as a GAP for Rag D causing it to switch from its inhibitory GTP bound state to a non-inhibitory GDP bound state that allows the other Rag protein in the Rag dimer to switch to an active GTP bound form (46). The active Rag GTPases target mTORC1 to vesicles containing the mTORC1 activator GTPase Rheb through a complex termed “the regulator” that contains the MAPK scaffold MP1, p14 and p18 (encoded by the MAPKSP1, ROBLD3, and c11orf59 genes) (47). The Rag GTPases were shown to directly bind mTORC1 but did not stimulate the phosphorylation of S6K in vitro indicating that these GTPases function to bring mTORC1 to Rheb for activation rather than directly stimulate mTORC1 themselves (43).

The mechanisms by which glucose regulates mTORC1 are less clear. The most characterized mechanism centers around AMPK-mediated phosphorylation of TSC2. AMPK is directly controlled by cellular AMP concentration, which is increased in the absence of glucose due to decline of ATP. Many studies have shown that AMPK directly phosphorylates TSC2 and enhances its Rheb GAP activity (32, 33). This results in decreased Rheb stimulation of mTORC1. Additionally, AMPK can directly phosphorylate the raptor subunit of mTORC1 and this event has also been shown to be inhibitory (48). So what about AMPK-independent mechanisms? Under low glucose conditions, glyceraldehyde 3-phosphate dehydrogenase (GAPDH) has been shown to bind Rheb and prevent it from stimulating mTORC1 activity (49). This inhibition occurs in TSC2-null cells silenced for AMPK expression, indicating that GAPDH directly affects Rheb’s ability to stimulate mTORC1 (49). George Thomas' lab has also produced an alternative explanation regarding the TSC2/AMPK-independent inhibition of mTORC1 during nutrient starvation. They find that metformin blocks the ability of mTORC1 to relocate during amino acid stimulation, and the mTORC1 inhibition resulting from metformin treatment can be reversed by overexpressing an activated mutant of Rag B (50). These results suggest glucose depletion may be signaling to mTORC1 through a mechanism similar to amino acids.

Oxygen concentration can also control mTORC1 signaling and occurs through both direct and indirect mechanisms. Under hypoxic conditions, the promyelocytic leukemia (PML) tumor suppressor has been shown to bind and sequester mTORC1 to the nucleus, preventing its activation (51). The TSC1/2 interacting protein REDD1 is upregulated by HIF1α in the absence of oxygen whereupon binding to the TSC1/2 complex results in activation of TSC2's Rheb-GAP activity and the inhibition of mTORC1 (52). In addition to REDD1 control of the tuberin-hamartin complex, the hypoxia-inducible Bcl family member BNIP3 binds directly to Rheb and inhibits its ability to activate mTORC1 (53).

1.6 mTORC1 integration of growth and metabolism to control protein synthesis

As shown in figure 1-2, mTORC1 regulates protein synthesis directly and indirectly through its regulation of S6K and 4E-BP. The rate-limiting step in protein synthesis is translational initiation. In this process the small ribosomal subunit is recruited to the 5'-end of mRNA and scans for the start codon where the complete ribosome assembles and translation begins. For this recruitment to occur, the eukaryotic initiation factor 4F (eIF4F) complex must assemble on the 5'-cap of mRNA (54). This complex is made up of eIF4E, eIF4G, and eIF4A (54). The assembly of the 5'-mRNA cap is regulated by mTORC1 through its most characterized substrates, 4E-binding protein (4E-BP) and S6 kinase (S6K). Hypophosphorylated 4E-BP binds to eIF4E and antagonizes formation of the mRNA capping complex by preventing eIF4G and eIF4A from binding to eIF4E. When mTORC1 hyperphosphorylated 4E-BP, it dissociates from eIF4E, the capping complex assembles, and translation of cap-dependent mRNAs is increased (54).

Activation of S6K by mTORC1 additionally increases mRNA translation through several mechanisms. These include cap-dependent translation, elongation, and ribosome biogenesis. S6K accomplishes this through its regulation of SKAR, PDCD4, eIF4B, eEF2K, and ribosomal protein S6. SKAR binds to newly-made mRNA in the exon-junction complex where it recruits activated S6K to drive translation of these new transcripts (55, 56). PDCD4 is a tumor suppressor that binds to the mRNA capping complex helicase eIF4A preventing it from removing secondary structures that hamper efficient translation (57, 58). When phosphorylated by S6K it is targeted for degradation and eIF4A becomes activated (57, 58). In addition to blocking PDCD4 inhibition, S6K also increases the activity of eIF4A by activating eIF4B (54). S6K also inhibits the activity of eIF2K, a stress-regulated kinase that phosphorylates and inhibits eEF2 (59). Thus S6K action enables more rapid peptide elongation. Although ribosomal protein S6 is a well-characterized substrate of S6K that is frequently used as a readout for S6K activity, no clear roll in the growth of cells has been establish for the phosphorylation of this substrate (54).

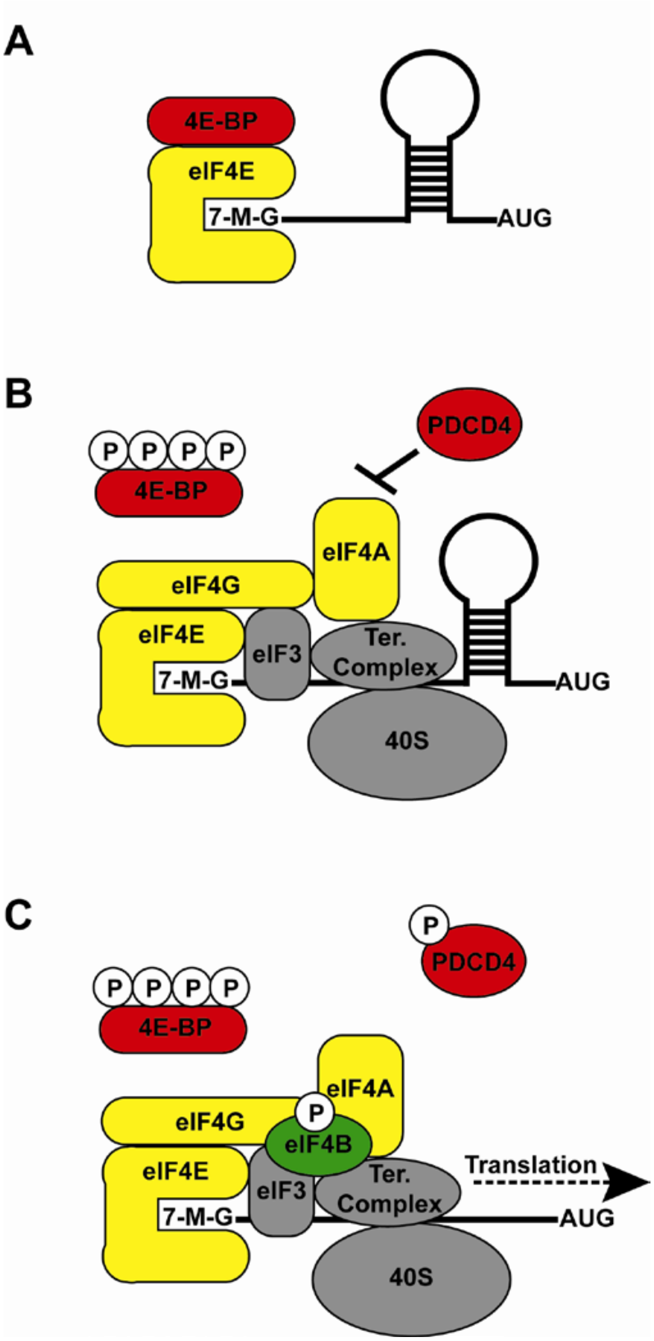
A
4E-BP
eIF4E
7-M-G
AUG
B
PDCD4
P
P
P
P
4E-BP
eIF4A
eIF4G
eIF4E
eIF3
Ter.
Complex
7-M-G
AUG
40S
C
P
PDCD4
P
P
P
P
4E-BP
eIF4A
eIF4G
P
eIF4B
eIF4E
eIF3
Ter.
Complex
Translation
7-M-G
AUG
40S

Figure 1-2. Cap-dependent translation tightly controls translational initiation

1.7 Autophagy

Macroautophagy, a process whereby intracellular proteins and organelles are degraded in double-membrane vacuolar structures known as autophagosomes, is potently inhibited by mTORC1 activity as shown in figure 1-3. This seems logical since under conditions of nutrient excess and active protein synthesis there is no need to recycle macromolecules. However, inhibiting mTORC1 by amino acid depletion, hypoxia, or other nutritional stresses as outlined earlier induces macroautophagy.

The first point where mTORC1 controls macroautophagy is through the regulation of a protein complex consisting of ULK1 (unc-51-like kinase), ATG13 (autophagy-related gene 13), and FIP200 (focal adhesion kinase family-interacting protein of 200 kDa). mTORC1 blocks macroautophagy by directly phosphorylating and inhibiting ULK1 and ATG13 (60-62). Interestingly, AMPK has recently been shown to also phosphorylate the ULK1/ATG13 complex to induce autophagy directly (63-65). The fact that both mTORC1 and AMPK can control the same signaling process to initiate autophagy suggests there are possible different agonists for each kinase (e.g. amino acids verses glucose starvation). The second point where mTORC1 affects macroautophagy is through inhibition of the VPS34-beclin complex. Although the mechanism behind this latter inhibition is unclear, it prevents an elevation of PI3P levels that is required to generate autophagosomes (41). A complex series of events follows these two regulatory steps, reviewed in Dikic et al , subsequently leads to the incorporation of LC3 into the autophagosome membrane (41). Ubiquitinated proteins that are to be degraded within autophagosomes are then coupled to this LC3 by $p62^{SQSTM1}$ (41).

This process and its regulation by mTORC1 have been implicated in both cell death and cell survival. Mice lacking beclin1 have increased incidence of lymphomas, lung and liver tumors indicating that macroautophagy may play a role in cell death and tumor surveillance (66). However, neurons lacking ATG7 (an E1 ubiquitin ligase required for LC3 incorporation into autophagosomes) accumulate toxic protein aggregates and acquire damaged mitochondria that ultimately lead to cell death indicating that macroautophagy is required for basic survival of this cell type (67). Adding to this paradox, macroautophagy has been shown to be required for both healthy and cancer cells alike to survive nutrient depletion and hypoxia (68). While certain chemotherapeutic treatments such as the proteasome inhibitor, bortezomib (PS341/Velcade) seem to require macroautophagy to induce cell death (69). These facts highlight the dualities and complexities of macroautophagy we are just beginning to understand.

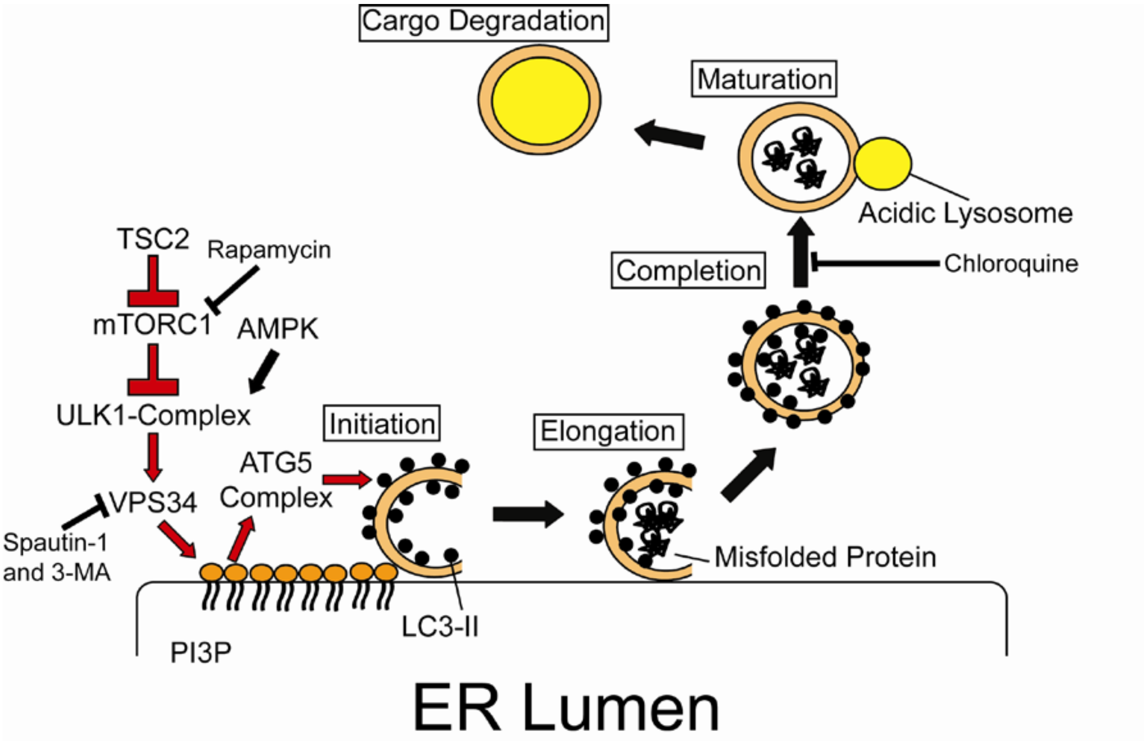
Cargo Degradation
Maturation
Acidic Lysosome
Completion
Chloroquine
TSC2
Rapamycin
mTORC1
AMPK
ULK1-Complex
Initiation
Elongation
ATG5
Complex
VPS34
Spautin-1
and 3-MA
Misfolded Protein
LC3-II
PI3P
ER Lumen

Figure 1-3. mTORC1 and the ER participate in the regulation of autophagosome formation

1.8 Lipid synthesis

Cellular lipids are used to make membranes, activate or inhibit certain biological processes, and to store energy. Due to the many important processes these molecules participate in, their synthesis is a complex and highly regulated process. Both mTORC1 and mTORC2 play major roles in the control lipid biogenesis by influencing the expression of key transcription factors such as SREBP-1, PPARγ, C/EBP1-δ, and C/EBP1-α.

mTORC1 is required for insulin-induced fatty acid synthesis and controls SREBP1-mediated transcription of target genes, such as fatty acid synthase and acetyl-coA carboxylase (70-72). The activation of this transcriptional program favors the synthesis of triglycerides, leading to the synthesis of PPARγ ligands. This is just one of several mechanisms whereby mTORC1 increases PPARγ activity. For example, mTORC1 additionally increases cap-dependent translation of C/EBP-1δ and C/EBP-1α, triggering a transcriptional cascade that results in increased PPARγ expression (73). Outside of the control of transcription factors, mTORC1, and possibly mTORC2, has also been shown to phosphorylate Lipin1 with unknown consequences (74). Lipin1 is a lipid phosphatase that converts phosphatidic acid into diacylgycerol that may then be incorporated into trigycerides, which may lead to the synthesis of more PPARγ ligands, or it can be converted into phospholipids that are essential for membrane synthesis. PPARγ activation has been shown to play a role in fatty acid storage and glucose metabolism (75).

1.9 Mitochondrial metabolism and biogenesis

Control of mitochondrial number and activity is essential to cellular homeostasis and both are influenced by mTORC1. Inhibition of mTORC1 activity in skeletal muscle and cultured fibroblasts decreases expression of the mitochondrial transcriptional regulators PGC-1α, estrogen-related receptor alpha and nuclear respiratory factors, resulting in a decrease in mitochondrial gene expression and oxygen consumption (76). The transcription factor YY1 also associates with mTORC1 and PGC-1α. Knockdown of YY1 caused a significant decrease in mitochondrial gene expression and in respiration, and YY1 was required for rapamycin-dependent repression of those genes (76).

1.10 Cell cycle

mTORC1 is a major regulator of the G_1/S cell cycle checkpoint. This checkpoint allows cells to be held in G_1 phase in the presence of stresses, such as amino acid depletion or hypoxia, that inhibit mTORC1. This arrest mechanism prevents cells from entering into the cell cycle when nutrient and other conditions are not apt for cell division similarly to the way p53 prevents cell division until DNA damage has been repaired. The major points where mTORC1 affects these processes are by controlling the expression of cyclin D1 and localization of p27(Kip).

Cyclin D1 mRNA is a cap-dependent transcript whose translation and possible nuclear export may be regulated by mTORC1 antagonism of 4EBP binding to eIF4E (77). Cyclin D1 binds to CDK2 in a kinase complex that phosphorylates substrates required for exit from G_1 phase. In addition to the cap-dependent regulation of transcripts required to exit S phase, mTORC1 regulates the cytoplasmic localization of p27, a protein inhibitor of the CDK2-cyclin D complex. mTORC1-mediated mislocalization of p27 to the cytoplasm prevents the inhibition of the cyclin kinase complex. Cell lacking TSC2 that consequently have elevated mTORC1 activity also have higher levels of CDK2-Cyclin D1 activity and cytoplasmic localization of p27 (78). The reason behind this relocalization of p27 is likely twofold: Cells lacking TSC2 have increased AMPK-mediated phosphorylation of p27 at T170 (78). This phosphorylation is in the nuclear localization signal of p27 and results in its cytoplasmic accumulation and stabilization. In addition to AMPK-mediated phosphorylation of p27, mTORC1 has been shown to promote SGK-mediated phosphorylation of p27 at T157 (79). Phosphorylation of both sites has a similar outcome. The regulation of p27 localization is important because cytoplasmic p27 may be an indicator of poor prognosis in certain types of cancer, including those of breast and prostate (80, 81). In the clinic, rapamycin has been shown to decrease the cytoplasmic localization of p27 during prostate cancer treatment, indicating that mTORC1 inhibition may be combined with other treatments to improve the therapeutic response in this patient group (82).

1.11 mTORC1 and mTORC2 in cancer

Research on the two mTOR complexes has highlighted their roles in control of cellular growth, metabolism, and survival. It has also revealed that regulation of these complexes is lost or compromised in multiple types of cancer. Underscoring this fact, loss of multiple tumor suppressors such as NF1, PTEN, LKB1, TSC1, and TSC2 results in the downstream activation of mTORC1 (83). In the case of the tumor suppressor lipid phosphatase PTEN, both mTOR complexes are activated and it has been shown in a PTEN-heterozygous mouse model of prostate cancer that mTORC2 is required for the development of cancer (84). It was the importance of these pathways to the growth of cancer and the availability of a potent selective inhibitor that initiated interest in using analogs of the mTORC1 inhibitor rapamycin in chemotherapy.

Although rapamycin has had limited success in the treatment of many cancers, the rapamycin analog CCI-779 (temsirolimus) has been approved for treatment of renal clear cell carcinoma (RCC) where its effects are due to inhibition of HIF-1α, a proangiogenic transcription factor downstream of mTORC1 (85).

1.12 Directly targeting mTOR kinase activity

The failure of rapamycin and rapalogs to potently inhibit the growth of other tumors in the clinic has been disappointing. However, research has shed light on why they may be failing. Firstly, rapamycin does not inhibit the mTORC2 complex whose activity is required for the growth of several types of cancer. Secondly, these compounds are allosteric inhibitors of mTORC1that fail to completely block its regulation of cell cycle, autophagy inhibition, and protein synthesis (86, 87). Lastly, mTORC1 inhibition often results in feedback activation of mTORC2 as well as other upstream growth and survival signals (88).

These problems have been addressed by a new class of compounds that directly compete for the binding of ATP to mTOR's catalytic domain. These drugs which include PP242, Torin1, and WYE-354 were shown to block cell cycle, induce autophagy, and potently reduce translation in cell lines where rapamycin had little to no effect (86, 89, 90). Since these compounds were also effective on Rictor-null cells, the failure of rapamycin to block tumor growth is likely due to its incomplete inhibition of mTORC1 rather than inability to affect mTORC2 (86).

An additional class of compounds has been identified that will antagonize mTOR complexes as well as PI3-kinase signaling. mTOR is a member of the PI kinase-related kinase (PIKK) family and off-target effects of anti-PI3 kinase drugs have been shown to directly inhibit mTOR activity as well as other PIKK family members such as ATM and ATR. The latest generation of these drugs includes GDC-0941 and NVP-BEZ235 (91). These dual mTOR/PI3 kinase inhibitors show great promise due not only to their ability to block growth and survival signals from mTOR but to quash the feedback activation loops associated with mTOR inhibition by rapamycin. GDC-0941 has entered phase I while NVP-BEZ235 has begun phase II clinical testing for breast cancer treatment (91).

1.13 Targeting Rheb

Apart from antagonizing mTORC1 using rapalogs or ATP-competitive inhibitors, other strategies have been proposed with varying degrees of success. Many of these focus on blocking the ability of the small GTPase Rheb to activate mTORC1. Like many other small GTPases, Rheb1 and 2 are post-translationally modified by three enzymes: an isoprenyl transferase, Ras converting enzyme 1 (RCE1), and isoprenylcysteine carboxyl methyl transferase (ICMT) (92, 93). These enzymes reside on the endoplasmic reticulum and modify Ras-family proteins by adding a farnesyl or geranylgeranyl moiety to a cysteine located 4 residues from the C terminus, removing the amino acids C-terminal to the isoprenylated cysteine, and then methylating the new carboxy-terminus of the Ras protein, respectively. These modifications are important to many Ras family members for proper localization. Loss of these signals impairs or completely blocks their ability to activate downstream effectors.

A class of drugs, known as farnesyl transferase inhibitors (FTIs), has been designed to inhibit the farnesylation and subsequent C-terminal modifications of Ras proteins. These drugs have the ability to block the farnesylation of Rheb, cause its mislocalization, and reduce or block its ability to activate mTORC1. This effect has been shown by many groups using overexpressed Rheb (24, 94-96). In studies not covered in this thesis we found that it took higher concentrations of FTI to block glioma cell growth than was required to inhibit the farnesylation of endogenous Rheb. However, inhibiting the ability of endogenous Rheb to activate mTORC1 using FTIs seems to be cell line specific (97). Despite the incongruencies in blocking Rheb-mediated activation of mTORC1, FTIs do inhibit the growth of specific cancer cells and sensitize them to other drug treatments in a Rheb-dependent manner (94, 95, 97). These compounds have been most effective in treating hematological malignancies, such as acute or chronic myeloid leukemias, myelodysplastic syndrome, and multiple myeloma (98). Interestingly, Rheb expression has been shown to be upregulated at the mRNA level in Burkitts' lymphoma and FTI treatment is very effective in a Rheb overexpression mouse model of lymphoma (95).

In addition to FTIs, HMG-CoA reductase inhibitors (statins) are also currently being explored as inhibitors of Rheb and other Ras family members. These inhibitors block the rate-limiting step of the mevalonate synthesis pathway leading to depletion of the isprenyl pyrophosphates used to post-translationally modify Rheb and other proteins. In this way, statins differ from FTIs because they will inhibit all isoprenylation whereas FTIs are specific for farnesylation. Statins have been tested for their effects on Rheb/mTORC1 in both cell culture and mouse models with differing results (99-101). In TSC2-null cells where Rheb is the primary driver for mTORC1 activity, treatment with statins was able to block Rheb farnesylation and inhibit mTORC1 (99). These drug treatments also blocked signaling from RhoA (99). However in mouse models of TSC, statins as a single-agent failed to inhibit the mTORC1 pathway or the growth of tumors despite potently affecting the synthesis of cholesterol and the isoprenylation of Ras-family proteins in healthy tissue (100, 101).

1.14 Genotoxic stress

Even though mTORC1 is a strong promoter of growth and survival, it has been shown by several groups to sensitize cells to specific types of stress (20, 33, 102-104). Based on these observations, it has been proposed that these stresses can be used to eliminate cancer cells with high mTORC1 activity while leaving the healthy tissue with low mTORC1 activity relatively unharmed. These new and exciting ideas are currently being developed by several groups who have shown that mTORC1 activation sensitizes the cell to genotoxic stress, nutrient depletion, and endoplasmic reticulum (ER) stress (20, 33, 102, 105).

Some of the most effective cancer treatments used today rely heavily on DNA damage-induced cell death. Many factors affect the sensitivity of cells to DNA damaging agents and it has been frequently shown that mTORC1 activation is one of those factors. As discussed earlier, when mTORC1 is active it inhibits the activation of mTORC2 leading to reduced Akt activity. Akt is a major contributor to cell survival through the NFκB pathway and anti-apoptotic pathways (106). When healthy cells with low mTORC1 activity are treated with DNA damaging agents, the Akt/NFκB pathway keeps the cell from entering apoptosis (20). However, these pathways are inhibited by mTORC1 so DNA damaging agents potently induce apoptosis (20).

In addition to its effects on NFκB, mTORC1 also increases the translation of the p53 tumor suppressor, both in cell culture and patient samples. p53 is the cells major coordinator for genotoxic stress, and its activation leads to cell cycle arrest or apoptosis (105). Interestingly, p21, a major player in p53 mediated cell cycle arrest and senescence, requires mTORC1 activation to carry out these activities. When p21 expression is induced in rapamycin treated or serum starved cells with low mTORC1 activity, it induces quiescence instead of senescence and the cells maintain their ability to grow (107). These findings may indicate that rapamycin or other compounds that inhibit mTORC1 directly or indirectly may antagonize DNA damaging agents in the clinic. It is also possible that by reducing translation, more ATP is available for DNA synthesis.

1.15 Nutrient depletion

In healthy tissue, mTORC1's response to amino acids and glucose is tightly controlled. The sensitivity to these stimuli allows healthy cells to coordinate their growth with available nutrients. However, these controls are lost in cancer leading to growth regardless of nutrient access. This growth in the absence of nutrients puts excess stress on the cell, that if severe, can induce apoptosis. For example, it has been shown that TSC2-null fibroblasts are much more sensitive to glucose starvation than wild-type fibroblast (32, 33). These findings indicate that, 2-deoxy-glucose (2-DG), a glucose mimetic that blocks the uptake of glucose by inhibiting hexokinase, would be able to treat tumors that have unregulated mTORC1 signaling.

Even though the mTORC1's response to glucose is lost in many cancer cells, the response to amino acids remains intact. This may allow for mTORC1 inhibition by amino acid depletion in cancer patients. It has been shown by injecting the bacterial enzyme, asparaginase, into mice that both asparagine and glutamine can be depleted from the blood leading to mTORC1 inhibition and reduced growth of TSC2-null cysts (104, 108). Interestingly, this amino acid depletion can also activate the GCN2 eIF2α kinase leading to activation of the proapoptotic transcription factor CHOP (108). This type of amino acid depletion treatment may be combined with additional drugs to enhance the cell death that is initiated by nutrient depletion.

1.16 Endoplasmic Reticulum Stress

The unfolded protein response (UPR) is activated when the cell's protein folding and secretory machinery, that is located in the endoplasmic reticulum (ER), becomes overwhelmed by misfolded protein as shown in figure 1-4. This stress response consists of three parallel pathways: inositol requiring enzyme 1 (IRE1), activating transcription factor 6 (ATF6), and the protein kinase like-ER kinase (PERK). The UPR enhances the cells ability to adapt to ER stress; however in cases of prolonged or severe stress, the UPR will induce cell death through apoptosis or autophagy (109). The UPR pathways help the cell adapt to anabolic stress in several ways. Firstly, activation of the PERK branch leads to the phosphorylation of eIF2α. This mechanism of inhibiting global protein synthesis is conserved from yeast to mammals (110). While the decrease in protein synthesis reduces the overall burden on the ER, phosphorylation of eIF2α also induces the translation of the ATF4 transcription factor. The other 2 branches of the UPR trigger the transcription of additional stress response genes. ATF6 translocates from the ER to the Golgi where it becomes activated by cleavage. Meanwhile, IRE1 facilitates the splicing of XBP1 (X-box protein 1) mRNA in the cytoplasm to an actively translated form using its endoribonuclease activity. This splicing requires tRNA ligase. ATF4, ATF6 and XBP1 help overcome the UPR by increasing the expression of ER resident chaperones, protein disulfide isomerase, and enzymes that regulate both lipid and amino acid metabolism. However, these same transcription factors also induce the expression of a proapoptotic transcription factor CHOP following prolonged stress, leading to cell death (109).

Interestingly, it has been shown that loss of either the TSC1 or TSC2 genes results in activation of the UPR in cultured MEFs, neurons, mice with TSC2-loss-induced cysts as well as in TSC patients (102, 111). It is currently believed that the loss of these genes leads to high levels of mTORC1-induced translation and that this puts an excessive burden on the ER folding machinery. The activation of mTORC1 sensitizes these cells to the ER stressing agents thapsigargin and tunicamycin and it is anticipated that other ER stressors could selectively promote the demise of cancer cells exhibiting high mTOR activity (102, 111). It is also noteworthy that glucose starvation is an inducer of ER stress through loss of N-linked protein glycosylation. This fact may explain the heightened sensitivity of TSC1 and 2 null cells to glucose deprivation.

In addition to the adaptive response of the UPR, the endoplasmic reticulum also uses a proteasomal degradation pathway to ubiquitinate and degrade proteins that cannot be correctly folded. This pathway known as ER-associated degradation (ERAD) can be inhibited by proteasome inhibitors such as MG-132 and bortezomib. When cells are treated with these inhibitors, unfolded proteins accumulate in the endoplasmic reticulum and hyper-activate the UPR. It has been shown that TSC2-null MEFs and cancer cell lines overexpressing Rheb1 have increased sensitivity to proteasome inhibitors; however, this study linked drug-sensitivity to failure to target ubiquitinated proteins to the aggresome (103).

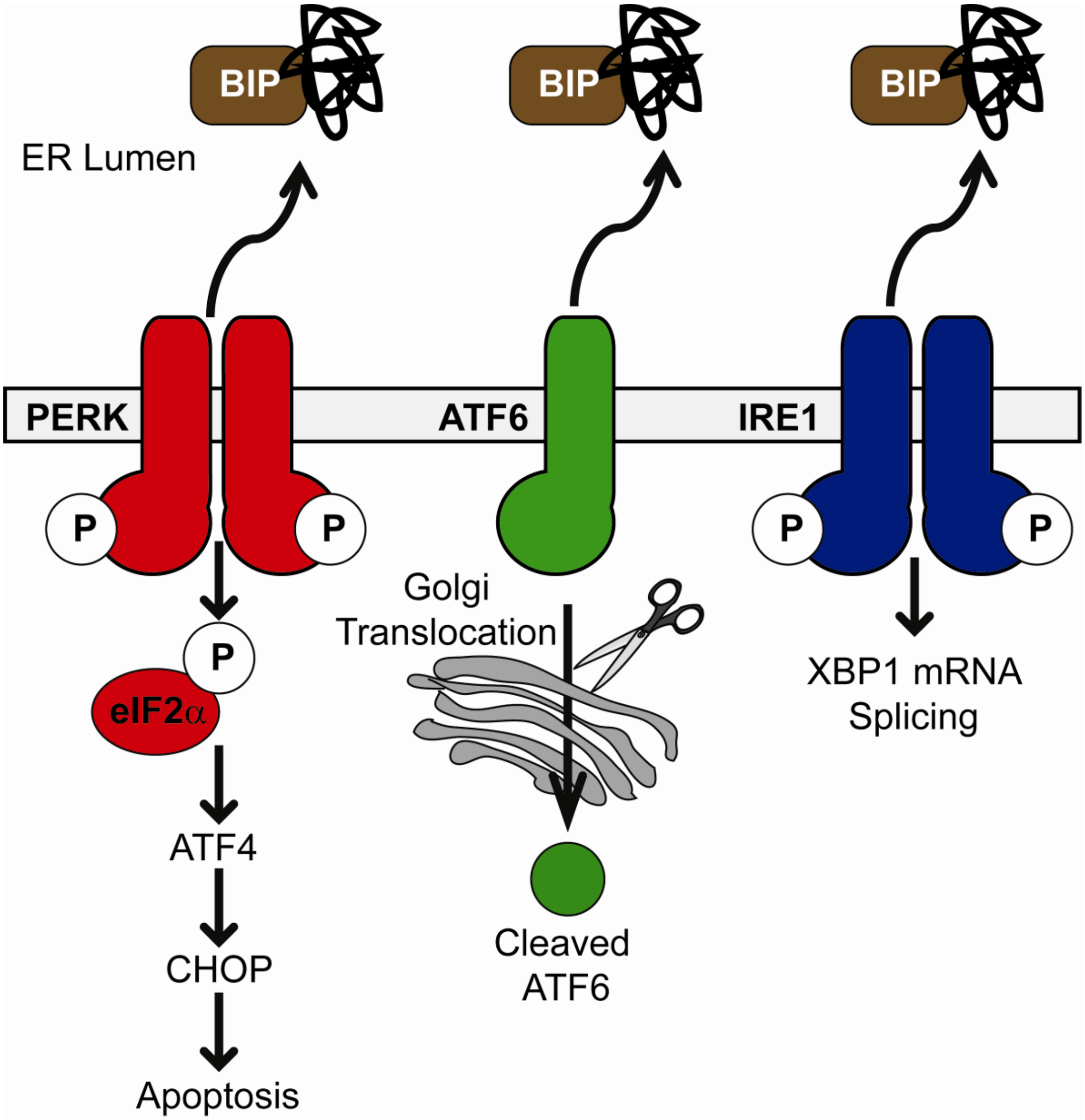
BIP
BIP
BIP
ER Lumen
PERK
ATF6
IRE1
P
P
P
P
P
eIF2α
ATF4
CHOP
Apoptosis
Golgi
Translocation
Cleaved
ATF6
XBP1 mRNA
Splicing

Figure 1-4. The Unfolded Protein Response

1.17 mTORC1 control of c-MYC

mTORC1's control of the c-MYC transcription factor is a well-established phenomenon that likely explains how mTORC1 indirectly orchestrates so many different genes and processes. mTORC1 controls the amount of c-MYC protein in the cell through a complex regulation of translation which is not completely understood (112-114). The c-MYC oncogene controls between 10-15% of genes which operate in diverse cellular processes (115, 116). These processes include growth and metabolism as well as senescence and apoptosis (117). While the mechanisms c-MYC uses to drive tumor growth have been well studied and characterized, its ability to suppress tumor growth or cooperate with certain anticancer drugs have been the intense focus of recent study and may be a possible way to induce apoptosis in cells with high mTORC1 activity.

c-MYC sensitizes cells to apoptosis induced by activation of the Fas death receptor, serum deprivation, hypoxia, glucose starvation, and cytotoxic drugs indicating that c-MYC is a general factor that induces apoptosis (116, 118, 119). Although the exact mechanism by which c-MYC induces apoptosis is unknown at least three pathways may contribute to this mechanism of cell death. First, c-MYC induces expression of the tumor suppressor protein Arf which prevents MDM2 from targeting p53 for degradation (116, 118, 119). Expression of Arf allows p53 to induce the transcription of proapoptotic genes like BAX and PUMA as well as mediators of cell cycle arrest such as p21 and p27. However, c-MYC represses expression of p21 through interaction with Miz-1 which overrides p53-induced cell cycle arrest (120, 121). This ability to override p53 induced cell cycle arrest may explain why c-MYC, unlike other oncogenes such as K-RAS, has both apoptotic and progrowth activities. Second, c-MYC has been shown to bind to and activate the transcription of the NOXA oncogene which promotes apoptosis (122). Finally, c-MYC represses expression of the anti-apoptotic members of the BCL-2 family that prevent cytochrome c release from the mitochondria (123). c-MYC's participation in apoptosis has been shown to be a major barrier in its ability to drive tumor development. Mouse models of Myc-induced tumor development have found that for c-MYC to potently drive tumor development inactivating mutations to p53, Arf, Bax and Bim or overexpression of anti-apoptotic genes such as Bcl-2 and Bcl-XL must be present(123-126). Further, c-MYC mutants that are deficient for stimulating apoptosis, but retain the ability to stimulate progrowth genes, accelerates lymphomagenesis without the need for complementary mutations in apoptosis-regulatory genes (127).

1.18 Summary

Studying the mechanism of action of rapamycin has allowed researchers to decipher how cells coordinate transcription, ribosome biogenesis, translation initiation, and autophagy in both yeast and mammals in response to wide-ranging stimuli (oxygen, growth factors, amino acids, and intracellular energy supply). In humans these processes are integrated through the serine/threonine protein kinase, mammalian target of rapamycin (mTOR). Improper activation of mTOR in cancer, diabetes, and aging suggested that rapamycin may be useful in the treatment of multiple diseases. However, recent evidence suggests that there might be more advantageous methods of blocking mTOR activation. These include targeting the Rheb GTPases, amino acid signals to mTOR, cellular stresses generated by mTOR activation, or directly inhibiting the kinase activity of mTOR.

CHAPTER 2. MATERIALS AND METHODS

2.1 Elt3 Cell culture

Elt3 cells were a gift from Cheryl Walker (MD Anderson). All experiments were performed on cells between passages 40-50 that were maintained in DF-8 media as described by Walker and Ginsler (128). Cells were plated at 70% confluence. The following day, DF-8 media was replaced with serum-free DMEM (Lonza) containing DMSO vehicle control or 50 nM rapamycin (Calbiochem). 24 hours later, bortezomib (LC laboratories) was added to each plate to a final concentration of 20 nM. In experiments using c-MYC inhibitor II (EMD Millipore), cells were starved of serum overnight and treated with 5µM c-MYC inhibitor II 2 hours prior to treatment with 20 nM bortezomib. Experiments also used 10mM 2-DG and 1µM thapsigargin when described.

2.2 621-101 Cell culture

621-101 cells were a gift from Lisa Henske (Harvard). All experiments were performed on cells between passages 14-30 that were maintained in DF-8 media as described by Walker and Ginsler (128). Cells were plated at 70% confluence. The following day, DF-8 media was replaced with serum-free DMEM (Lonza) containing DMSO vehicle control or 50 nM rapamycin (Calbiochem). 24 hours later, MG-132 (LC laboratories) was added to each plate to a final concentration of 1µM. In experiments using 10 µM spautin-1 (Cayman-are you sure), 10µM bhloroquine (Sigma), or 10mM 3-methyl adenine (Sigma), cells were treated 2 hours prior to treatment with MG-132. In experiments using 10 µM of the JNK inhibitor SP60012 (Calbiochem), cells were treated for 24 hours similar to rapamycin.

2.3 Nuclear lysates

Nuclear lysates were collected in experiments where the levels of ATF4 or CHOP proteins were measured in order to increase the detectability of these nuclear proteins. 60 mm plates of Elt3 cells were washed with ice-cold PBS. Cells were then harvested into 1 mL of 10 mM HEPES pH 7.9, 1.5 mM $MgCl_2$, 10 mM KCl, and 0.25% IGEPAL. Cells were incubated with rotation at 4°C, for 10 min. Nuclei were then pelleted at 3,000 rpm in an accuSpin Micro 17R microcentrifuge (Fisher Scientific) at 4°C, 10 min. The supernatant was discarded and the pellet was resuspended in high detergent lysis solution (20 mM Tris-HCl pH 7.4, 150 mM NaCl, 2 mM EDTA, 1% TX-100, and 1% SDS). Nuclear lysates were incubated for 10 minutes on ice and pelleted for 10 minutes at 13,300 rpm, 4°C. Supernatants were transferred to ice-cold tubes and frozen in liquid nitrogen for later analysis.

2.4 Western blotting and antibodies

For experiments where ATF4 and CHOP proteins were not measured, whole cell lysates were prepared using high detergent lysis solution with protease and phosphatase inhibitors. Cell lysates were normalized by protein concentration using a Bradford assay (Bio-Rad) and analyzed using 10 or 15% SDS-PAGE gels. Proteins separated in these gels were transferred to PVDF-FL membranes (Millipore). Membranes were blocked in 5% non-fat dry milk and probed with primary antibodies. Antibodies specific to LC3(#3868), cleaved caspase-3 (#9661), Lamin A/C (#4777), and c-MYC (#5606) were obtained from Cell Signaling Technologies. Antibodies specific to p62 (sc-28359), U1snRNP70 (sc-9571), ATF4 (sc-200), CHOP (sc-7351), and β-actin (sc-47778) were obtained from Santa Cruz Biotechnology. Western blots were visualized by X-ray film using SuperSignal West Femto Maximum Sensitivity substrate (Thermo Scientific) or scanned using an Odyssey LiCOR machine.

2.5 qRT-PCR

RNA was isolated from cells using TRIzol (Invitrogen) according to the manufacturer’s protocol. First-strand cDNA synthesis was performed using M-MuLV reverse transcriptase (New England Biolabs) and qRT-PCR detection of transcripts was performed using the Light Cycler

480 (Roche) and the Roche Universal Probes Library according to the manufacturers' protocols. Primer sequences and probe numbers are located in Appendix 1.

2.6 Trypan blue cell viability assays

After bortezomib treatment, cells were washed with ice-cold PBS and trypsinized for 5 minutes at 37°C. The media from the plate, PBS wash, and trypsinized cells were pooled into a 15 mL conical tube and cells were pelleted for 5 min at 1,000 rpm in a Beckman GS-15R centrifuge at 4°C. The supernatant was discarded and cells resuspended in a 1:1 solution of PBS:0.4% Trypan blue (Sigma-Aldrich). The number of live and dead cells was counted by using a hemocytometer (Reichert). Clumps of cells where individual cells could not be accurately counted were excluded from these counts.

2.7 Chromatin immunoprecipitation

Chromatin immunoprecipitation was performed on 10^7 Elt3 cells that had been treated for 4 hr with 20 nM bortezomib using the SimpleChIP Chromatin IP kit (Cell Signaling #9003) according to the manufacturer's specifications. PCR detection of immunoprecipitated DNA fragments was performed using Maxima Hot Start 2x PCR master mix (Fermentas). Primer sequences are located in Appendix 1.

2.8 Cloning and lentiviral production

The c-MYC lentiviral expression plasmid was generated by the addition of 5'-BamHI and 3'-NotI sites to human c-MYC cDNA by PCR. This DNA fragment was then cloned into the same sites of the pCDH1-CMV-MCS-EF1-Hygro expression vector (System Bioscience). pCSCGW-GFP-mCherry-ER and pCSCGW-GFP-mCherry-LC3 were cloned as follows. The KDEL endoplasmic reticulum retention signal was added during PCR amplification of RFP using the forward primer TAGCTACCGGTTCTAGAGCCTCCTCCGAGGACGTCATC and the reverse primer AGCTACTCGAGTCACAGCTCGTCCTTCGAAGCTTGGGCGCCGGTGGA. This fragment was then digested with AgeI and XhoI and ligated into the pCSCGW lentiviral vector backbone. The ER targeting signal from calreticulin was then added to this newly created plasmid by digesting with AgeI and XbaI and ligating to the annealed oligonucleotides CCGGTATGCTGCTATCCGTGCCGTTGCTGCTCGGCCTCCTCGGCCTGGCCGTCGCCATCGATT and CTAGAATCGATGGCGACGGCCAGGCCGAGGAGGCCGAGCAGCAACGGCACGGATAGCAGCATA. LC3 was subcloned from pEGFP-LC3 was subcloned using AgeI and XhoI into the pCSCGW plasmid. mCherry was PCRed and inserted into the NheI and AgeI sites of these plasmids. All lentiviral plasmids were co-transfected using calcium phosphate into 293T cells with pCMV-VSV-G (Addgene #8454), pRSV-REV (Addgene #12253), and pMDLg/pRRE (Addgene #12251). Two days post-transfection the viral supernatant was filtered using a 0.45 μm syringe filter and stored at -80°C until needed. Empty vector or the pCDH1-c-MYC plasmid were co-transfected into 293T cells, along with with pCMV-VSV-G (Addgene #8454), pRSV-REV (Addgene #12253), and pMDLg/pRRE (Addgene #12251) plasmids following calcium phosphate precipitation. Two days post-transfection the viral supernatant was filtered (0.45 μm) and stored at -80°C until needed.

2.9 Generation of c-MYC and empty vector stable cell lines

Elt3 stable cell lines were generated by plating the cells into media containing lentivirus and 5 μg/mL polybrene. An additional plate was set up on the first day that was not infected. This plate served as a control for complete drug selection. On the day following infection cells were selected using 300 μg/mL hygromycin B. This selection was continued by refreshing the media and selection drug every 2 days until cells on the uninfected control plate were completely killed.

2.10 Imaging and measuring ER volume

Cells were plated into 35mm plates containing glass cover slips. Each plate contained 100 µl of mCherry-ER lentivirus supernatant and DF-8 media. The next day the media on these plates was replaced with serum-free media and drug treatments were done as describe in each experiment. The third day more drug treatments were done pertinent to the experiment and slides were washed with cold PBS 3 times while still in the plates. Cells were then fixed in 4% paraformaldehyde (PFA) in PBS pH 7.4 for 15 minutes. Plates were washed 3 times with PBS pH 7.4 to remove PFA. Each plate was soaked in a solution of 5µg/mL AF488-wheat germ agglutinin (WGA) in PBS pH7.4 overnight in the cold room. WGA only labels the plasma membrane because these cells have not been permeabilized with detergent. Excess WGA was washed away using 3 PBS pH 7.4 washes. Cover slips were removed and mounted using hard set mounting media with DAPI (VECTRASHIELD H-1500). Fluorescence images were acquired on a Zeiss 468 AxioObserverZ1 microscope, and ER and plasma membrane area were measured using AxioVision software.

2.11 Florescent live cell imaging

Cells were plated into 35 mm MatTek dishes with glass bottoms. Each plate contained 100µl of lentivirus in DF-8 media. Cells were allowed to adhere overnight before the media was changed to serum-free DMEM containing the drug treatments described in each experiment. The following day these cells were treated again with a stress drug without changing the media. Fluorescence images were acquired on a Zeiss 468 AxioObserverZ1 microscope.

2.12 shRNA sequences and 293T shRNA knockdowns

shRNA sequences are cloned into the AgeI and EcoRI sites of the pLKO.1 vector. These sequences can be found in Appendix 2. shRNA lentiviruses were created as described in section

2-8. 293T cells were then infected with the viral supernatant and then selected with 2µg/mL puromycin. Once completely selected, cells were replated as needed for the experiments.

2.13 Luciferase Assays

2.5-kb of the rat ATF4 promoter were amplified from the Elt3 genomic DNA. This 2.5-kb fragment was cloned into the pGL3-basic plasmid into the NheI and XhoI sites. The E-boxes located at -855 and -141 of the ATF4 promoter were deleted using the primer overlap method. 0.5 µg of luciferase reporter and 0.5 µg of c-MYC or empty vector plasmid were transfected into 293T cells. Cells were lysed and measured 48 hours later according to the Promega luciferase assay system protocol.

2.14 Statistical Analysis

Bar graphs represent the mean measurement of 3 or 4 experiments with error bars representing the standard deviation from this mean. P-values were calculated using the T-test function in Microsoft Excel.

CHAPTER 3. mTORC1 ENHANCES BORTEZOMIB-INDUCED DEATH IN TSC-NULL CELLS BY A C-MYC-DEPENDENT INDUCTION OF THE UNFOLDED PROTEIN RESPONSE

3.1 Introduction

Bortezomib is a potent inhibitor of the 26S proteasome. Its early promise as a treatment for relapsed/refractory multiple myeloma prompted the United States Food and Drug Administration (US FDA) to grant the drug accelerated approval (129). Subsequently there has been significant interest in the use of bortezomib as a treatment for other forms of cancer and clinical trials are underway using the drug as a single agent or in combination with several additional compounds.

Despite positive results in the treatment of multiple myeloma, the mechanism of action of bortezomib remains unclear due to the pleiotropic effects of proteasome inhibition. Recent work by multiple labs has found a convergence of two signaling pathways that contribute to apoptosis induced by the UPR and may influence bortezomib induced cell death (102, 111, 130). The first pathway involves the activation of the mammalian target of rapamycin complex-1 (mTORC1) that increases protein synthesis in response to the small GTPase Rheb (Ras homologue enriched in brain). The activity of Rheb is in turn controlled by a complex of the *TSC1* and *TSC2* tumor suppressor gene products, designated hamartin and tuberin, respectively. Tuberin acts as a GTPase activating protein (GAP), which switches Rheb from an active GTP-bound state to an inactive GDP-bound form (23, 24, 26, 131). Meanwhile hamartin stabilizes tuberin to prevent its degradation (22). Inactivating mutations in either *TSC1* or *TSC2* are found in the genetic disorder tuberous sclerosis complex (TSC) and the rare cystic lung disease lymphangioleiomyomatosis (LAM) (1). Mutation of *TSC1* or *TSC2* in these diseases also results in the development of neoplasms that are characterized by activation of mTORC1 and high levels of protein synthesis (1).

The second pathway that converges with the TSC2/mTORC1 pathway to sensitize cells to bortezomib-induced death is the unfolded protein response (UPR). The UPR is activated when unfolded proteins accumulate in the endoplasmic reticulum (ER) causing an excessive burden on the protein folding and secretory machinery of cells (132, 133). Bortezomib and other proteasome inhibitors can activate the UPR by inhibiting the cells ability to degrade unfolded protein via the ER-associated degradation (ERAD) pathway (134, 135). Therefore, unfolded proteins can build up in the ER and activate all three branches of the UPR: inositol-requiring enzyme-1 (IRE-1), activating transcription factor-6 (ATF6), and protein kinase-like ER kinase (PERK) (132, 133). Activation of these 3 branches allows the cell to adapt to the unfolded protein stress by arresting global protein synthesis, preferentially translating prosurvival transcription factors, and inducing the expression of proteins that facilitate the folding, processing, and trafficking of secretory proteins. However, if unfolded protein stress is severe or prolonged, the cell will undergo apoptosis through PERK-dependent translation of the transcription factors ATF4 and CCAAT/enhancer-binding protein homologous protein (CHOP) (136, 137).

PERK is a member of the eIF2α kinase family. By phosphorylating eIF2α at serine 51, PERK causes a global arrest of mRNA translation but enables the preferential translation of specific stress responsive mRNAs that contain complex 5’UTRs (138, 139). These mRNAs, including ATF4 and CHOP, are also transcribed more effectively during PERK-activation (140, 141). ATF4 and CHOP are essential for unfolded protein-induced death and knockout MEFs lacking either of these transcription factors are more resistant to drugs that induce the UPR (140, 142). Therefore, signaling pathways that alter *ATF4* and *CHOP* expression may provide the key to understanding bortezomib sensitivity.

TSC1 or *TSC2* knockout MEFs have been reported to experience increased sensitivity to the chemical stressors, thapsigargin and tunicamycin, that activate the UPR (102). This increased sensitivity was attributed to a significant increase in the basal levels of UPR markers in *TSC1*- or *TSC2*-null MEFs compared to their wild-type counter parts. These markers included phosphorylated PERK, *CHOP* mRNA, and *GRP78* mRNA that encodes an ER molecular chaperone (102). Expression of these stress markers, as well as UPR-induced apoptosis could be decreased by treating these knockout MEFs with the mTORC1 inhibitor rapamycin (102). 4-phenylbutyrate, a chemical suggested to improve protein folding also decreased basal levels of

UPR components and UPR-induced apoptosis in *TSC*-null MEFs (102). These results strongly support the hypothesis that mTORC1 activity predisposes a cell to apoptosis by inducers of the UPR, such as bortezomib. However, the mechanism(s) of mTORC1 action in this process is not well understood.

To address how mTORC1 activity sensitizes cells to bortezomib-induced ER stress and apoptosis we studied these events in the *TSC2*-null Elt3 cell line. Bortezomib promoted both the UPR and UPR-induced apoptosis, responses that were suppressed by the mTORC1 inhibitor, rapamycin. Both the mRNA and protein expression of ATF4 and CHOP were increased upon exposing Elt3 cells to bortezomib. This suggested that mTORC1 may regulate the expression of a transcription factor, such as c-MYC, that is required for the induction of these two genes. In support of this notion, rapamycin treatment decreased c-MYC protein expression in Elt3 cells. c-MYC was also shown to bind both the *ATF4* and *CHOP* promoters during bortezomib treatment. Exogenous expression of c-MYC overcame the suppressive effects of rapamycin. These findings are consistent with mTORC1 functioning in conjunction with bortezomib to induce cell death by driving c-MYC expression, which in turn upregulates *ATF4* and *CHOP* to drive apoptosis.

3.2 Bortezomib induced cell death is reduced by rapamycin and by inhibition of the unfolded protein response

It was previously reported that 24 hour pretreatment with the mTORC1 inhibitor rapamycin decreased the ability of UPR inducers, such as thapsigargin and tunicamycin, to induce the death of *TSC2*$^{-/-}$ MEFs (102). This suggested that ER stress is only lethal in the presence of high mTORC1 activity and that this might be taken advantage of in the elimination of TSC1/2-null lesions. We began our study by confirming that Elt3 cells, a *TSC2*-null rat leiomyoma cell line, respond similarly to the proteasome inhibitor and UPR inducer, bortezomib. Elt3 cells were pretreated with 50 nM rapamycin for 24 hours and then exposed to 20 nM bortezomib for 8, 12, or 24 hours. Bortezomib treatment induced apoptosis of Elt3 cells as shown by an increase in cleaved caspase-3 at 24 hours (Figure 3-1a). However, cells pretreated with rapamycin showed significantly less caspase activity or overall cell death. In support of the notion that caspase-3 cleavage accompanies apoptosis, Elt3 cells at the same 24 hour time point showed reduced viability as determined by trypan blue staining: bortezomib lowered the viability of Elt3 cells to 43% while it only modestly decreased the survival of the rapamycin pretreated cell from 84% to 76% (Figure 3-1b). Bortezomib treatment caused cells to round and lose adherence whereas rapamycin pretreated cells remained mostly flat and attached (Figure 3-1c).

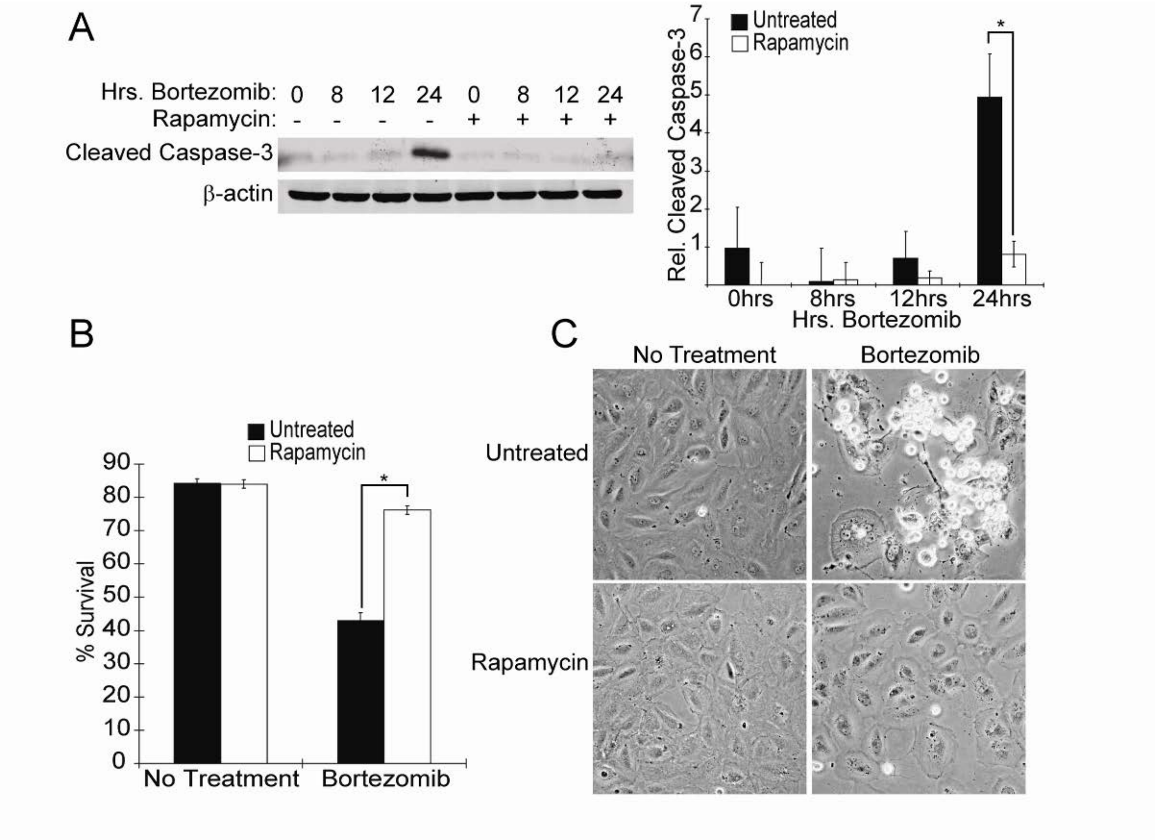

Figure 3-1. Elt3 cells undergo rapamycin-sensitive apoptosis when treated with bortezomib

(A) Elt3 cells were pretreated with 50 nM rapamycin or vehicle control for 24 hours before being exposed to 20 nM bortezomib for an additional 8, 12, or 24 hours. Lysates were prepared after these drug treatments and analyzed by Western blot using an antibody selective for cleaved caspase-3 or β-actin. (B) Trypan blue staining of Elt3 cells exposed to bortezomib for 24 hours in the presence or absence of rapamycin pretreatment. (C) Phase contrast microscopy of the Elt3 cells treated with rapamycin and bortezomib, as indicated. (*P<0.05)

3.3 Early UPR markers are induced by bortezomib but unaffected by rapamycin in Elt3 cells

In its earliest stages, ER stress leads increased PERK-dependent phosphorylation of eIF2α at serine 51, cleavage of ATF6 to its active form, and IRE1 splicing of XBP1 mRNA. This splicing facilitates translation of XBP1 mRNA by causing a reading frame shift. Phosphorylation of eIF2α not only attenuates global translation but also promotes the transcription and translation of the proapoptotic transcription factors ATF4 and CHOP (132, 133). Both of these transcription factors have been linked to proteasome inhibitor-induced apoptosis, and both factors likely contributed to the cell death that was observed in figure 1 (141, 142).

We found that eIF2α phosphorylation was increased at 4 and 6 hours following bortezomib treatment. However, there was no statistically significant effect of rapamycin pretreatment on eIF2α phosphorylation at any time point tested. Likewise, there was no observable difference in the accumulation of the cleaved (active) fragment of ATF6 in the nucleus after bortezomib treatment (Figure 3-2). However, there was a significant elevation in the amount of cleaved ATF6 in cell pretreated with rapamycin alone. We are currently unsure of the role this elevation in ATF6 activation may play in rapamycin-induced resistance to bortezomib induced cell death. Phosphorylation of the mTORC1 substrate, S6 kinase (S6K), was completely inhibited by rapamycin in these experiments indicating that drug treatment had effectively blocked mTORC1. The lack of effect of rapamycin pretreatment on bortezomib-induced eIF2α phosphorylation and activated ATF6 suggested that activation of mTORC1 in these cells does not greatly impact the level of unfolded protein to further exacerbate ER stress and PERK phosphorylation of eIF2α when combined with proteasome inhibition.

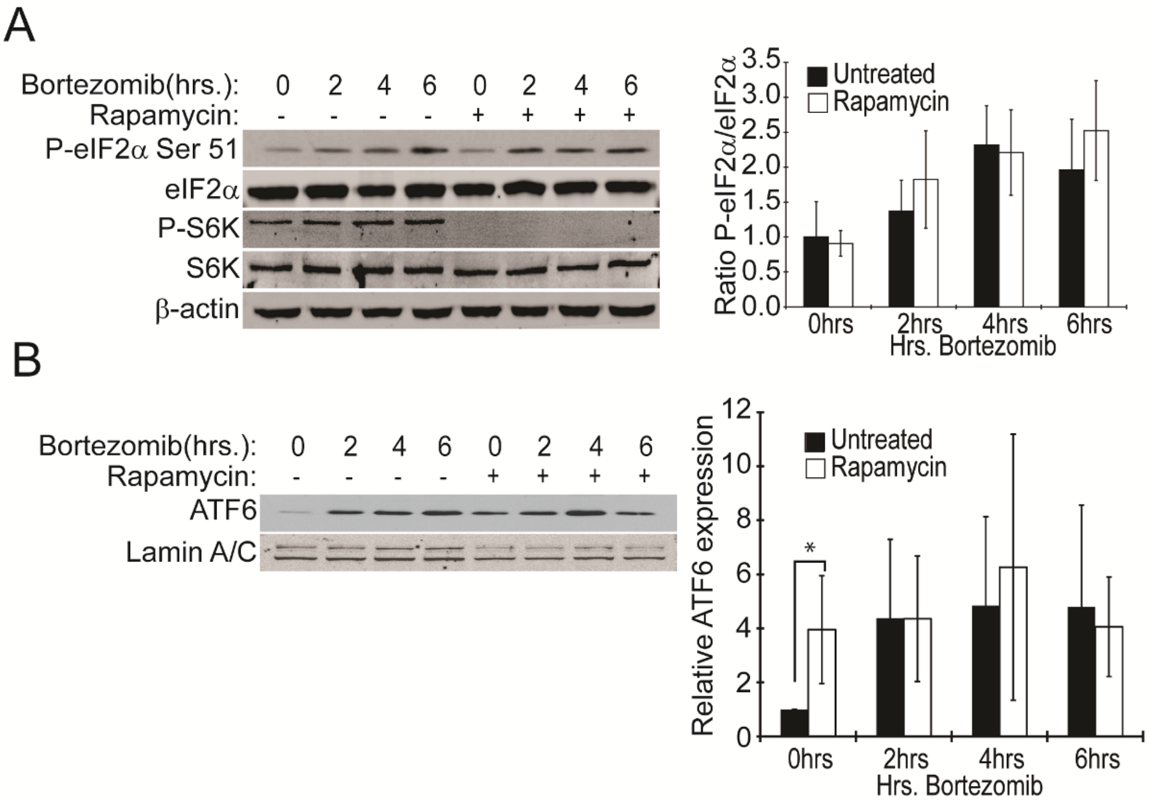

Figure 3-2. Early UPR markers are induced by bortezomib but unaffected by rapamycin in Elt3 cells

Elt3 cells were pretreated with 50nM rapamycin for 24 hours before being exposed to 20nM bortezomib for the amount of time shown in the figure. (A) Whole cell lysates were prepared and probed using the antibodies list above. (B) Nuclear lysates were prepared and probed for the nuclear cleaved fragment of ATF6. ($P<0.05$)

3.4 ATF4 and CHOP protein and mRNA levels are induced by bortezomib in a rapamycin-dependent manner

Coincident with elevated eIF2α phosphorylation, the expression of both ATF4 and CHOP was induced following 4 or 6 hours bortezomib exposure (Figure 3-3b). However, in contrast to eIF2α phosphorylation, rapamycin reduced expression of the ATF4 and CHOP proteins. Further investigation determined that the induction of both *ATF4* and *CHOP* mRNAs by bortezomib was also suppressed by rapamycin pretreatment (Figure 3-3c and d). These data indicate that while proximal events of the UPR are not mTORC1-dependent, the downstream pro-apoptotic signals emanating from the ATF4/CHOP portion of this pathway are inhibited at the level of transcription by rapamycin pretreatment.

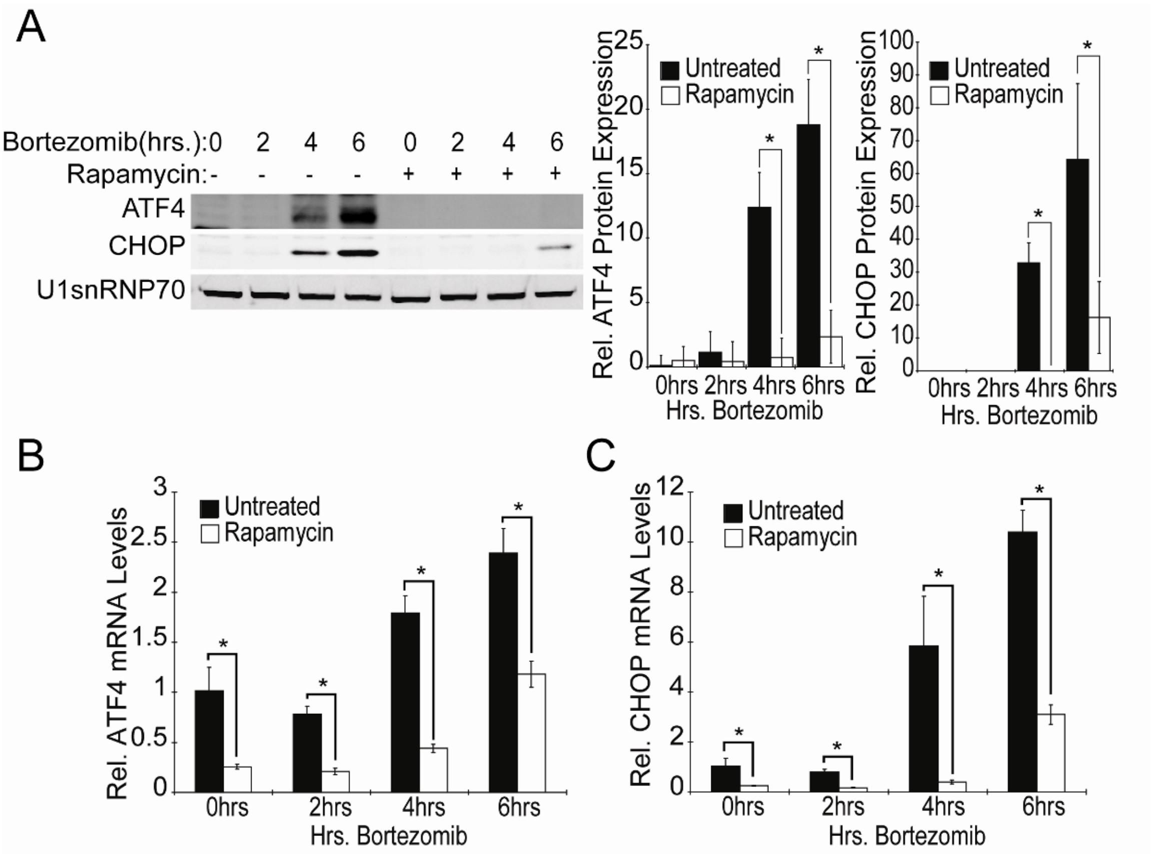

Figure 3-3. Rapamycin prevents induction of downstream UPR markers at the mRNA level

Elt3 cells were pretreated with 50 nM rapamycin or vehicle control for 24 hours before being exposed to 20 nM bortezomib for 2, 4 or 6 hours. (A) Nuclear lysates were prepared from Elt3 cells pretreated with rapamycin, followed by exposure to bortezomib. Equal amounts of the nuclear proteins were then subjected to SDS-PAGE, and ATF4, CHOP and U1snRNP70 were measured by Western blot. Relative levels of ATF4 and CHOP proteins in each treatment group are presented as histograms in the right side of the panel. (B and C) qRT-PCR measurement of ATF4 and CHOP mRNA levels in Elt3 cells pretreated with rapamycin (24 hr) followed by exposure to bortezomib for up to 6 hr, as indicated. (*$P<0.05$)

3.5 Bortezomib-induced expression of ATF4 and CHOP requires new mRNA and protein synthesis

The ability of rapamycin to inhibit ATF4 and CHOP protein expression, combined with the reduced mRNA expression of these genes following drug pretreatment, suggested that rapamycin may deplete cells of a transcription factor that is required for bortezomib to induce *ATF4* and *CHOP* expression. Alternatively, during bortezomib treatment, the increase in *ATF4* and *CHOP* expression may be caused by their inability to be degraded by the proteasome. If rapamycin pretreatment decreased the synthesis of these proteins, it could result in reduced accumulation in the presence of proteasome inhibitor. In order to determine if the increase in ATF4 and CHOP protein levels is the result of stress-induced synthesis (transcription and/or translation), or the result of protein accumulation due to inhibition of the proteasome, we conducted experiments using the RNA polymerase inhibitor actinomycin D and the protein synthesis inhibitor cycloheximide. We found that simultaneously treating Elt3 cells with bortezomib and actinomycin blocked ATF4 and CHOP protein expression (Figure 3-4a). This result suggested that bortezomib requires new mRNA synthesis in order to induce expression of either transcription factor. Cycloheximide similarly suppressed bortezomib-induced accumulation of ATF4 and CHOP proteins, indicating that new protein synthesis is also required and that the observed increase in protein expression is not merely the result of its accumulation due to proteasome inhibition (Figure 3-4c). As a control, we also measured the phosphorylation of eIF2α and cleavage of ATF6 during actinomycin or cycloheximide treatment time courses. Neither actinomycin nor cycloheximide prevented bortezomib from inducing the phosphorylation of eIF2α (Figure 3-4 b and d). We also observe that ATF6 cleavage was somewhat enhanced by actinomycin treatment (Figure 3-4b). Cycloheximide treatment did prevent ATF6 cleavage which is consistent with the report by Teske et al. where it is reported that ATF6 cleavage requires new protein synthesis and is completely inhibited by cycloheximide (Figure 3-4d) (143). These control experiments confirm that our observed block of ATF4 and CHOP expression during actinomycin and cycloheximide treatment is not merely a result of relieving ER stress by decreasing the load on the ER’s protein folding machinery.

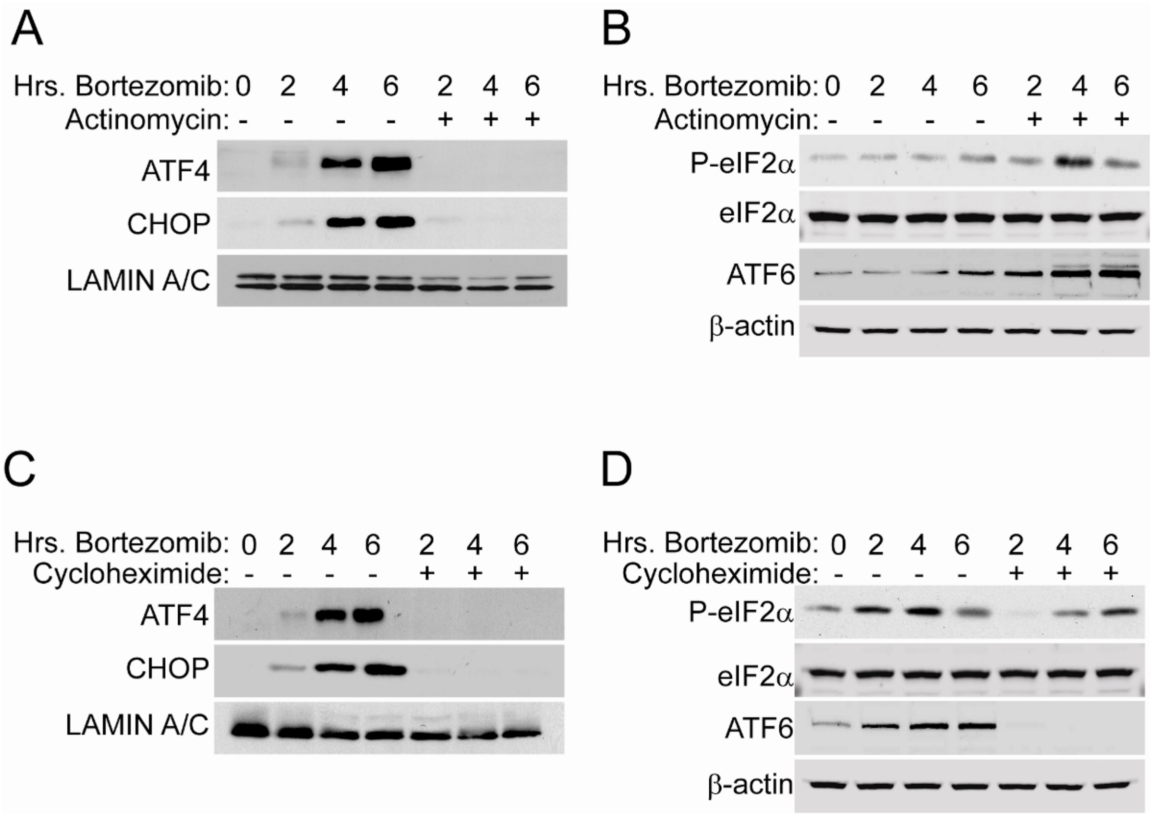
A
Hrs. Bortezomib: 0 2 4 6 2 4 6
Actinomycin: - - - - + + +
ATF4
CHOP
LAMIN A/C
B
Hrs. Bortezomib: 0 2 4 6 2 4 6
Actinomycin: - - - - + + +
P-eIF2α
eIF2α
ATF6
β-actin
C
Hrs. Bortezomib: 0 2 4 6 2 4 6
Cycloheximide: - - - - + + +
ATF4
CHOP
LAMIN A/C
D
Hrs. Bortezomib: 0 2 4 6 2 4 6
Cycloheximide: - - - - + + +
P-eIF2α
eIF2α
ATF6
β-actin

Figure 3-4. Increased levels of ATF4 and CHOP proteins in response to bortezomib treatment require the synthesis of new mRNA and protein

(A) Elt3 cells were treated with 20 nM bortezomib for 2, 4, 6 hours in the presence or absence of 5 μg/mL actinomycin D. ATF4, CHOP and lamin A/C levels in cell lysates were determined by Western blot. (B) Elt3 cells were treated as in part A of this figure. Phosphorylation of eIF2α, total eIF2α, the cleaved fragment of ATF6, and β-actin in cell lysates were determined by western blot.(C) Elt3 cells were treated with 20 nM bortezomib at 2, 4, 6 hours in the presence or absence of 100 μg/mL cycloheximide. Protein levels were measured as in part A of this figure. (D) Elt3 cells were treated as in C of this figure. Protein levels were measured as in part B of this figure.

3.6 c-MYC is upregulated by ER stressing agents at the transcriptional level in Elt3 cells

The above findings indicated that rapamycin inhibits induction of *ATF4* and *CHOP* expression by blocking the synthesis of ATF4 and CHOP mRNA but does not alter upstream PERK activation. This selective targeting of downstream UPR components could be the result of expressing and/or activating a transcription factor(s) in response to elevated mTORC1 signaling, by exposure to bortezomib, or a combination of both stimuli. The oncogenic transcription factor c-MYC is a strong candidate for this link between mTORC1 and bortezomib: c-MYC is translationally upregulated by mTORC1 activation and down-regulated by rapamycin treatment (144, 145). Additionally, c-MYC is a short-lived protein whose expression is increased rapidly during proteasome inhibition, and c-MYC has been shown to contribute to bortezomib-induced death of cultured melanoma cell lines (122, 146, 147). Finally, the *ATF4* gene promoter contains E-box consensus binding sites for basic helix-loop-helix transcription factors such as MYC (Figure 3-7a).

We found that treating Elt3 cells with bortezomib for 2, 4, or 6 hours increased c-MYC protein expression. Consistent with its potential role as mediator of mTORC1-induced *ATF4* and *CHOP* expression, c-MYC induction by bortezomib was dampened by pretreatment with rapamycin (Figure 3-5a). Interestingly, while we additionally observed increased levels of c-MYC transcripts in response to bortezomib treatment, this upregulation was insensitive to rapamycin pretreatment (Figure 3-5b). This is consistent with rapamycin specifically inhibiting only the translation of c-MYC into protein. Two other ER stress-inducing drugs, 2-deoxyglucose and thapsigargin, also increased the expression of both c-MYC mRNA and protein (Figure 3-5c and d). In order to examine the effect of rapamycin on c-MYC activity, we measured mRNA levels of the stress induced c-MYC transcriptional target NOXA. In these studies, we also evaluated the effectiveness of the small molecule, c-MYC inhibitor II, which was originally reported to inhibit c-MYC activity in Rat1a fibroblasts (148). In order to measure c-MYC transcriptional activity, we measured the transcript levels of NOXA which is directly regulated by c-MYC binding to its promoter (122). We found that both rapamycin and the c-MYC inhibitor block the induction of NOXA after bortezomib treatment. Additionally, we show that knockdown of eIF4E, a necessary component for mTORC1 control of translation, reduces c-MYC protein levels in 293T cells (Figure 3-6a). This same eIF4E shRNA also blocked ATF4 induction in 293T cells by bortezomib (Figure 3-6b). These findings collectively suggest that ER stress, caused by bortezomib or other ER stressing-inducing agents, promoted the transcription of c-MYC, resulting in upregulation of c-MYC levels/activity. Rapamycin is able to block the translation of c-MYC under the conditions we studied, thereby inhibiting transcription of the c-MYC target, NOXA.

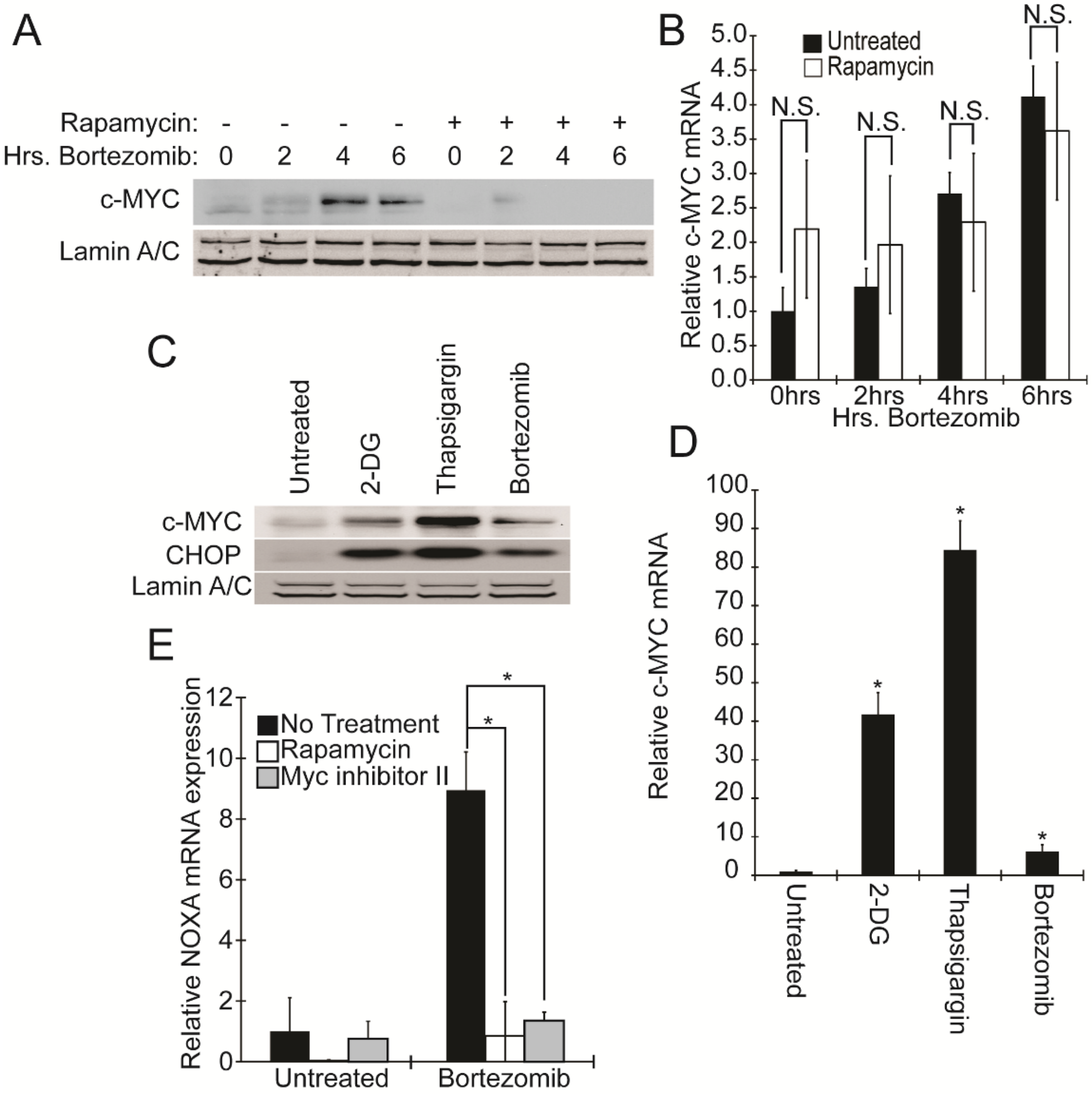

Figure 3-5. Bortezomib and other ER stressors induce expression and activity of c-MYC in a rapamycin-sensitive manner

Elt3 cells were pretreated with 50 nM rapamycin or vehicle control for 24 hours before exposure to 20 nM bortezomib for 2, 4 or 6 hr, as indicated. (A) Lysates were then prepared and the levels of c-MYC and lamin A/C measured by Western blot. (B) c-MYC mRNA levels were measured under the same conditions as part A of this figure. (C-D) 10 mM 2-DG, 1 µM thapsigargin, and 20 nM bortezomib were all used to induce ER stress for 6 hours. c-MYC protein and mRNA levels were measured. (E) Bortezomib treatment induces expression of the c-

MYC transcriptional target NOXA. Rapamycin and Myc inhibitor II blocked induction of NOXA.

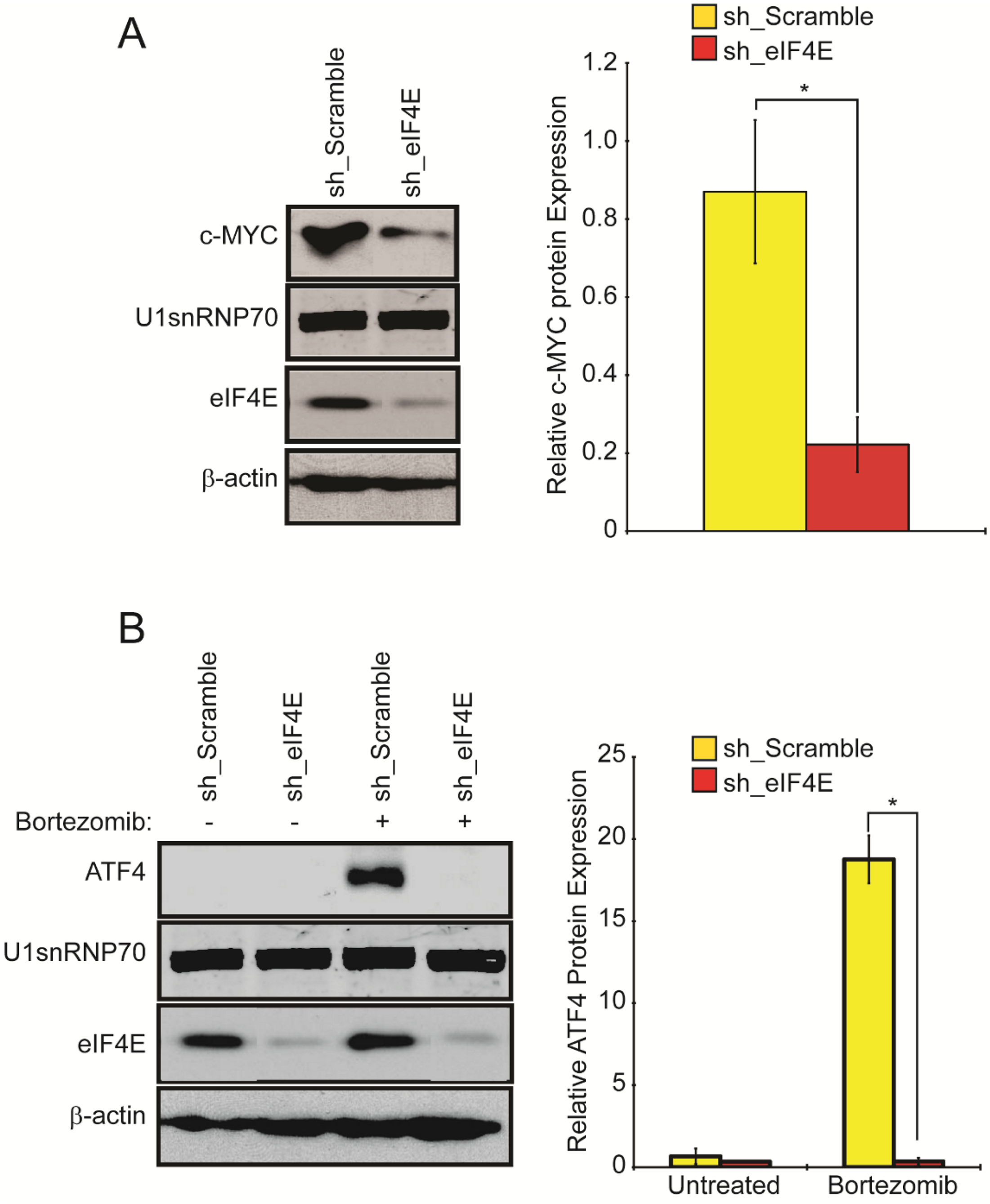

Figure 3-6. eIF4E knockdown reduces c-MYC and ATF4 expression

(A) 293T cells were transduced and selected for expression of either sh_Scramble or sh_eIF4E. Nuclear and cytosolic fractions were then prepared from these cells. Western blots of these lysates show reduced c-MYC expression after eIF4E deletion. (B) 293T cells were prepared as in part A of this figure. These cells were then treated for 4 hours with 20 nM bortezomib.

Nuclear and cytosolic fractions were prepared and probed to detect changes to ATF4 expression resulting from eIF4E knockdown. ($P<0.05$)

3.7 Rapamycin inhibits bortezomib-induced c-MYC expression and binding to the ATF4 gene promoter

To determine if c-MYC plays a direct role in the transcription of ATF4 we performed chromatin immunoprecipitation (ChIP) assays on the ATF4 promoter. ChIP revealed binding of c-MYC to the canonical E-box (CACGTG) at -855 of the *ATF4* promoter following 4 hours of bortezomib treatment (Figure 3-7a). We also found that deleting the E-box at -855 but not the similar sequence at -141 of the ATF4 promoter blocks the induction of luciferase during c-MYC overexpression in 293T cells (Figure 3-7b). It is not clear why loss of the -141 E-box positively impacted gene expression. These results indicate that c-MYC binds the *ATF4* promoter during bortezomib treatment and may play a role in its transcriptional upregulation. Bortezomib treatment also upregulates c-MYC expression in this cell line in a rapamycin-sensitive manner. These findings support the idea that c-MYC is a transcription factor that is induced by mTORC1 and bortezomib that directly activates transcription of the *ATF4* genes during the UPR. Although these studies were done on rat cells which have a different *ATF4* promoter than human cells, there is an E-box found in the *ATF4* promoter in human cells which may be regulated by c-MYC. Further, c-MYC has been shown to drive the expression of *ATF4* in a human cell model (149).

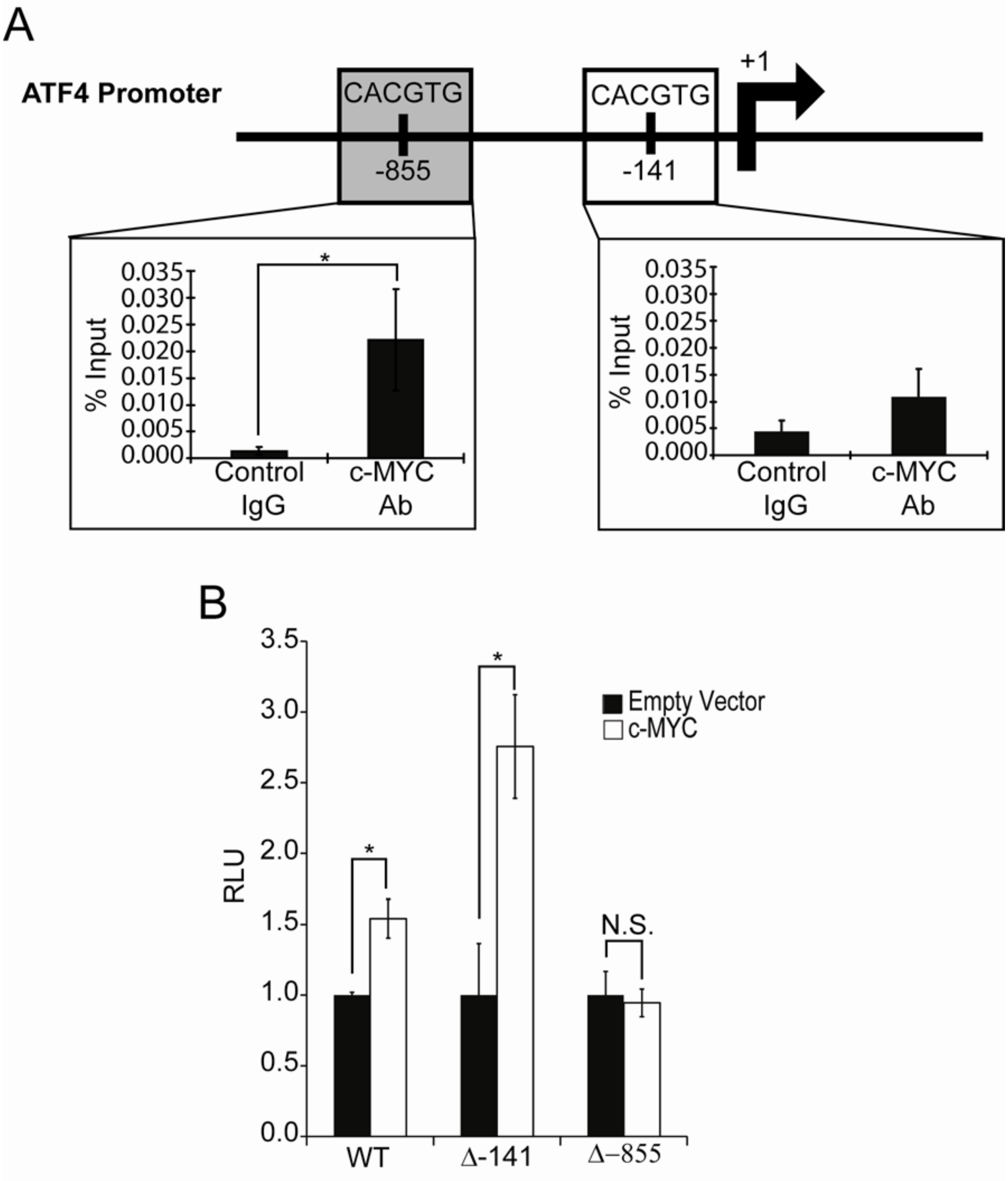

Figure 3-7. c-MYC binds to and stimulates the ATF4 promoter

(A) Elt3 cells were treated with 20 nM bortezomib for 4 hours. The cells were then fixed and analyzed by ChIP for c-MYC binding to the E-boxes at positions -855 and -141 of the rat ATF4 promoter. Graphs represent the mean ± standard deviation of 3 independent ChIP experiments. (B) 2.5kb of the region 5’ of the rat ATF4 gene were cloned upstream of the luciferase gene. The E-boxes located at -141 and -855 were mutated to prevent c-MYC binding and activation of luciferase transcription. These reporters were then transfected into 293T cells with empty vector or c-MYC. ($P<0.05$)

3.8 c-MYC overexpression rescues rapamycin-mediated suppression of bortezomib-induced ATF4 and CHOP expression

Taken together, the above results suggest that rapamycin prevents the induction of ATF4 and CHOP, and the accompanying apoptosis, in response to bortezomib treatment by decreasing the expression levels of c-MYC. This decrease in c-MYC expression would reduce its binding to the *ATF4* gene promoter, thus lowering its transcription. Consequently rapamycin protects the cell from bortezomib-induced apoptosis due to a reduction in the expression of each of these transcription factors. To test this model, we used a lentiviral expression system to restore the c-MYC protein expression that had been lost as a resulted of rapamycin treatment. We also used Myc inhibitor II to block c-MYC activity to demonstrate the requirement for c-MYC activity in the bortezomib induction of ATF4 and CHOP.

Elt3 cells were transduced with lentiviruses carrying either empty vector or c-MYC sequences. Cells transduced with empty vector showed a similar lowering of bortezomib-induced c-MYC, ATF4 and CHOP expression upon rapamycin pretreatment (Figure 3-8a, compare lanes 3 and 4) as had been observed in uninfected cells in previous experiments. Meanwhile, c-MYC transduced cells showed high c-MYC expression basally, after 6 hours of bortezomib treatment, and even following pretreatment with rapamycin (Figure 3-8a, lanes 5-8) Additionally, cells expressing exogenous c-MYC showed induction of ATF4 and CHOP when treated with bortezomib alone or following rapamycin pretreatment (Figure 3-8a, lanes 7 and 8). We also show that blocking c-MYC activity using Myc inhibitor II blocks the induction of ATF4 and CHOP protein by bortezomib (Figure 3-8b). c-MYC overexpression did not induce eIF2α phosphorylation or enhance eIF2α phosphorylation after bortezomib treatment (Figure 3-8c). Similarly, shRNA knock down of c-MYC in 293T cells is able to block induction of ATF4 by bortezomib treatment without blocking induction of eIF2α phosphorylation (Figure 3-9). This result suggests that c-MYC is not causing stress or enhancing the stress caused by bortezomib. These results as a whole suggest that the ability of rapamycin to suppress *ATF4* and *CHOP* expression is dependent on its downregulation of c-MYC. These findings also support the notion that c-MYC plays a central role in the induction of the *ATF4* and *CHOP* mRNAs during bortezomib treatment.

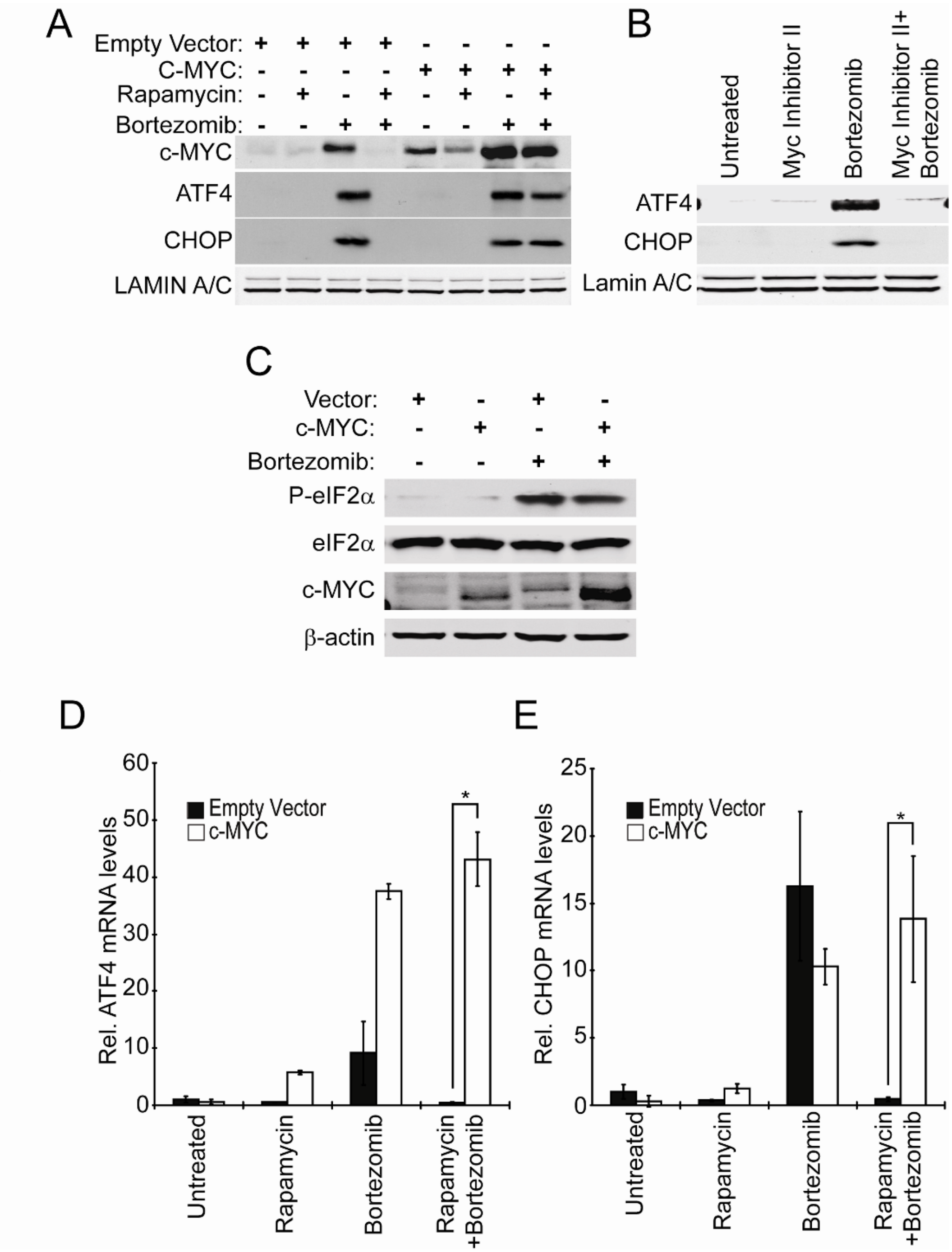

Figure 3-8. Overexpression of c-MYC rescued bortezomib-induced ATF4 and CHOP expression following pretreatment with rapamycin

A lentivirus was used to stably express c-MYC in Elt3 cells. (A) Vector and c-MYC expressing cells were then pretreated with vehicle control or 50 nM rapamycin (24 hr) prior to treatment with bortezomib for 6 hours. (A) Nuclear lysates were prepared and levels of ATF4, CHOP, and Lamin A/C were measured by Western blot. (B) Elt3 cells were pretreated with Myc inhibitor II 2 hours before being treated with bortezomib for 6 hours. Western blots were executed as in part A of this figure (C) ELT3 cells overexpressing c-MYC were treated with bortezomib for 6 hours. Whole cell lysates were probed for the phosphorylation of eIF2α , total eIF2α, c-MYC, and β-actin. (D-E) Under the same conditions, ATF4 and CHOP mRNAs were measured by qRT-PCR. ($^*P<0.05$)

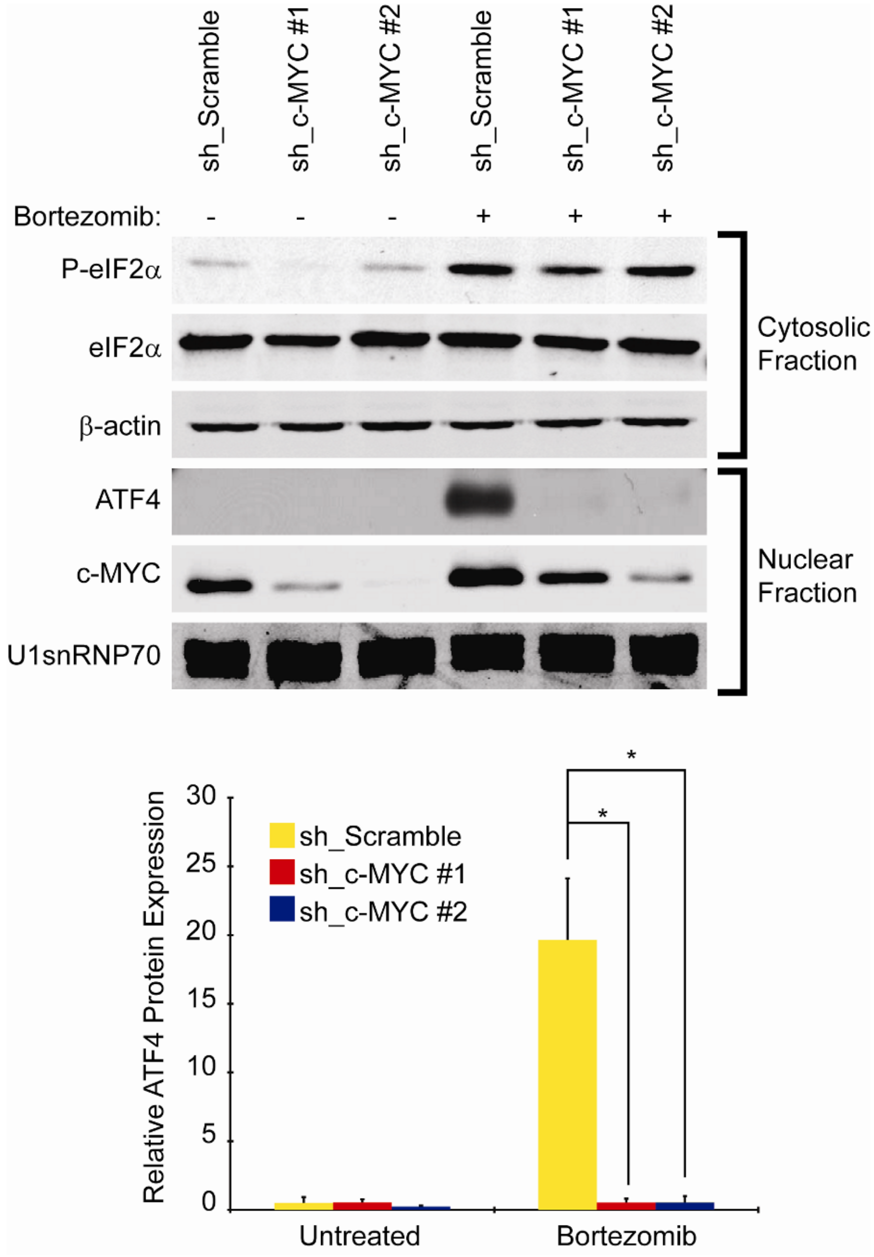

Figure 3-9. c-MYC knockdown blocks bortezomib-induced induction of ATF4

293T cells were puromycin selected to express sh_Scramble, sh_c-MYC #1, or sh_c-MYC #2. Cells were then replated and treated with 20nM bortezomib for 4 hours. Lysates were fractionated to better visualize ATF4 and c-MYC. Western blots were performed for phosphorylated eIF2α, total eIF2α, β-actin, ATF4, c-MYC, and U1snRNP70. (*P<0.05)

3.9 c-MYC overexpression rescues rapamycin-mediated suppression of bortezomib-induced Elt3 cell apoptosis

Next we used the lentiviral c-MYC overexpression system to test if c-MYC rescue of *ATF4* and *CHOP* expression in the presence of rapamycin is sufficient to restore bortezomib-induced apoptosis. Elt3 cells transduced with empty vector virus showed caspase-3 cleavage after 24 hours of exposure to bortezomib that was dramatically reduced by rapamycin pretreatment (Figure 3-10a), similarly to that reported in figure 3-1. Importantly, cells transduced with c-MYC-expressing virus showed caspase-3 cleavage after 24 hours of bortezomib treatment with or without rapamycin pretreatment, indicating that restoring c-MYC expression is sufficient to restore bortezomib induced apoptosis (Figure 3-10a). A similar outcome was seen on cell viability as measured by trypan blue staining: Cells transduced with only empty vector showed a 57% decrease in cell viability after bortezomib treatment that was significantly inhibited by rapamycin pretreatment (Figure 3-10b). By comparison, c-MYC transduced cells showed a similar decrease in cell viability that could not be rescued by pretreating cells with the mTORC1 inhibitor (Figure 3-10b). This decrease in cell viability was also readily apparent by microscopy where c-MYC overexpressing cells showed a rounded non-adherent morphology after bortezomib treatment, with or without rapamycin (Figure 3-10c). In contrast, the vector transduced cells remained flat and adherent when pretreated with rapamycin prior to exposure to bortezomib.

As anticipated, blocking the activity of c-MYC using c-MYC inhibitor II resulted in reduced ATF4 and CHOP expression after bortezomib treatment. Caspase-3 activation was also reduced following 24 hours of bortezomib treatment for those cells treated with the c-MYC inhibitor II (Figure 3-10d). These results indicate that in this cell line c-MYC expression contributes to cell death and induction of ATF4 and CHOP during bortezomib treatment.

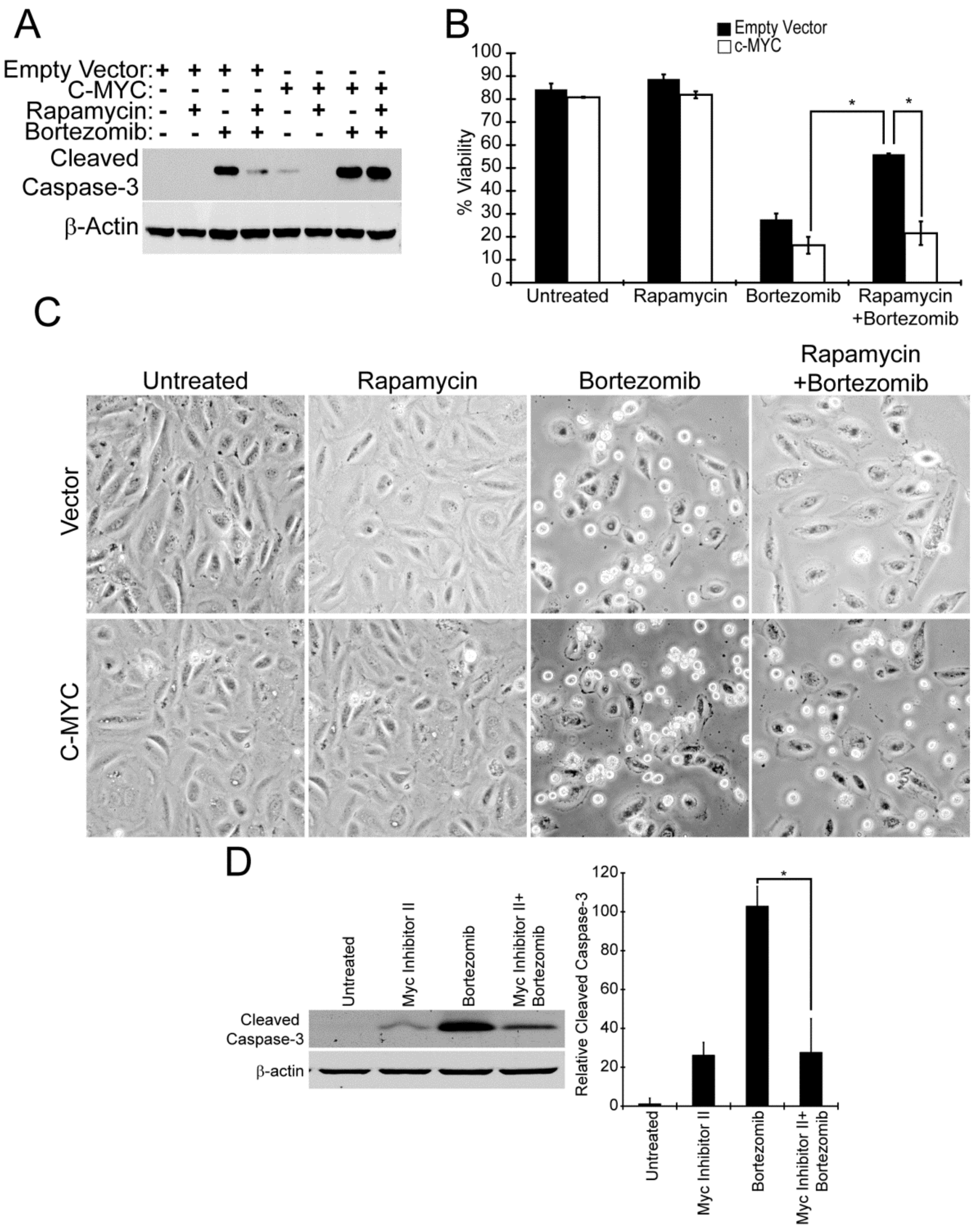

Figure 3-10. Overexpression of c-MYC restores bortezomib-induced apoptosis

Elt3 cells over-expressing c-MYC, or containing empty vector were subjected to 24 hr treatment with 20 nM bortezomib with or without an additional 24 hr rapamycin pretreatment. (A) Cleaved caspase-3 and β-actin were detected in cell lysates by Western blotting. The levels of cleaved caspase-3 are shown in a histogram to the right of this panel. (B) Trypan blue staining was carried out to measure the survival of Elt3 ells overexpressing c-MYC versus cells containing the empty lentivirus vector alone, upon exposure to bortezomib. (C) Photographs of the two cell lines after 24 hours of bortezomib exposure in the presence or absence of rapamycin pretreatment. (D) Elt3 cells were pretreated with Myc Inhibitor II 2 hours prior to being treated with bortezomib for 24 hours. Cleaved caspase-3 and β-actin were detected in cell lysates by Western blotting. Levels of cleavage caspase-3 are shown in the histogram to the right of these western blots.

3.10 Discussion

This study demonstrates the feasibility of using a clinically approved drug to induce the death of cells that have elevated mTORC1 activity due to the loss of TSC2. It also demonstrates, for the first time, that mTORC1 can regulate the UPR at the level of ATF4 and CHOP transcription factors by promoting increased transcription of these genes. This is achieved, at least in part, by the translation of c-MYC that regulates the transcription of ATF4 as shown in figure 3-11. In concert with bortezomib treatment, which elevates ER stress and induces the expression of c-MYC, high mTOR activity contributes to cell death in a manner that can be prevented by rapamycin pretreatment. These data not only suggest a means of eradicating cells exhibiting high mTOR activity but may also help explain why myeloma cells with elevated c-MYC levels are more sensitive to bortezomib/Velcade.

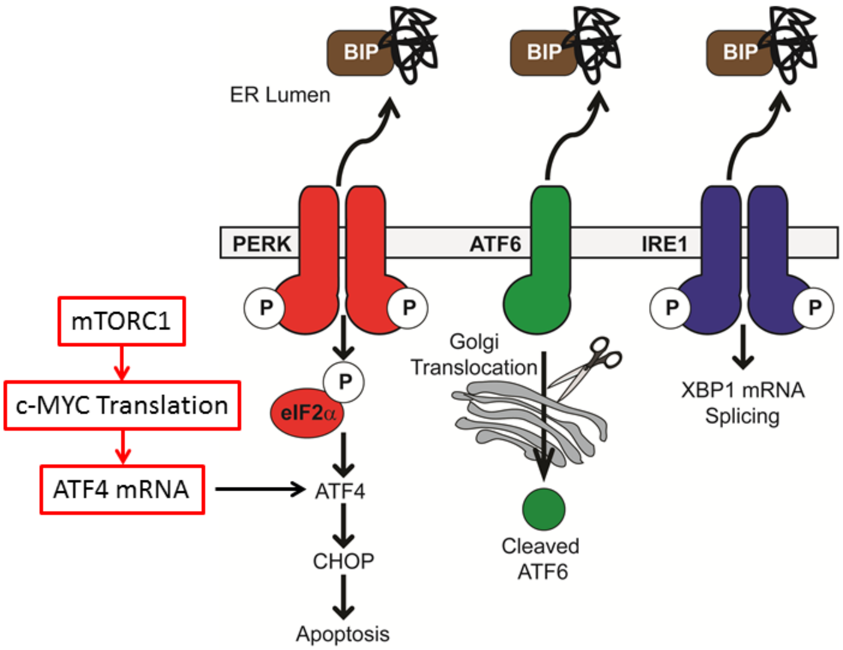
BIP
BIP
BIP
ER Lumen
PERK
ATF6
IRE1
P
P
P
P
mTORC1
c-MYC Translation
ATF4 mRNA
P
eIF2α
ATF4
CHOP
Apoptosis
Golgi
Translocation
Cleaved
ATF6
XBP1 mRNA
Splicing

Figure 3-11. mTORC1/c-MYC play a role in inducing the ER stress response

Our study was able to make these contributions to our understanding of how mTORC1 affects the UPR thanks to a key difference in the Elt3 cell line compared to the MEF cells used in previous studies. The key difference between these cell lines that allowed this advance was the fact that Elt3 cells treated with bortezomib and rapamycin shown no statically significant difference in the phosphorylation of eIF2α compared to cells treated with bortezomib alone; however, this same rapamycin treatment blocked the induction of the downstream ATF4 and CHOP transcription factors. This key difference allowed us to focus on possible direct effects of mTORC1 on signaling processes downstream of eIF2α phosphorylation which led us to explore possible contributions from the mTORC1 translational target c-MYC. While our results demonstrate direct control of ATF4 expression by mTORC1, the effect of mTORC1 driven protein synthesis may play a major role in causing ER stress in some situations and may be the prevailing effect in other cell lines.

Three previous studies have reported increased ER stress-induced apoptosis following the knockout of TSC1 or 2 (102, 111, 130). Two of these studies by the laboratories of Hotamisligil and Sahin show that rapamycin reduces this ER stress induced apoptosis; whereas, the study by Guan lab shows no effect of rapamycin on ER stress induced apoptosis. Our current study not only confirms aspects of the Hotamisligil observations but contributes additional mechanistic insight into how mTORC1 contributes to ER stress and cell death. The two studies using MEFs reported increased PERK and eIF2α phosphorylation upon TSC1 or 2 loss while a third study of TSC-null rodent neurons focused on the induction of CHOP expression and did not measure eIF2a phosphorylation (102, 111, 130). Since eIF2α phosphorylation was not affected by rapamycin treatment in the current study prior to the addition of bortezomib, it allowed us to unmask layers of UPR regulation by mTORC1 distal to eIF2α phosphorylation. At this time we have not established why the Elt3 cells have an attenuated response compared to MEFs. However, this is likely related to other genetic differences between cell lines. For example, Elt3 cells retain wild type p53 whereas the TSC-null MEFs required deletion of p53 for survival or may have lower basal MYC expression (19). It should also be pointed out that the two MEF studies also conflict both in whether TSC loss impacts downstream ATF4 and CHOP activation (102, 130). Thus there are likely to be mechanistic differences based on both cell type and metabolic state.

Our studies findings are also similar to other studies which have found that specific stresses result in a truncated response to eIF2α phosphorylation where ATF4 and CHOP are not expressed. It has been observed that treatment of macrophages with lipopolysaccharide (LPS) or MEF cells with ultra violet (UV) light stimulate the phosphorylation of eIF2α without the induction of ATF4 and CHOP (140, 150). Additionally, it was shown that stimulation of eIF2α phosphorylation without inducing ATF4 or CHOP expression was a protective mechanism against UV induced cell death (140). This mechanism is consistent with our data which shows that rapamycin protects Elt3 cells from apoptosis by blocking ATF4 and CHOP expression but does not affect the phosphorylation of eIF2α.

Our studies also confirm previous reports concerning c-MYC and the unfolded protein response. Cavener lab shows that c-MYC is induced by the ER stressing agents thapsigargin and DTT in MEFs at the mRNA level (151). Our data shows that c-MYC is induced by thapsigargin, 2-DG, and bortezomib at the mRNA in our rat model. Wei and Ren laboratories show that c-MYC binds to the human ATF4 gene in ChIP on ChIP experiments (152, 153). Similarly, we find that c-MYC binds to and simulates the rat ATF4 promoter at the -855 position. Despite the poor conservation of the 5’ promoter region from rats to mice to humans, all three species have at least two c-MYC binding sites either in the promoter region or first exon. This data suggest that c-MYC plays a role in controlling ATF4 expression which likely is conserved. Other labs have also found that c-MYC combines with bortezomib to induce cell death. The Soengas and Lightcap labs have shown that c-MYC enhances bortezomib induced cell death in melanoma and colon cancer, respectively (122, 146).

In terms of clinical implications, our studies may partially contribute to our understanding of why multiple myeloma is sensitive to bortezomib. Multiple myeloma responds well to bortezomib treatment for two reasons both of which relate to c-MYC and the UPR. Multiple myeloma is a B cell cancer and B cells secrete their own weight in antibodies every day. This massive amount of secretion puts stress on these cells endoplasmic reticulum and may sensitize them to ER stress induced cell death by bortezomib. Synergizing with this effect, these cells typically have high levels of c-MYC expression which has been shown to control total ER content, protein synthesis, and aggregate formation in these cells (147). Knocking down c-MYC has been shown to protect multiple myeloma cells from bortezomib induced cell death similar to our observation that the Myc inhibitor II prevents apoptosis (147). Our studies may link these two aspects of bortezomib-sensitivity in multiple myeloma, because we show that the UPR directly involves c-MYC when it induces cell death. Additionally, c-MYC and ATF4 have been shown to control the expression of the proapoptotic gene NOXA which may also be involved in bortezomib induced cell death in Elt3 cells (154).

CHAPTER 4. PROTEASOME INHIBITION-INDUCED ER VACUOLATION REQUIRES mTORC1 ACTIVATION

4.1 Introduction

Autophagy gives a cell the ability to adapt to changes in environment and maintain homeostasis through the destruction of unwanted or damaged proteins and organelles. In order to respond appropriately to specific types of nutrient and environmental stress, organelle specific forms of autophagy have evolved. These forms of autophagy specifically target mitochondria (mitophagy), peroxisomes (pexophagy), ribosomes (ribophagy), and endoplasmic reticulum (reticulophagy) for degradation. For example when a cell switches from a fatty-acid nutrient source to other food sources, peroxisomes are no longer needed and cells will undergo pexophagy (155). Similarly, mitophagy is induced when cells are exposed to starvation conditions and no longer need excess mitochondria (156). The focus of this chapter will be autophagic degradation of the endoplasmic reticulum or reticulophagy and its regulation by the mammalian target of rapamycin complex-1 (mTORC1) pathway and the unfolded protein response (UPR).

mTORC1 is a master suppressor of the initiation phase of autophagy. When amino acids and other nutrients are abundant, Rag and Rheb small GTPases bind to and activate mTORC1 by localizing it to specific perinuclear endosomes (43, 44). Active mTORC1 phosphorylates and inhibits unc-51-like kinase 1 (ULK1) which participates in a complex with mammalian Atg13 and focal adhesion kinase interacting protein of 200 kD (FIP200) (60-62). In the absence of these nutrients, mTORC1 becomes delocalized and inactive. This allows ULK1-mATG13-FIP200 complex to autophosphorylate and promote the downstream initiation of autophagy (60-62). mTORC1 inhibition and induction of autophagy can also be achieved by treatment with the mTORC1-specific inhibitor rapamycin. Autophagy will then progress though four additional phases: elongation, closure, maturation, and degradation. During these stages the autophagic target is enclosed within a double membrane vacuole which is subsequently fused to lysosomes, acidified, and degraded (157).

In addition to mTORC1 inhibition, autophagy can be induced by damage to the cell caused by various toxins. Our research and that of others has shown that chemicals which disrupt the protein folding processes of the ER are strong promoters of autophagy (158-160). These chemicals, such as tunicamycin, thapsigargin, and dithiothreitol (DTT), cause proteins which are folding in the ER to misfold by altering the environment within the ER or by inhibiting chaperones that promote proper protein folding. These unfolded proteins accumulate within the ER and ultimately activate the UPR which consists of three branches: inositol-requiring enzyme-1 (IRE-1), activating transcription factor-6 (ATF6), and protein kinase-like ER kinase (PERK) (132, 133). These three branches help the cell adapt to the unfolded protein stress by promoting the synthesis of ER membrane, protein folding machinery, and arresting global protein synthesis. The UPR does this primarily by activation of PERK as activation of the other UPR branches rely on PERK for their downstream signaling. PERK is responsible for the phosphorylation of eIF2α and subsequent arresting of global protein synthesis (85, 132). During this global arrest of protein synthesis, stress responsive mRNAs with complex signaling sequences in their 5'-untranslated regions (5'-UTR) are translated more efficiently. Two of these mRNAs code for the transcription factors ATF4 and CHOP (139, 161). These transcription factors will promote the return to homeostasis; however, their prolonged activation will cause the cell to undergo cell death through apoptosis or other forms of cells death.

The ER-associated decay (ERAD) pathway is another pathway involved in the clearance of misfolded proteins from the ER and is essential for both ER and cellular homeostasis. When the UPR is activated the ERAD pathway is also activated and disulfide bonds and sugar moieties are removed from unfolded proteins destined for degradation. These proteins are then ubiquitinated and translocated from the ER for either proteasomal or autophagic degradation (133). Chemicals that inhibit the proteasome, such as MG-132 and bortezomib, inhibit the proteasomal degradation arm of the ERAD pathway and may place an extra burden on autophagic degradation to clear misfolded proteins. Treatment with either of these inhibitors results in an accumulation of unfolded proteins within the ER, activation of the UPR, and ultimately cell death. Proteasome inhibitors are currently being explored as a chemotherapeutic tools because of their ability to induce cell death via the UPR (162). These inhibitors may be useful in the treatment of diseases such as tuberous sclerosis complex (TSC) and lymphangioleiomyomatosis (LAM) where the activity of the TSC2 tumor suppressor is lost. TSC1 and 2-null cells have high mTORC1 activity, high protein synthesis rates, and reduced levels of autophagy (3). These cells have also been shown to be more sensitive to ER stressing drugs than their wild-type counter parts (102, 111, 130). These traits of TSC1 and 2-null cells may make them an ideal candidate for treatment with inhibitors that target the proteasome.

In this chapter, we show that treating the TSC2-null 621-101 cell line with proteasome inhibitors induces the UPR and the mTORC1 inhibitor rapamycin is able to suppress this activation of the UPR. Rapamycin pretreatment increased levels of LC3 cleavage and decreased p62 levels compared to untreated cells indicating higher levels of autophagy in rapamycin treated cells. Additionally, the cytoplasm of the non-rapamycin treated cells is filled with MG-132 induced vesicles derived from the ER that do not appear in rapamycin pretreated cells. Using a novel imaging technique, we demonstrate that these vesicles may represent a failure of mature ER derived vesicles to become acidified autolysosomes. However, acidified autolysomes derived from the ER could be detected in the rapamycin cells during proteasome inhibition.

4.2 MG-132 induces vacuolation and cell death in a rapamycin-sensitive manner

eIF2α is phosphorylated in response to the accumulation of unfolded protein within the ER. This phosphorylation also controls the arrest in global protein synthesis and directs the transcription and translation of downstream UPR targets that include ATF4 and CHOP. We began our study by determining if rapamycin reduced activation of the UPR in 621-101 cells. Cells were treated with 50 nM rapamycin for 48 hours in serum-free media. We found that these treatments significantly reduced the basal levels of eIF2α phosphorylation as shown in figure 4-1a. Messenger RNA levels of ATF4 and CHOP as well as the ATF4 transcriptional targets LC3B and asparagine synthase (ASNS) were also reduced by the rapamycin treatments after 48 hours of rapamycin treatment (Figure 4-1b). Both of these transcription factors have been shown to promote cell death during the UPR. The higher levels of ATF4 and CHOP in the cells that were not pretreated with rapamycin correlated with increased cell death after 24 hours of MG-132 treatment according to trypan blue staining (Figure 4-2a). Strikingly, these cells also showed massive vacuolation within their cytoplasm which was not seen in the rapamycin pretreated cells (Figure 4-2b, upper and lower right).

In order to determine if these vacuoles were derived from the ER, we used an mCherry red fluorescent protein probe which is targeted to and retained within the ER through a 5’-amino terminal ER targeting signal from the ER-resident chaperone calreticulin and a 3’-carboxyl terminal-KDEL peptide sequence, which facilitates ER retention. In untreated cells or rapamycin treated cells, this probe labeled the ER, which appears as a smooth reticulated perinulear signal. Cells treated with MG-132 without rapamycin were found to contain the mCherry label within the cytoplasmic vacuoles. MG-132 and rapamycin co-treated cells appeared to have normal ER structures (Figure 4-3).

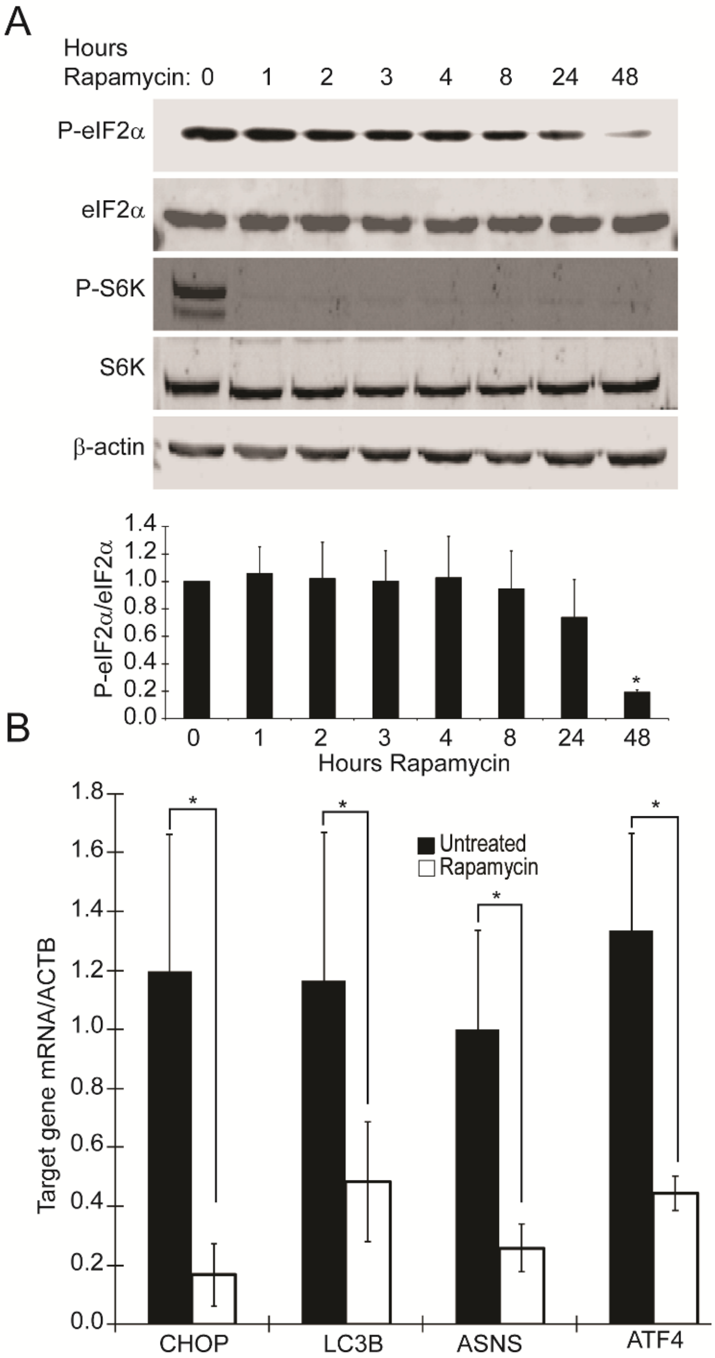

Figure 4-1. Rapamycin decreases ER stress markers

(A) 621-101 cells were treated with 50 nM rapamycin for different time points over 48 hours in serum-free DMEM. eIF2α phosphorylation was measured by western blot and quantified. This ER stress readout decresased over time after rapamycin treatment. (B) CHOP, LC3B, ASNS, and ATF4 mRNA levels were measured after 48 hours of rapamycin treatment. Rapamycin decreased all four stress readouts. (*P<0.05)

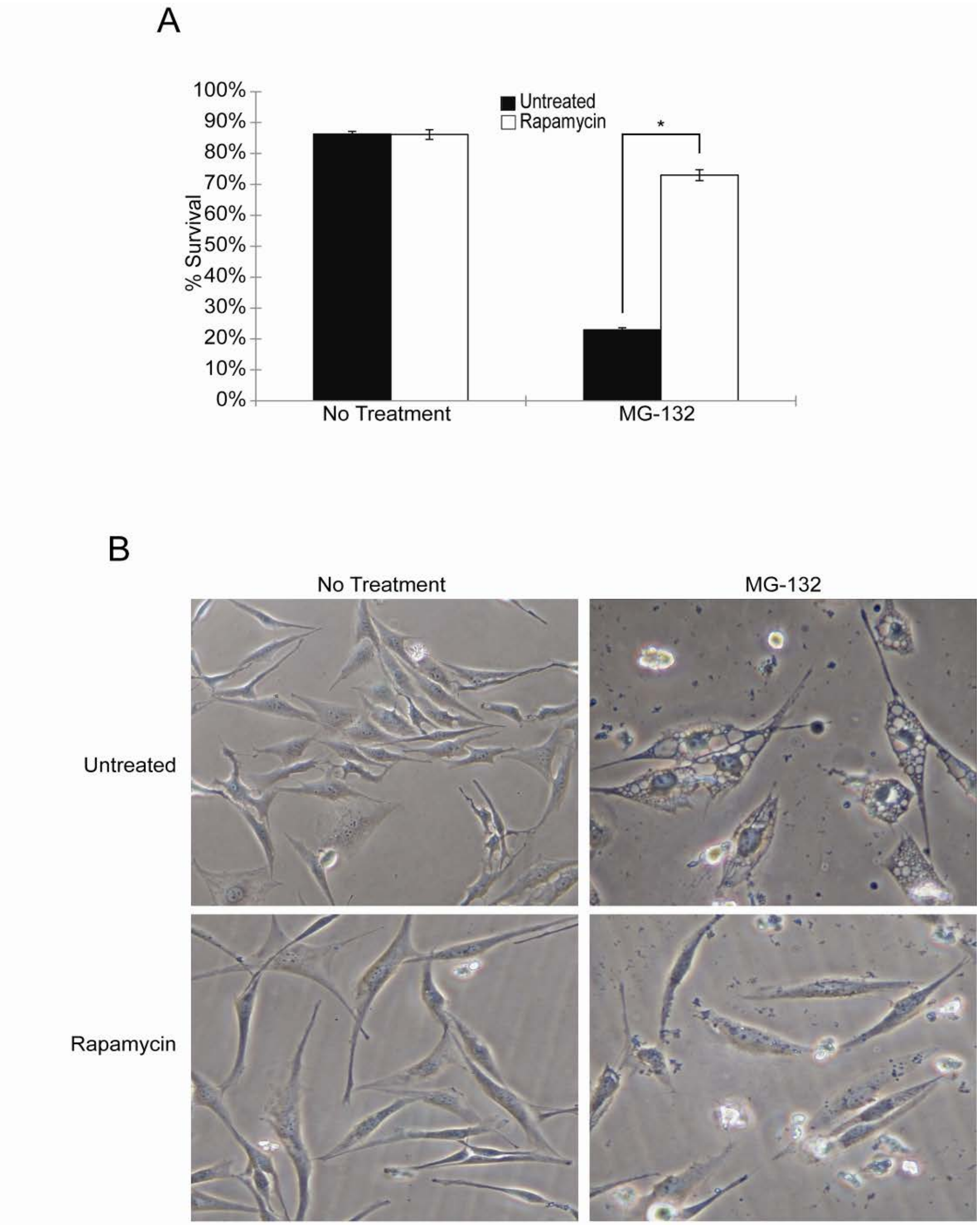

Figure 4-2. Rapamycin treatment prevents vacuolation and cell death induced by MG-132

A) 621-101 cells were treated with rapamycin 24 hours prior to being stressed with MG-132 from 24 hours. Cells treated only with MG-132 show decreased viability; however, rapamycin prevented this decrease in viability. B) Rapamycin also prevented the vacuolation observed after MG-132 treatment. (*$P<0.05$)

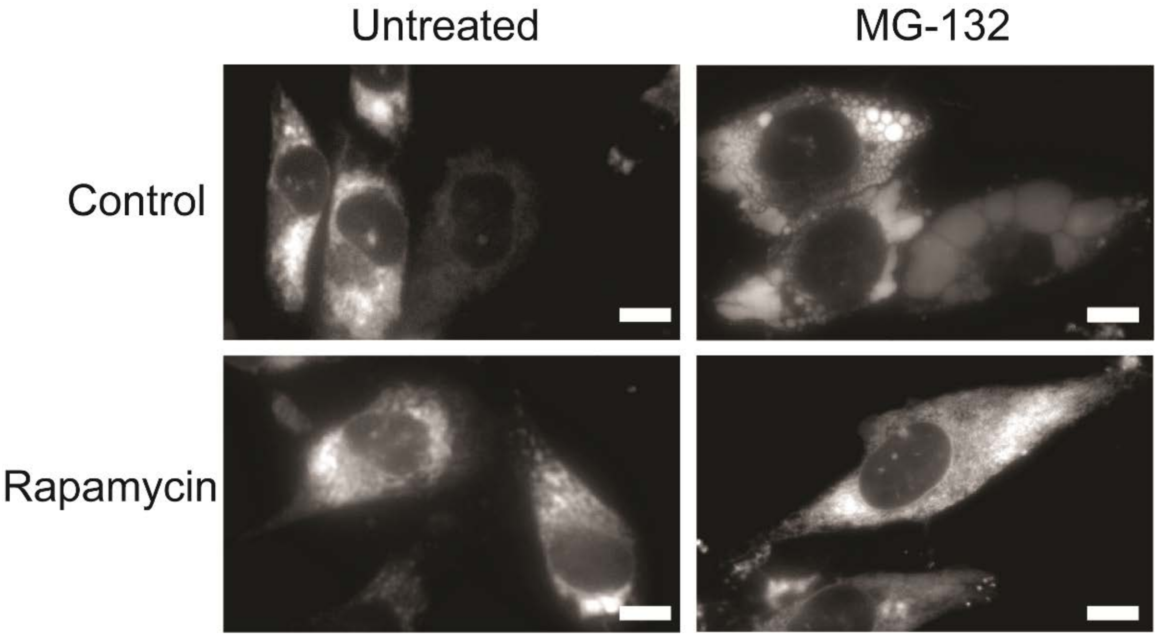

Figure 4-3. Vacuoles induced by proteasome inhibition contain ER

The ER of 621-101 cells was labeled using mCherry targeted to the ER. We found that when vacuoles form during MG-132 treatment they contain the ER label (upper right panel). These results suggest that these membrane structures are derived from the ER. Cells pretreated with rapamycin have normal ER morphology (lower right panel).

4.3 Cell death and vacuolation is not associated with caspase-dependent apoptosis

Cell death through the formation of cytoplasmic vacuoles is commonly associated with non-apoptotic forms of cell death, such as autophagy. However, it has been reported that loss of TSC2, as is the case for 621-101 cells, reduced autophagy due to mTORC1 repression of the ULK1-mATG13-FIP200 complex (Figure 1-3). Additionally, these vacuoles appear to have an endoplasmic reticulum origin rather than an endosomal/lysosomal origin and are very large (~3-10 µm) compared to a typical autophagosome (~0.2-0.5 µm) (Measurements are based on size bars on florescent images in figure 4-3 which represent 10 µm).

In order to determine what role, if any, caspase-dependent apoptosis plays in the formation of the cytoplasmic vacuoles or the cell death observed after MG-132 treatment, we blocked this protease activity using the pan-caspase inhibitor, Z-VAD-FMK. Cells were co-treated with MG-132 with or without 50 µM Z-VAD-FMK for 12 hours at which time cell were assayed for viability using trypan blue staining. Caspase inhibitor treatment failed to enhance cell survival (Figure 4-4a). Additionally, cells co-treated with MG-132 and Z-VAD-FMK showed a similar amount of vacuolation to those treated with MG-132 alone (Figure 4-4b).

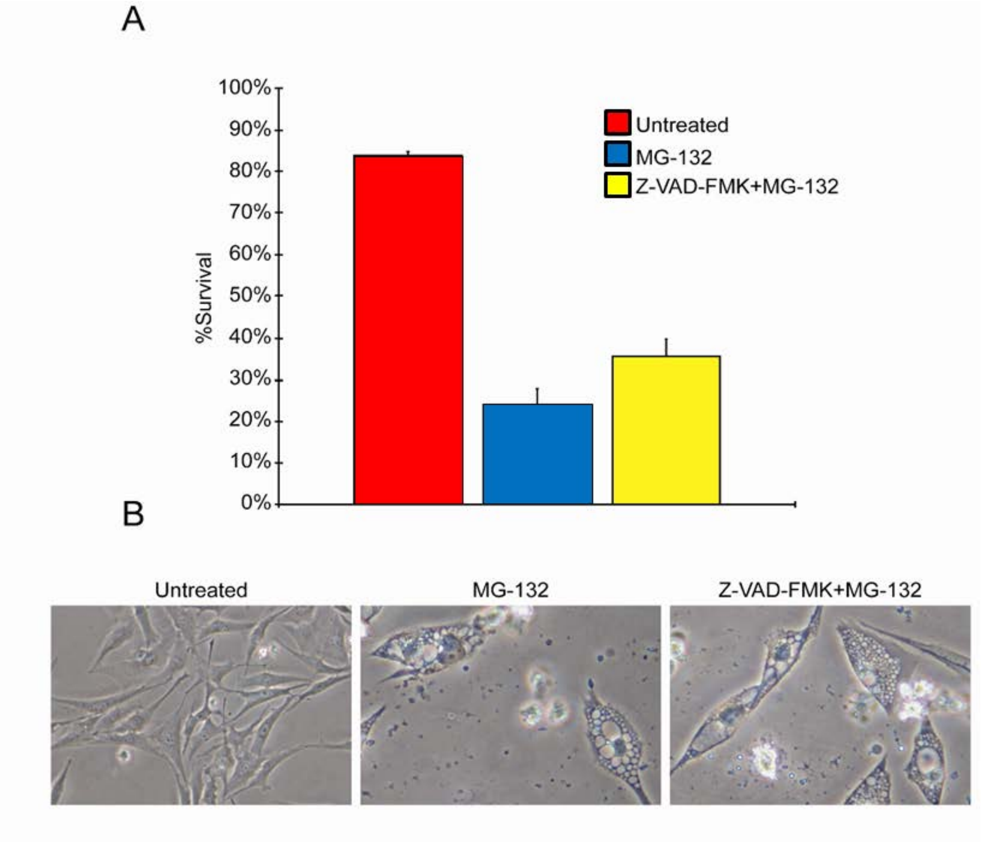

Figure 4-4. Caspase activation is not required for MG-132-induced cell death or ER vacuolation

621-101 cells were pretreated with 50μM Z-VAD-FMK 2 hours before being stressed with MG-132 for 24 hours. (A) Trypan blue staining shows a decreased viability of cells treated with MG-132. Cells pretreated with Z-VAD-FMK showed a similar amount of cell death. (B) Cells pretreated with Z-VAD-FMK showed ER vacuolation similar to that seen in cells treated only with MG-132.

4.4 Rapamycin pretreatment enhances basal autophagic processes

Having seen no significant contribution to cell death or vacuolation from caspase activation, we next addressed whether autophagic cellular processes may be contributing to the cell death. Autophagy is characterized by the conversion of unprocessed LC3-I to cleaved and lipidated LC3-II which coats autophagic vesicles. These vesicles then form and fuse with lysosomes to degrade the autophagomes' contents. The contents of these vesicles are targeted to the autophagosome by p62 which is itself degraded during the completion of autophagic degradation. These processes have been reported to be inhibited in TSC2-null cell lines, like 621-101, leading to an accumulation of p62 and low levels of processes LC3-II (3).

Both LC3 and p62 marker levels suggested the induction of autophagy by the combination of rapamycin and MG-132. Rapamycin treated cells show much less p62 accumulation at all time-points indicating that rapamycin has allowed the cell to once again process its autophagic cargos. Additionally, this autophagy is enhanced after 2 hours of MG-132 treatment as shown by increased LC3-II cleavage (Figure 4-6b, lane 6).

The maturation of autophagosomes by fusion to lysosomes can be tracked by the visualization of GFP-mCherry dual tagged LC3 as shown in figure 4-5. This technique takes advantage of the acid-labile nature of GFP. At the typical cytosolic pH, ~7.2-7.4, GFP and mCherry are both able to fluoresce, and when both fluoresce proteins are used as a dual tag for LC3 the overlapping image of autophagosomes generated will appear green or yellowish. However inside an autolysosome the pH is very acidic, GFP will become bleached and only the mCherry component of the chimera will fluoresce. Under these acidic conditions, the autolysosme will appear red (163). In this manner, one can view the progression of autophagosome to autolysosomes.

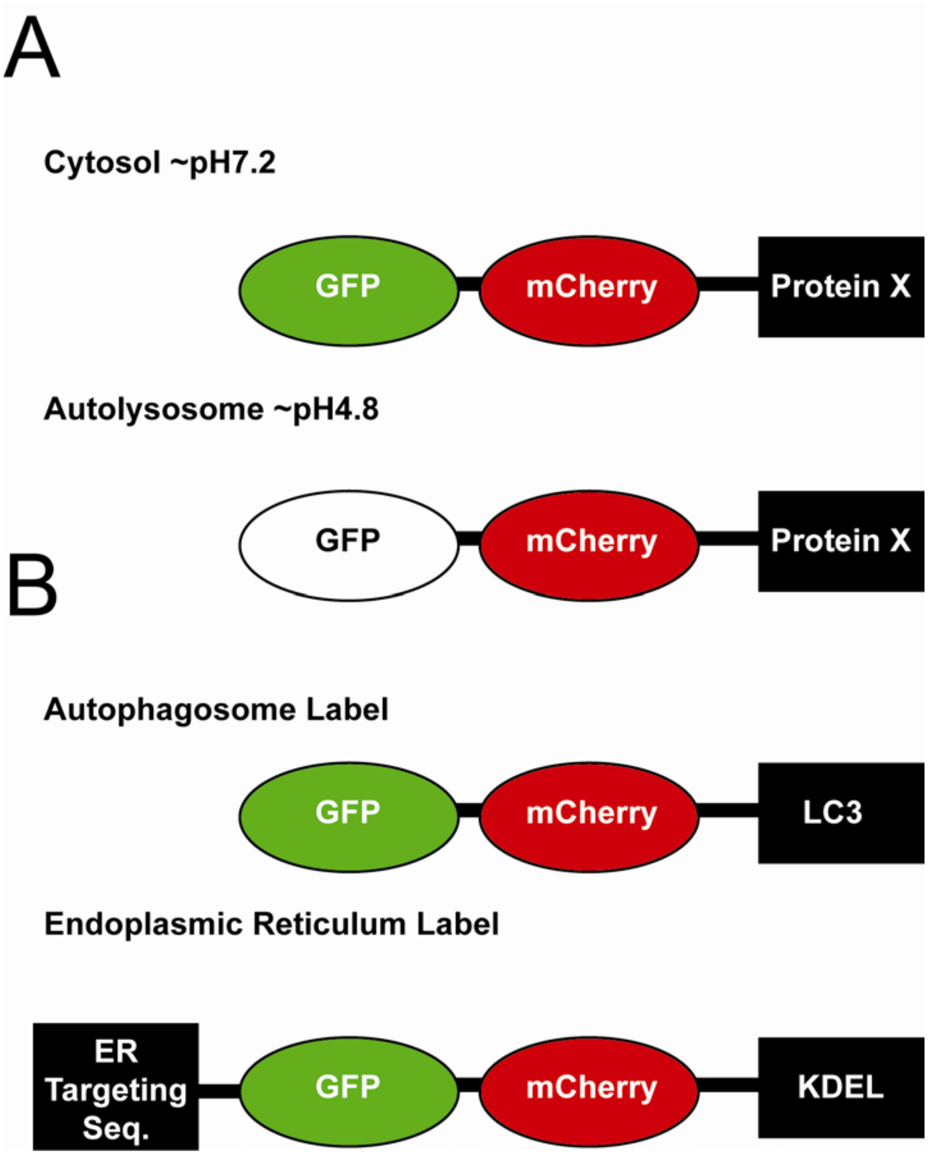
A
Cytosol ~pH7.2
GFP
mCherry
Protein X
Autolysosome ~pH4.8
GFP
mCherry
Protein X
B
Autophagosome Label
GFP
mCherry
LC3
Endoplasmic Reticulum Label
ER Targeting Seq.
GFP
mCherry
KDEL

Figure 4-5. Fluorescent proteins used to measure cellular pH

A) The normal pH of the cytosol is about 7.2. At this pH, both GFP and mCherry fluoresce. This dual signal is depicted as yellow/orange in micrographs; however, the pH inside an autolysosome is about 4.8. At this pH, GFP bleaches but mCherry retains fluorescence and lysosomes are visualized red. This effect means that one can use a lack of GFP fluorescence and the presence of mCherry fluorescence to visualized acidic regions of the cell. B) We created LC3 with this dual tag and also targeted it to the endoplasmic reticulum (ER) using the calreticulin ER targeting sequence and the KDEL ER-retention signal as indicated above.

When dual tagged GFP-mCherry-LC3 was visualized in 621-101 cells that had been pretreated with rapamycin, both yellow autophagosomes and red autolysosomes could be seen in cells treated with or without MG-132 indicating that autophagy was progressing through its mature stages under both rapamycin treated conditions. However in cells not treated with rapamycin, GFP-mCherry-LC3 appeared in much fewer and larger vesicles. These vesicles were yellow indicating they likely did not fuse with lysosomes and consequently not progress through autophagy correctly (Figure 4-6a). Additionally, there was an accumulation of p62 in 621-101 cells that was suppressed by rapamycin pretreatment. LC3-II levels are also higher when cells are treated with both MG-132 and rapamycin compared to MG-132 treatment alone (Figure 4-6b).

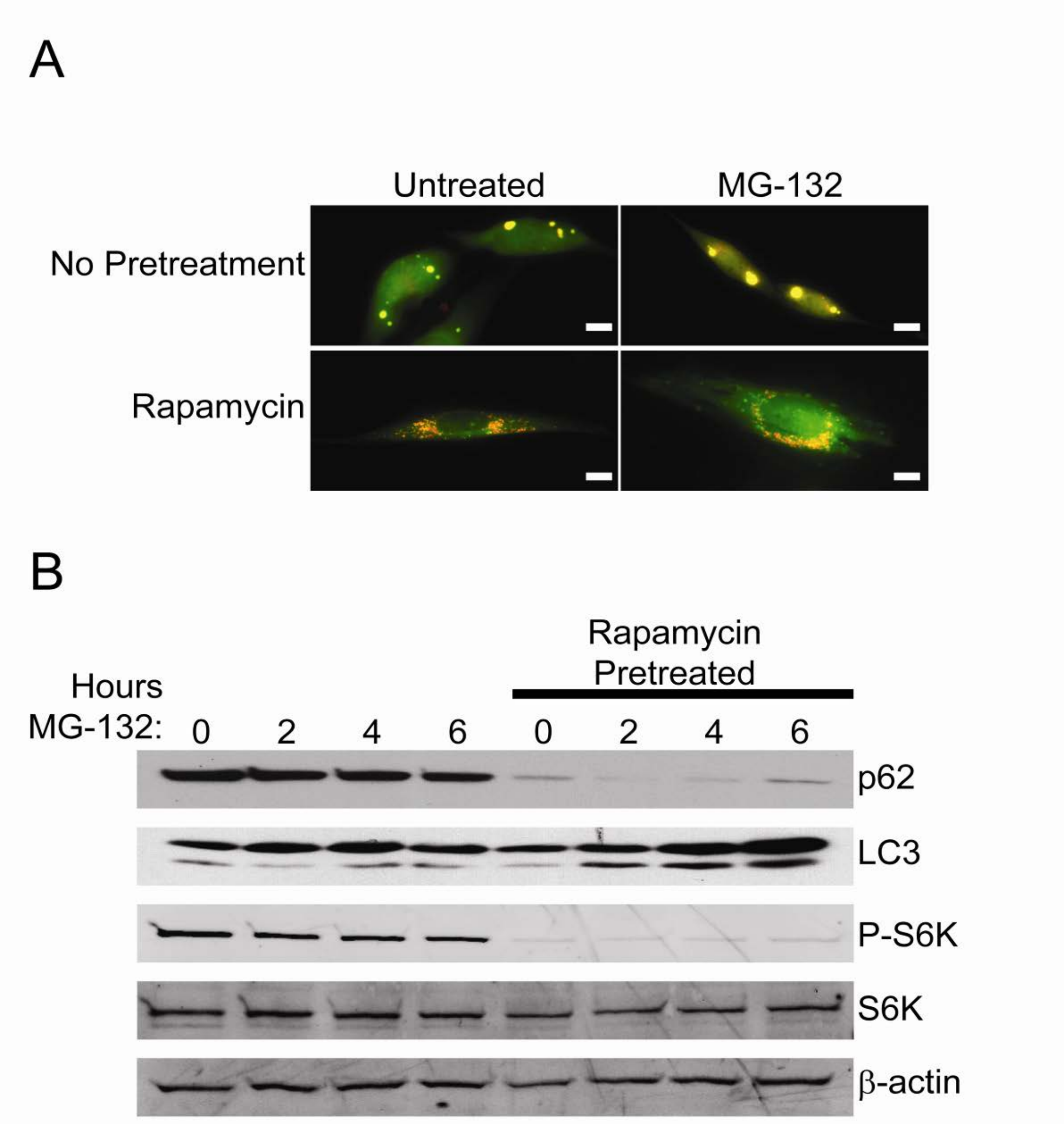
A
Untreated
MG-132
No Pretreatment
Rapamycin
B
Rapamycin Pretreated
Hours MG-132:
0
2
4
6
0
2
4
6
p62
LC3
P-S6K
S6K
β-actin

Figure 4-6. Rapamycin treatment restores autophagic processes

(A) 621-101 cells expressing mCherry-GFP-LC3 fusion protein were treated with 1µM MG-132 for 6 hours with or without 24 hours 50 nM rapamycin pretreatment. Images of GFP and mCherry localization are overlaid to illustrate regions of LC3 acidification. (B) 621-101 cells were treated for the indicated time with 1µM MG-132 with or without 24hrs of 50nM rapamycin pretreatment. Lysates were prepared and western blotted.

4.5 Autophagy may play a role in ER expansion during MG-132 treatment

During activation of the UPR, cells will expand the ER. This increase in ER volume will decrease the concentration of unfolded protein contained within the ER relieving the unfolded protein stress. Typically, this expansion is accompanied by increases in ER-resident chaperones and other components that promote proper protein folding; however, these components are not absolutely required for resolution of the unfolded protein stress by membrane expansion (164).

We find that despite rapamycin suppressing the UPR stress components ATF4 and CHOP, treatment with this macrolide antibiotic alone is sufficient to promote expansion of the ER. Rapamycin further cooperates with MG132 to enhance ER expansion. On the other hand, 621-101 cells which were not treated with rapamycin fail to show any significant increase in ER volume when exposed to MG-132 (Figure 4-7). Due to the fact that ER expansion was only observed under the conditions of increased autophagy, we tested two autophagy inhibitors for their ability to block ER expansion in rapamycin treated cells. We found that 3-methyl adenine (3-MA) or spautin-1 treatment reversed the ER expansion phenotype in cells that were treated with rapamycin. Additionally, these inhibitors blocked the further expansion of the ER after MG-132 treatment (Figure 4-8).

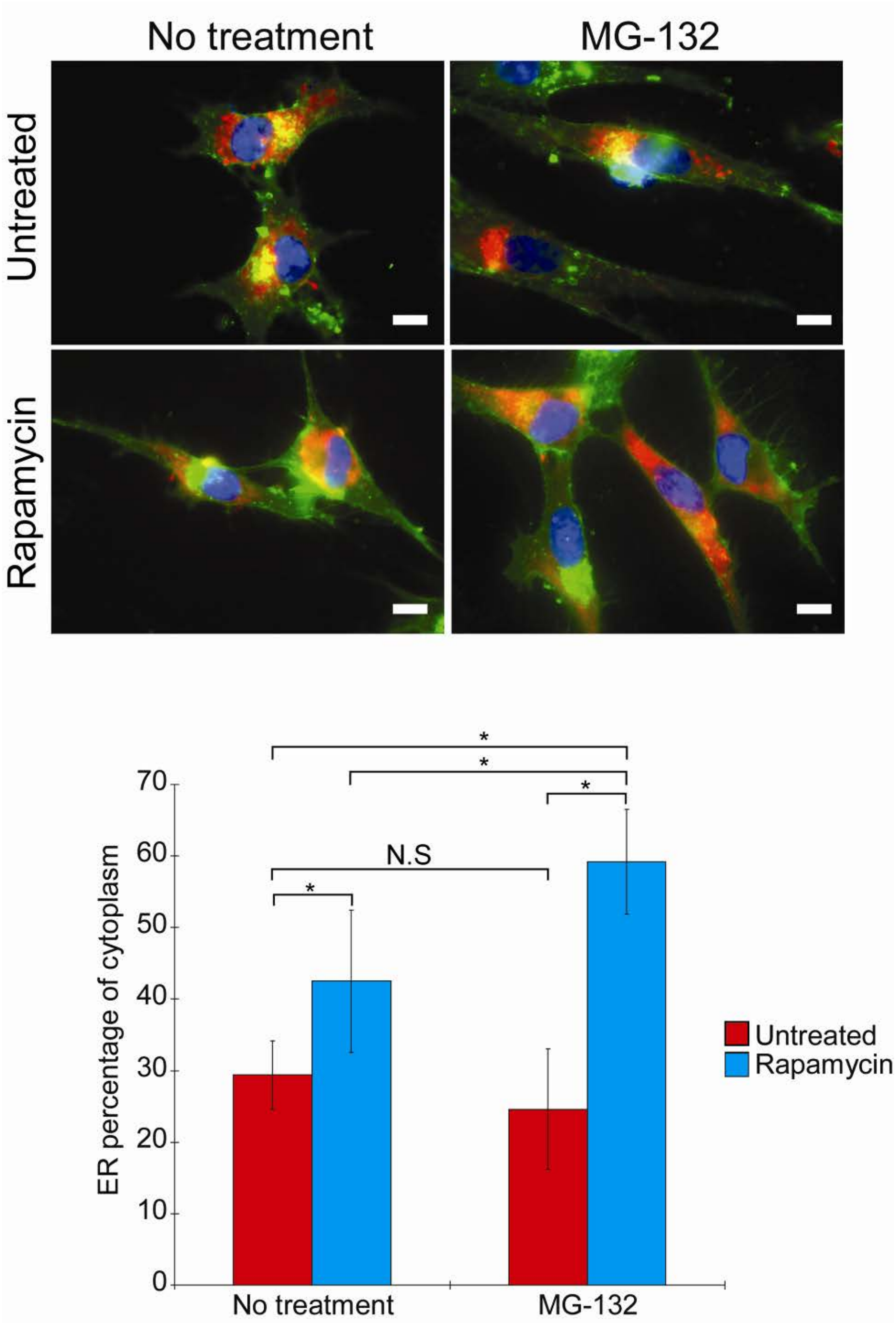
No treatment
MG-132
Untreated
Rapamycin
ER percentage of cytoplasm
0
10
20
30
40
50
60
70
N.S
*
*
*
*
No treatment
MG-132
🟥 Untreated
🟦 Rapamycin

Figure 4-7. mTORC1 inhibition is required for ER expansion

The ER of 621-101 cells was labeled using mCherry targeted to the ER (Red). These cells were then treated with 50nM rapamycin or vehicle control for 48 hours prior to being treated with 1µM MG-132 for 6 hrs. These cells were then fixed. The plasma membrane was labeled using AF488-wheat germ agglutinin (Green) and the nucleus was labeled using DAPI (Blue). The area of each cell’s plasma membrane and ER was measured using Zeiss software. We find that only cells treated with rapamycin showed increased ER volume when treated with MG-132. (*$P<0.05$)

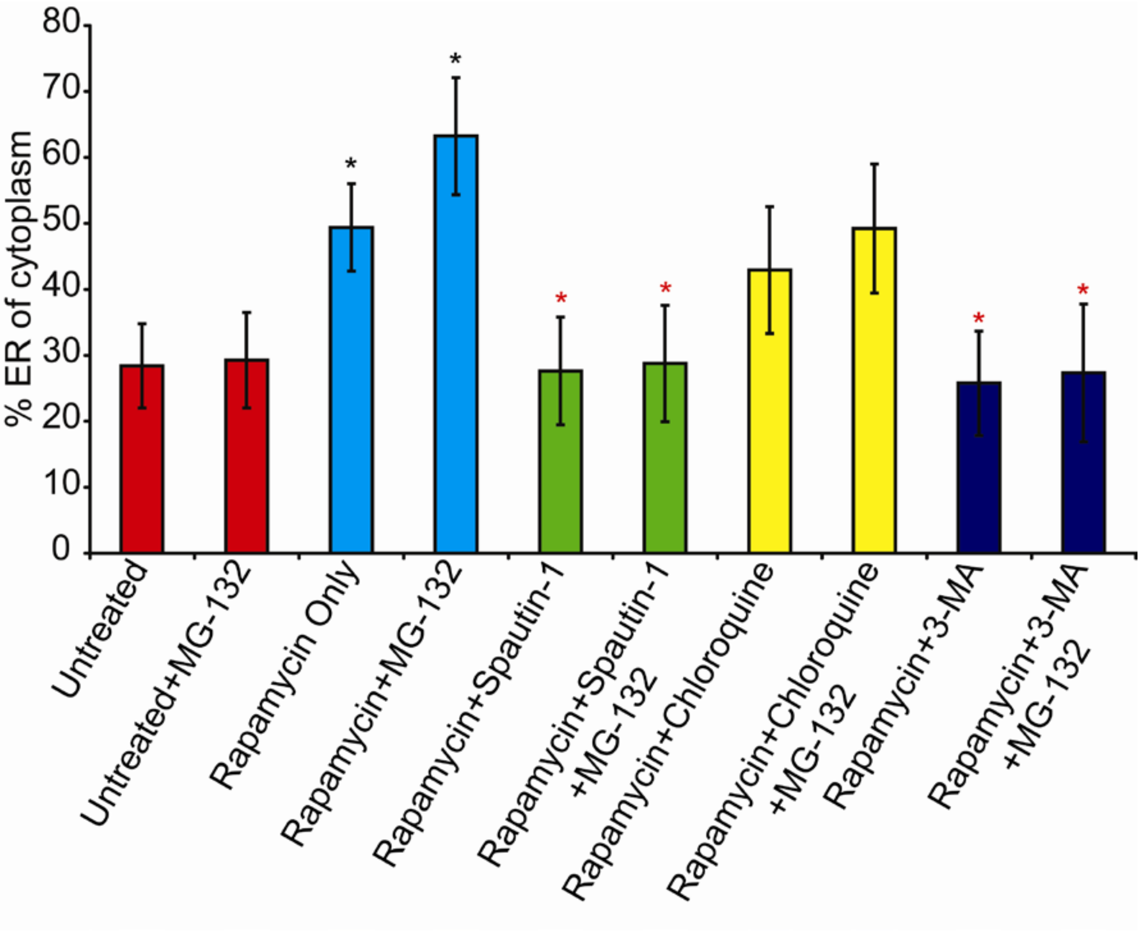

Figure 4-8. Autophagy inhibitors reverse rapamycin-associated ER expansion

Cells were treated as in figure 4-7 except 2 hours prior to MG-132 treatment cells were treated with 1µM Spautin-1, 2µM Chloroquine, or 10mM 3-MA. The area of each cell's ER and plasma membrane were determined. (*P<0.05 vs. untreated control) (*P<0.05 vs. rapamycin control)

4.6 Vacuoles may represent failed autophagosomal degradation of ER

The changes we observe in ER expansion in the presence or absence of autophagy suggest a possible role of autophagy in expansion of the ER and also in the formation of the cytoplasmic vacuoles seen during late stages of MG-132 treatment. Previous reports have shown that autophagy is induced during UPR induction and that the ER is a substrate for autophagic degradation (158-160, 165, 166). In order to observe the specific degradation of the ER by autophagy, we created an ER targeted GFP-mCherry expression construct. This construct functions similar to the GFP-mCherry-LC3 expression construct used to track all autophagosome maturation. However, the GFP-mCherry-ER labels the ER and should only track the acidication of autophagosomes containing the ER as a substrate.

We find that in non-rapamycin treated cells the GFP-mCherry-ER construct labels the ER a yellow color indicating that very little ER is being degraded by acidic autolysosomes (Figure 4-9 upper left panel). However, rapamycin treated cells show red punctate regions (Figure 4-9 lower left panel) in a similar area to where the LC3 labeled autophagosomes in figure 4-6, suggesting the ER is actively being turned over by autophagy. When these cells were treated with MG-132, the non-rapamycin treated cells formed vacuoles which contained the GFP-mCherry-ER probe and appear yellow suggesting that these vacuoles are likely derived from the ER and ultimately fail to acidify due to low levels of autophagic activity (Figure 4-9 upper right panel). However, the rapamycin treated cells show an increase in the amount of red vesicles suggesting an increase in autophagosomal degradation of the ER after MG-132 treatment (Figure 4-9 lower right panel).

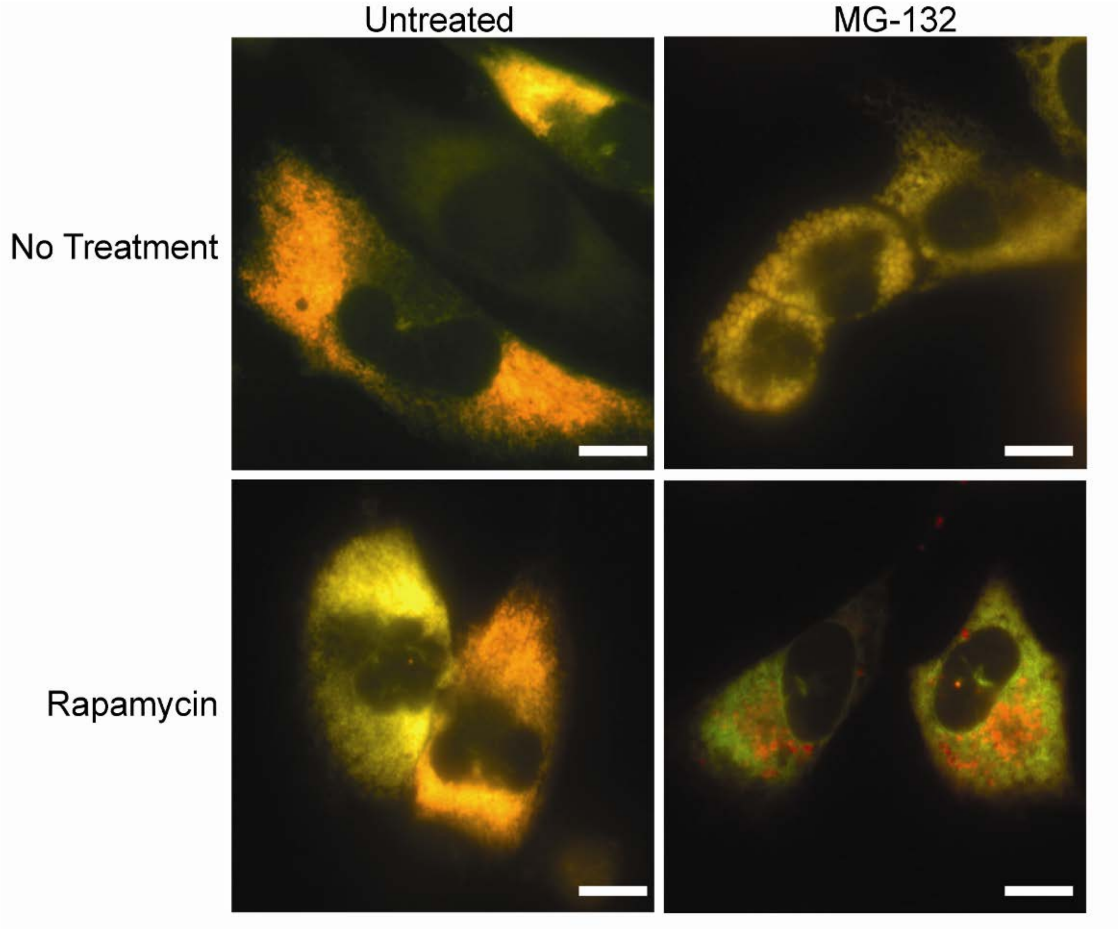

Figure 4-9. Vacuoles derived from the ER do not acidify in the absence of rapamycin

The ER of 621-101 cells was labeled using GFP-mCherry targeted to the ER. We find that the large vacuoles that form after MG-132 treatment are yellowish-orange indicating that these vacuoles are not acidic. However, the small vesicles that form in rapamycin treated cells are acidic (Red) and contain the ER label.

4.7 PI3P fails to accumulate in the ER in the absence of rapamycin

One of the proposed origins of the membranes autophagosomes are made of is the ER, where it has been shown that the lipid PI3P accumulates at regions named “omegasomes” (167). These omegasomes are believed to be a precursor for autophagomes. Using a GFP-tagged FYVE domain that is specifically targeted to the cytosolic face of the ER membrane, one can measure the accumulation of PI3P into these structures (168). We find that untreated cells do not have many omegasomes (Figure 4-11); however, cells treated with rapamycin form many omegasomes. This effect is even more pronounced when cells are treated with MG-132. We presume this increase in omegasome formation during MG-132 treatment is the result of increased demand on autophagic processes.

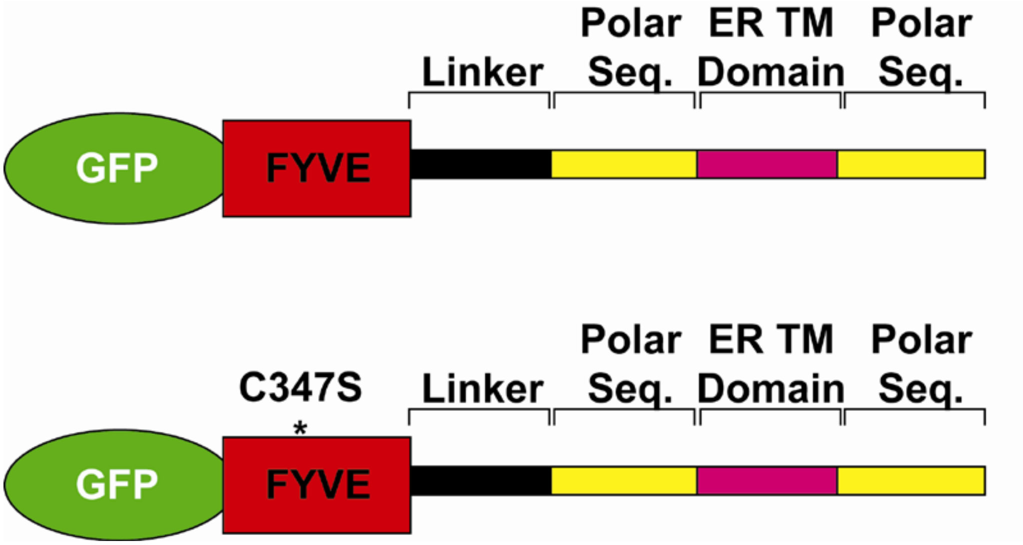
Polar Seq.
ER TM Domain
Polar Seq.
Linker
GFP
FYVE
C347S
*
Linker
Polar Seq.
ER TM Domain
Polar Seq.
GFP
FYVE

Figure 4-10. Measuring PI3P specifically in the ER

We used a construct that labels the PI3P specifically in the ER which is constructed using a PI3-binding FYVE domain from FENS1 fused to GFP and an ER transmembrane domain. A C347S mutation was introduced into the FYVE domain in order to prevent it from binding lipid. This mutant serves as a negative control.

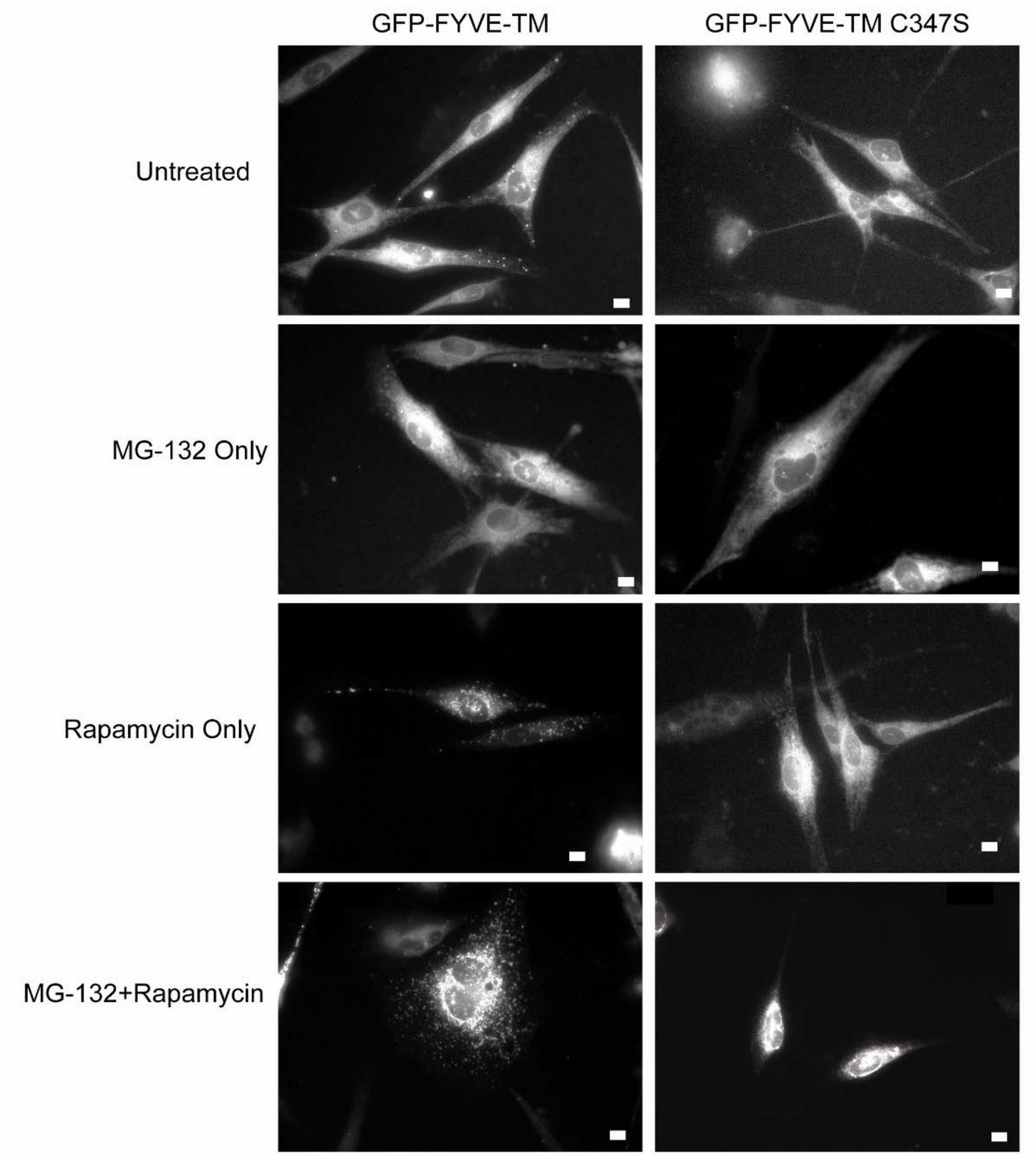
GFP-FYVE-TM
GFP-FYVE-TM C347S
Untreated
MG-132 Only
Rapamycin Only
MG-132+Rapamycin

Figure 4-11. mTORC1 activation inhibits accumulation of PI3P in the ER

Cells were treated as described in figure 7.We find that PI3P is present at higher levels in the ER when treated with rapamycin as evidenced by the punctate pattern of GFP in these cells.

4.8 JNK activation is required for omegasome formation during UPR induced autophagy

c-Jun N-terminal kinase (JNK) is a protein kinase that is activated by an assortment of different stresses, including genotoxic stress and UPR agonists (169, 170). Additionally, inhibition of mTORC1 with rapamycin has been shown to activate JNK (171). An inhibitor of JNK has previously been shown to block the induction of autophagy by the ER stressors tunicamycin and thapsigarin (158). However, it fails to block the induction of autophagy caused by non-ER stressors, such as amino acid starvation (158). To explore the relationship of these nutrient stressors with the activation of the UPR and formation of omegasomes on the ER membrane, we treated 621-101 cells that express the GFP-FYVE omegasome labeling construct with media that lacked either amino acids or glucose for 6hrs. We found that similar to rapamycin treatment, glucose starvation induced omegasome formation (Figure 4-12). Treatment of cells with the JNK inhibitor SP600125 resulted in strong inhibition of even the small amount of basal omeagasome formation. During rapamycin treatment, SP600125 blocked nearly all omegasome formation (Figure 4-12).

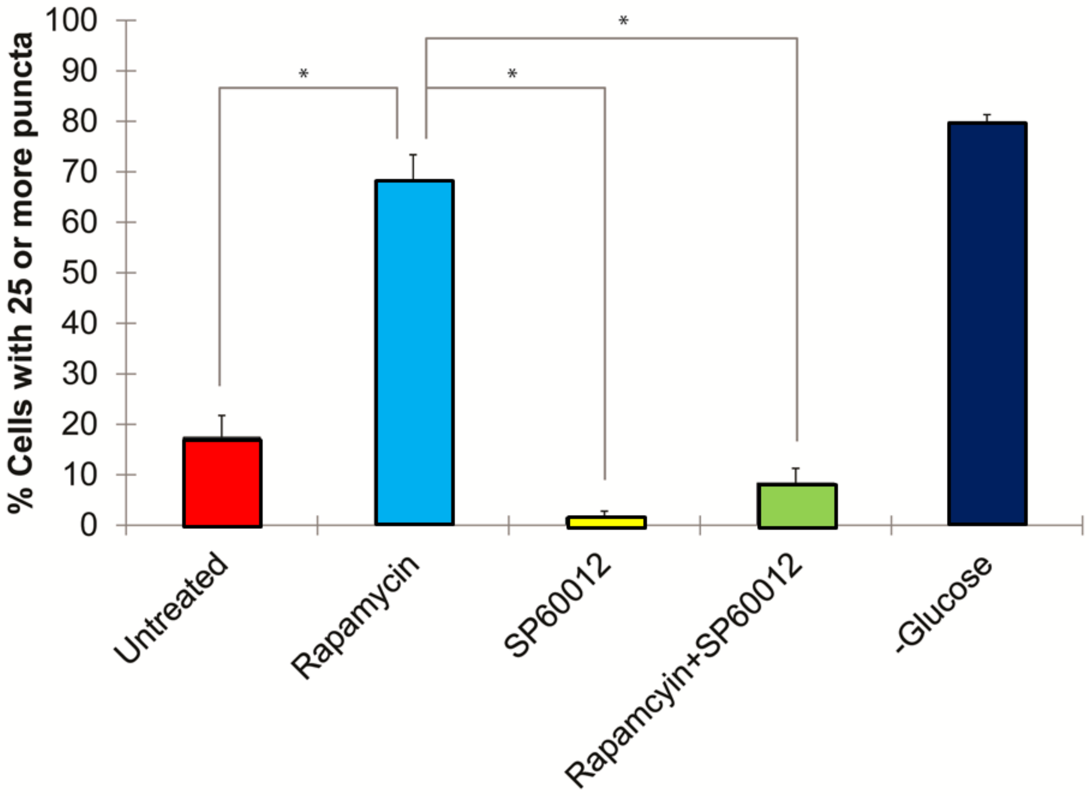

Figure 4-12. mTORC1 inhibition and JNK activation are required for accumulation of PI3P in the ER

Cells were treated as describe in figure 4-11.We find that PI3P is present at higher levels in the ER when treated with rapamycin as evidenced by the punctate pattern of GFP in these cells.

4.9.1 Discussion

The described ER expansion studies, although largely descriptive, significantly contribute to our understanding of the UPR and autophagy. These studies have also lead to the creation of two new techniques for measuring ER expansion and ER degradation by autophagy. These techniques may be adapted by other labs to create new and exciting angles for their research on the UPR. Because these techniques are new, the observations found in these studies are unique and may require validation with more established techniques. These studies also address the formation of omegasomes during the UPR for the first time.

4.9.2 Unifying Model Linking Autophagy and the UPR

The findings of this study and the results of other (158-160) have shown that activation of the UPR leads to expansion of the endoplasmic reticulum. The current studies are unique because we are studying cells that cannot correctly enter into autophagy without first inhibiting mTORC1 with rapamycin. We find that activation of autophagy by rapamycin treatment alone causes expansion of the ER. This is an interesting finding because we also find that rapamycin reduces basal levels of eIF2α phosphorylation as well as mRNA levels of ATF4 and CHOP. Interestingly when we look at only autophagy of the ER itself, we find that rapamycin treatment is required for the creation of mature autophagosomes which contain the ER as a substrate and become mature acidic autolysosomes. However when cells are stressed with MG-132 in the absence of autophagy, they will still form vesicles containing the ER marker which eventually fill the cytoplasm but will not acidify.

This lack of ER expansion may represent an inability of these cells to quickly reallocate building materials (lipids, carbohydrates, amino acids, etc.) to the synthesis of new ER. Rapamycin, by alleviating the blockade on autophagy imparted by TSC2 inactivation, leads to larger pools of available material to make ER. Additionally, the vacuoles formed from the ER in these cells during MG-132 treatment may fail to fuse with lysosomes and acidify because they lack the correct labeling or targeting signals as shown in the illustration below. These signals may include having high membrane concentrations of PI3P or binding to LC3 in some manner which will be discussed later in this section.

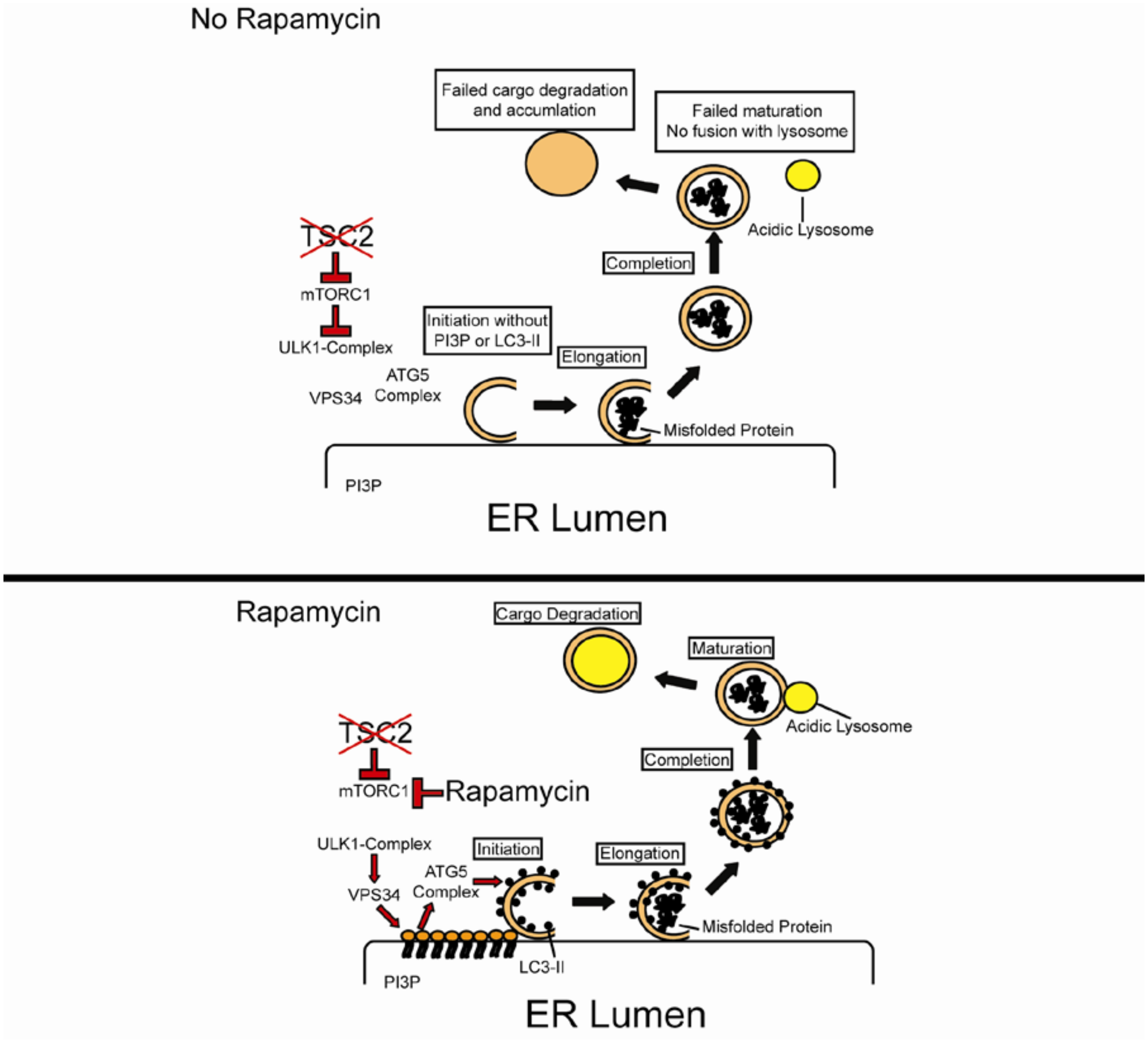
No Rapamycin
Failed cargo degradation and accumlation
Failed maturation No fusion with lysosome
Acidic Lysosome
TSC2
mTORC1
ULK1-Complex
Completion
Initiation without PI3P or LC3-II
Elongation
ATG5 Complex
VPS34
Misfolded Protein
PI3P
ER Lumen
Rapamycin
Cargo Degradation
Maturation
Acidic Lysosome
TSC2
mTORC1
Rapamycin
Completion
ULK1-Complex
Initiation
Elongation
ATG5 Complex
VPS34
Misfolded Protein
LC3-II
PI3P
ER Lumen

Figure 4-13. ER vacuole accumulation model

4.9.3 Parallels may exist between Mitophagy and Reticulophagy

There are very few studies in mammalian cells that focus on reticulophagy and other forms of cargo specific autophagy. Interestingly however, these processes have also been observed in yeast. In the yeast genetic system, the specific targeting of damaged mitochondria, misfolded proteins, and invading pathogens has been studied extensively. We may be able to better understand reticulophagy by applying the concepts we currently understand about mitophagy in yeast. Yeast genetic screens have identified proteins that are required for mitophagy. Some of these proteins are unique to mitophagy and others serve a purpose in general autophagy. In these screens, mitophagy was identified by the accumulation of mitochondrial proteins in the vacuole of stationary-phase respiring cells. One of the top hits found in these yeast screens was autophagy protein Atg32 (172, 173). Atg32 (which has no known metazoan homologue) is a 60-kDa protein that spans the outer mitochondrial membrane (174). It is required for mitophagy that occurs in response to enforced respiration but not for non-selective autophagy in response to nutrient deprivation or for pexophagy (172, 173). Under mitophagy-inducing growth conditions, Atg32 binds to Atg11, which is known to recruit a range of cargo, including peroxisomes, into autophagosomes by interacting with Atg8. Interestingly, the cytosolic domain of Atg32 contains a WXXL-like Atg8-binding motif, which is required for binding to Atg8 and for mitophagy (172, 173). Thus, Atg32 can interact with Atg8 indirectly through Atg11 and directly through the WXXL-like motif. The direct and indirect (when bridged by Atg11) association of mitochondrial membrane-anchored Atg32 with isolation membrane-bound Atg8 is thought to recruit mitochondria into autophagosomes (174). Although Atg32 expression increases under oxidizing conditions, which suggests that it might also participate in mitochondrial quality control, no defects in mitochondria were identified in Atg32-null yeast (174). How the expression and activity of Atg32 are regulated to eliminate the appropriate number of mitochondria remains unknown and is an intriguing area for further study.

We may be able to draw parallels between the yeast mitophagy regulation and what we observe in mammalian cells undergoing reticulophagy. First, there is likely an ER-linked autophagy signal protein similar to ATG32. This signal protein is likely a membrane-anchored protein or a protein that binds to another protein which is anchored to the cytosolic side of the ER membrane. This signal protein will likely interact with LC3 (ATG8) through either a WXXL-like motif or an indirect interaction with a WXXL-like motif containing protein. This targeting protein will either increase in expression, activity, or ER localization in times of extreme ER damage like during MG-132 treatment. This protein which targets LC3 to ER vesicles to be degraded by autophagy may be induced by inhibition of mTORC1 by rapamycin and its expression may be reduced in 621-101 cells where mTORC1 is constitutively active. This inability to label ER vesicles for degradation may explain their accumulation in the cytoplasm.

4.9.4 Reticuluophagy must have unique aspects from other cargo specific forms of autophagy

All forms of known autophagy have at least three general themes which they share in common. The cargo must be labeled in some manner. This labeling can be achieved by ubiquitination, phosphorylation, or through binding to another protein (174). The cargo must also interact with LC3 in some manner (174). This interaction can be either direct or indirect. Lastly, the cargo must be enveloped by membrane which then fuses with lysosomes to degrade the contents of the vesicle. It is this third theme where reticuluophagy appears to differ drastically from other forms of cargo specific autophagy.

The endoplasmic reticulum is orders of magnitude larger than other cargo specific autophagy targets like mitochondria, protein aggregates, and ribosomes. Additionally, there is only one ER in the cell and it must continue to exist in order to perpetuate its own existence, as the ER is the site of most *de novo* lipid synthesis (175). Therefore, a system must exist to remove damaged portions of the ER in small enough sections that they can be enveloped and degraded by an autophagosome. Removing these small sections of ER may be accomplished by the processes already associated with removing sections of the ER and transporting them elsewhere in the cell. There is some evidence that the ER to Golgi transport system is upregulated during activation of the UPR in a manner that relies on the activation of PERK and ATF4 (143). Interestingly, blocking ER to Golgi transport by brefeldin A (BFA) treatment leads to activation of the unfolded protein response in MEFs (143). This effect may be similar to proteasome inhibitors activating the UPR by blocking ERAD. BFA treatment would block the removal of bulk protein aggregates and undesired lipid membrane resulting in the activation of the UPR. Another possibility is that the ER to Golgi transport system shuttles the unfolded protein out of the cell; however, the bulk secretion of unfolded proteins by a cell would likely be highly toxic to a multicellular organism.

4.9.5 The ER as a coordinator of autophagy

The ER has been proposed to be the origin of the membrane used to make autophagosomes. This assertion is based on mainly two observations. First, the ER is the sight of omegasome formation which is a PI3P rich region of ER membrane that may provide a scaffold for an autophagosome to form and fill with their cargo (168). Second, the ER regulatory protein Beclin1 resides in the ER where it has been shown to regulate autophagy. This was demonstrated by overexpression of the BH3 only protein inhibitor Bcl2, engineered to specifically target to the ER. This Bcl2 mutant bound Beclin1 specifically in the ER, preventing both Beclin-VPS34 interaction and subsequent activation of autophagy. In contrast, Bcl2 targeted specifically to the mitochondria had no effect on autophagy (176). Accompanying these strong functional and spatial links between autophagy and the ER may be physical links to the ER’s UPR signaling machinery. JNK signaling from IRE1 activation has already been shown to drive the activation of autophagy after treatment with ER stressing drugs (158). Our data shows that in these cells there is a strong link between the expansion and contraction of the ER with activation or inhibition of autophagy, respectively. These links may be associated with expanding the ER to meet the demand for phospholipids for autophagic membranes. The ER may also actively operate as a platform for autophagic signaling processes similar to the actin cytoskeleton's role in other cell signaling events.

4.9.6 ER expansion, autophagy, and human health

In this chapter, we found that cells deficient for TSC2 fail to expand their ER and activate autophagy when stressed with MG-132. This inability to expand the ER may be related to the increased sensitivity to MG-132 we observe in this cell line and may contribute to our understanding of how TSC-associated cells respond to other ER stressing small molecules. This failed expansion may be used to kill tumors which cannot be removed by surgery in TSC patients. Despite the fact our study was conducted on cells which lack TSC2, we do not believe this mutation is required for this phenotype. We believe this because many mutations in cancer and other diseases can cause the activation of mTORC1, inhibition of autophagy, or directly lead to protein misfolding. Indeed, heavy vacuolation has been observed in cells with wild-type TSC1 and TSC2 expression (177, 178).

ER stress has been proposed to play a role in many chronic human ailments ranging from diabetes to neurodegenerative diseases (132, 133). General autophagy and ER-specific autophagy may help alleviate these and other disorders. For example, mutations to α-antitrypsin cause it to misfold in the ER where it cannot escape to be degraded by ERAD or it overwhelms the ability of the ERAD to export misfolded protein from the ER to the proteasome (177). In this disease, cells must rely almost exclusively on autophagy of the ER to dispose of the misfolded mutants of α-antitrypsin. Overexpression of mutants of α-antitrypsin has been shown to cause dilation/ vacuolation of the ER similar to what we observe in 621-101 cell with proteasome inhibition (177). Using drugs like rapamycin that enhance reticulophagy may be helpful for the elimination of protein aggregates trapped in the ER in diseases like α-antitrypsin deficiency.

This compartmental separation of misfolded protein from the proteasome may be a major theme in diseases like α-antitrypsin deficiency or cystic fibrosis. Additionally, diseases involving misfolded protein in the cytosol may also adversely affect ERAD’s ability to maintain healthy ER by tying up the proteasome. Huntington’s disease and Alzheimer’s disease are both characterized by the accumulation of protein aggregates and have been link to ER stress (179, 180). The progression of these diseases may be delayed by using rapamycin to improve clearance of ER protein aggregates. This approach would be superior to the cell’s natural mechanism of inducing autophagy because rapamycin induced autophagy is not linked to cell death; whereas, PERK activation is a strong inducer of both autophagy and apoptosis.

Additionally, TSC patients develop cortical tubers which present with cytoplasmic vacuolation similar to the vacuolation we observe after treatment with MG-132 (181). These patients also suffer from autism, seizures, and other problems associated with the brain (1). A mosaic mouse model of TSC1 loss in neural progenitors has been developed to mimic this aspect of TSC disease. Neural progenitors with loss of TSC1 develop vacuolation similar to that seen in the cortical tubers taken from patients (181). These mice also suffer from seizures. Rapamycin treatment of these mice effectively reduces both the seizures and appearance of vacuolated cells in these mice brains (181).

APPENDIX 1: qRT-PCR and CHIP PRIMERS

qRT-PCR Primers

Target Gene	Species	Forward Primer	Reverse Primer	Roche Probe
ATF4	Rat	tcagacaccggcaaggag	gtggccaaaagctcatctg	#85
CHOP	Rat	accaccacacctgaaagca	agctggacactgtctcaaagg	#13
MYC	Rat	gctcctcgcgttatttgaag	gcatcgtcgtgactgtcg	#10
NOXA	Rat	gcgaaagagcacgatgaga	gatcacactcgtccttcaggt	#117
ATF4	Human	tctccagcgacaaggctaa	caatctgtcccggagaagg	#76
CHOP	Human	cagagctggaacctgaggag	tggatcagtctggaaaagca	#9
LC3	Human	cgcaccttcgaacaaagag	cttctcacccttgtatcgttctatt	#89
ASNS	Human	cgtcaagctgtccacatcc	tggtattcaaattcaaaatgctgt	#30

ChIP Primers

ATF4 Gene Location	Forward Primer	Reverse Primer
-855	AAGCTGCTTCCTCCGGGTGG	GCAACGCTGCTGCTGGGTTTC
-141	CGGGCCAGAGCGTCAATGGG	CTGCAAAGGCCAACGCTGCC

APPENDIX 2: shRNA SEQUENCES

sh_RNA Name	**Sequence**
sh_Scramble	CCTAAGGTTAAGTCGCCCTCG
sh_c-MYC #1	GAACTATGACCTCGACTACGA
sh_c-MYC #2	GAATGTCAAGAGGCGAACACA
sh_eIF4E	CCAAAGATAGTGATTGGTTAT

REFERENCES

1. Crino PB, Nathanson KL, Henske EP. The tuberous sclerosis complex. The New England journal of medicine. 2006;355(13):1345-56. Epub 2006/09/29.

2. McCormack FX, Inoue Y, Moss J, Singer LG, Strange C, Nakata K, et al. Efficacy and safety of sirolimus in lymphangioleiomyomatosis. The New England journal of medicine. 2011;364(17):1595-606. Epub 2011/03/18.

3. Laplante M, Sabatini DM. mTOR signaling at a glance. Journal of cell science. 2009;122(Pt 20):3589-94.

4. Wang L, Harris TE, Roth RA, Lawrence JC, Jr. PRAS40 regulates mTORC1 kinase activity by functioning as a direct inhibitor of substrate binding. The Journal of biological chemistry. 2007;282(27):20036-44.

5. Vander Haar E, Lee SI, Bandhakavi S, Griffin TJ, Kim DH. Insulin signalling to mTOR mediated by the Akt/PKB substrate PRAS40. Nature cell biology. 2007;9(3):316-23.

6. Sancak Y, Thoreen CC, Peterson TR, Lindquist RA, Kang SA, Spooner E, et al. PRAS40 is an insulin-regulated inhibitor of the mTORC1 protein kinase. Molecular cell. 2007;25(6):903-15.

7. Guertin DA, Stevens DM, Thoreen CC, Burds AA, Kalaany NY, Moffat J, et al. Ablation in mice of the mTORC components raptor, rictor, or mLST8 reveals that mTORC2 is required for signaling to Akt-FOXO and PKCalpha, but not S6K1. Developmental cell. 2006;11(6):859-71.

8. Ikenoue T, Inoki K, Yang Q, Zhou X, Guan KL. Essential function of TORC2 in PKC and Akt turn motif phosphorylation, maturation and signalling. The EMBO journal. 2008;27(14):1919-31.

9. Facchinetti V, Ouyang W, Wei H, Soto N, Lazorchak A, Gould C, et al. The mammalian target of rapamycin complex 2 controls folding and stability of Akt and protein kinase C. The EMBO journal. 2008;27(14):1932-43.

10. Sarbassov DD, Guertin DA, Ali SM, Sabatini DM. Phosphorylation and regulation of Akt/PKB by the rictor-mTOR complex. Science. 2005;307(5712):1098-101.

11. Hsu PP, Kang SA, Rameseder J, Zhang Y, Ottina KA, Lim D, et al. The mTOR-regulated phosphoproteome reveals a mechanism of mTORC1-mediated inhibition of growth factor signaling. Science. 2011;332(6035):1317-22. Epub 2011/06/11.

12. Yu Y, Yoon SO, Poulogiannis G, Yang Q, Ma XM, Villen J, et al. Phosphoproteomic analysis identifies Grb10 as an mTORC1 substrate that negatively regulates insulin signaling. Science. 2011;332(6035):1322-6. Epub 2011/06/11.

13. Sarbassov DD, Ali SM, Sengupta S, Sheen JH, Hsu PP, Bagley AF, et al. Prolonged rapamycin treatment inhibits mTORC2 assembly and Akt/PKB. Molecular cell. 2006;22(2):159-68.

14. Peterson TR, Laplante M, Thoreen CC, Sancak Y, Kang SA, Kuehl WM, et al. DEPTOR is an mTOR inhibitor frequently overexpressed in multiple myeloma cells and required for their survival. Cell. 2009;137(5):873-86. Epub 2009/05/19.

15. Gao X, Zhang Y, Arrazola P, Hino O, Kobayashi T, Yeung RS, et al. Tsc tumour suppressor proteins antagonize amino-acid-TOR signalling. Nature cell biology. 2002;4(9):699-704.

16. Kwiatkowski DJ, Zhang H, Bandura JL, Heiberger KM, Glogauer M, el-Hashemite N, et al. A mouse model of TSC1 reveals sex-dependent lethality from liver hemangiomas, and up-regulation of p70S6 kinase activity in Tsc1 null cells. Human molecular genetics. 2002;11(5):525-34.

17. Inoki K, Li Y, Zhu T, Wu J, Guan KL. TSC2 is phosphorylated and inhibited by Akt and suppresses mTOR signalling. Nature cell biology. 2002;4(9):648-57.

18. Tee AR, Fingar DC, Manning BD, Kwiatkowski DJ, Cantley LC, Blenis J. Tuberous sclerosis complex-1 and -2 gene products function together to inhibit mammalian target of rapamycin (mTOR)-mediated downstream signaling. Proceedings of the National Academy of Sciences of the United States of America. 2002;99(21):13571-6.

19. Zhang H, Cicchetti G, Onda H, Koon HB, Asrican K, Bajraszewski N, et al. Loss of Tsc1/Tsc2 activates mTOR and disrupts PI3K-Akt signaling through downregulation of PDGFR. The Journal of clinical investigation. 2003;112(8):1223-33.

20. Ghosh S, Tergaonkar V, Rothlin CV, Correa RG, Bottero V, Bist P, et al. Essential role of tuberous sclerosis genes TSC1 and TSC2 in NF-kappaB activation and cell survival. Cancer cell. 2006;10(3):215-26.

21. Shah OJ, Wang Z, Hunter T. Inappropriate activation of the TSC/Rheb/mTOR/S6K cassette induces IRS1/2 depletion, insulin resistance, and cell survival deficiencies. Current biology : CB. 2004;14(18):1650-6.

22. Benvenuto G, Li S, Brown SJ, Braverman R, Vass WC, Cheadle JP, et al. The tuberous sclerosis-1 (TSC1) gene product hamartin suppresses cell growth and augments the expression of the TSC2 product tuberin by inhibiting its ubiquitination. Oncogene. 2000;19(54):6306-16. Epub 2001/02/15.

23. Inoki K, Li Y, Xu T, Guan KL. Rheb GTPase is a direct target of TSC2 GAP activity and regulates mTOR signaling. Genes & development. 2003;17(15):1829-34. Epub 2003/07/19.

24. Castro AF, Rebhun JF, Clark GJ, Quilliam LA. Rheb binds tuberous sclerosis complex 2 (TSC2) and promotes S6 kinase activation in a rapamycin- and farnesylation-dependent manner. The Journal of biological chemistry. 2003;278(35):32493-6. Epub 2003/07/05.

25. Garami A, Zwartkruis FJ, Nobukuni T, Joaquin M, Roccio M, Stocker H, et al. Insulin activation of Rheb, a mediator of mTOR/S6K/4E-BP signaling, is inhibited by TSC1 and 2. Molecular cell. 2003;11(6):1457-66.

26. Tee AR, Manning BD, Roux PP, Cantley LC, Blenis J. Tuberous sclerosis complex gene products, Tuberin and Hamartin, control mTOR signaling by acting as a GTPase-activating protein complex toward Rheb. Current biology : CB. 2003;13(15):1259-68. Epub 2003/08/09.

27. Huang J, Dibble CC, Matsuzaki M, Manning BD. The TSC1-TSC2 complex is required for proper activation of mTOR complex 2. Molecular and cellular biology. 2008;28(12):4104-15.

28. Huang J, Wu S, Wu CL, Manning BD. Signaling events downstream of mammalian target of rapamycin complex 2 are attenuated in cells and tumors deficient for the tuberous sclerosis complex tumor suppressors. Cancer research. 2009;69(15):6107-14.

29. Manning BD, Tee AR, Logsdon MN, Blenis J, Cantley LC. Identification of the tuberous sclerosis complex-2 tumor suppressor gene product tuberin as a target of the phosphoinositide 3-kinase/akt pathway. Molecular cell. 2002;10(1):151-62.

30. Ma L, Chen Z, Erdjument-Bromage H, Tempst P, Pandolfi PP. Phosphorylation and functional inactivation of TSC2 by Erk implications for tuberous sclerosis and cancer pathogenesis. Cell. 2005;121(2):179-93.

31. Lee DF, Kuo HP, Chen CT, Hsu JM, Chou CK, Wei Y, et al. IKK beta suppression of TSC1 links inflammation and tumor angiogenesis via the mTOR pathway. Cell. 2007;130(3):440-55.

32. Corradetti MN, Inoki K, Bardeesy N, DePinho RA, Guan KL. Regulation of the TSC pathway by LKB1: evidence of a molecular link between tuberous sclerosis complex and Peutz-Jeghers syndrome. Genes & development. 2004;18(13):1533-8.

33. Inoki K, Zhu T, Guan KL. TSC2 mediates cellular energy response to control cell growth and survival. Cell. 2003;115(5):577-90.

34. Inoki K, Ouyang H, Zhu T, Lindvall C, Wang Y, Zhang X, et al. TSC2 integrates Wnt and energy signals via a coordinated phosphorylation by AMPK and GSK3 to regulate cell growth. Cell. 2006;126(5):955-68.

35. Mao JH, Kim IJ, Wu D, Climent J, Kang HC, DelRosario R, et al. FBXW7 targets mTOR for degradation and cooperates with PTEN in tumor suppression. Science. 2008;321(5895):1499-502.

36. Hu J, Zacharek S, He YJ, Lee H, Shumway S, Duronio RJ, et al. WD40 protein FBW5 promotes ubiquitination of tumor suppressor TSC2 by DDB1-CUL4-ROC1 ligase. Genes & development. 2008;22(7):866-71.

37. Murthy V, Han S, Beauchamp RL, Smith N, Haddad LA, Ito N, et al. Pam and its ortholog highwire interact with and may negatively regulate the TSC1.TSC2 complex. The Journal of biological chemistry. 2004;279(2):1351-8.

38. Zheng L, Ding H, Lu Z, Li Y, Pan Y, Ning T, et al. E3 ubiquitin ligase E6AP-mediated TSC2 turnover in the presence and absence of HPV16 E6. Genes Cells. 2008;13(3):285-94.

39. Kuo HP, Lee DF, Chen CT, Liu M, Chou CK, Lee HJ, et al. ARD1 Stabilization of TSC2 Suppresses Tumorigenesis Through the mTOR Signaling Pathway. Science signaling.3(108):ra9.

40. Nobukuni T, Joaquin M, Roccio M, Dann SG, Kim SY, Gulati P, et al. Amino acids mediate mTOR/raptor signaling through activation of class 3 phosphatidylinositol 3OH-kinase. Proceedings of the National Academy of Sciences of the United States of America. 2005;102(40):14238-43.

41. Dikic I, Johansen T, Kirkin V. Selective autophagy in cancer development and therapy. Cancer research.70(9):3431-4.

42. Gulati P, Gaspers LD, Dann SG, Joaquin M, Nobukuni T, Natt F, et al. Amino acids activate mTOR complex 1 via Ca2+/CaM signaling to hVps34. Cell metabolism. 2008;7(5):456-65.

43. Sancak Y, Peterson TR, Shaul YD, Lindquist RA, Thoreen CC, Bar-Peled L, et al. The Rag GTPases bind raptor and mediate amino acid signaling to mTORC1. Science. 2008;320(5882):1496-501.

44. Kim E, Goraksha-Hicks P, Li L, Neufeld TP, Guan KL. Regulation of TORC1 by Rag GTPases in nutrient response. Nature cell biology. 2008;10(8):935-45.

45. Gong R, Li L, Liu Y, Wang P, Yang H, Wang L, et al. Crystal structure of the Gtr1p-Gtr2p complex reveals new insights into the amino acid-induced TORC1 activation. Genes & development. 2011;25(16):1668-73. Epub 2011/08/06.

46. Han JM, Jeong SJ, Park MC, Kim G, Kwon NH, Kim HK, et al. Leucyl-tRNA synthetase is an intracellular leucine sensor for the mTORC1-signaling pathway. Cell. 2012;149(2):410-24. Epub 2012/03/20.

47. Sancak Y, Bar-Peled L, Zoncu R, Markhard AL, Nada S, Sabatini DM. Ragulator-Rag complex targets mTORC1 to the lysosomal surface and is necessary for its activation by amino acids. Cell.141(2):290-303.

48. Gwinn DM, Shackelford DB, Egan DF, Mihaylova MM, Mery A, Vasquez DS, et al. AMPK phosphorylation of raptor mediates a metabolic checkpoint. Molecular cell. 2008;30(2):214-26.

49. Lee MN, Ha SH, Kim J, Koh A, Lee CS, Kim JH, et al. Glycolytic flux signals to mTOR through glyceraldehyde-3-phosphate dehydrogenase-mediated regulation of Rheb. Molecular and cellular biology. 2009;29(14):3991-4001.

50. Kalender A, Selvaraj A, Kim SY, Gulati P, Brule S, Viollet B, et al. Metformin, independent of AMPK, inhibits mTORC1 in a rag GTPase-dependent manner. Cell metabolism. 2010;11(5):390-401. Epub 2010/05/07.

51. Bernardi R, Guernah I, Jin D, Grisendi S, Alimonti A, Teruya-Feldstein J, et al. PML inhibits HIF-1alpha translation and neoangiogenesis through repression of mTOR. Nature. 2006;442(7104):779-85.

52. Brugarolas J, Lei K, Hurley RL, Manning BD, Reiling JH, Hafen E, et al. Regulation of mTOR function in response to hypoxia by REDD1 and the TSC1/TSC2 tumor suppressor complex. Genes & development. 2004;18(23):2893-904.

53. Li Y, Wang Y, Kim E, Beemiller P, Wang CY, Swanson J, et al. Bnip3 mediates the hypoxia-induced inhibition on mammalian target of rapamycin by interacting with Rheb. The Journal of biological chemistry. 2007;282(49):35803-13.

54. Ma XM, Blenis J. Molecular mechanisms of mTOR-mediated translational control. Nature reviews. 2009;10(5):307-18.

55. Ma XM, Yoon SO, Richardson CJ, Julich K, Blenis J. SKAR links pre-mRNA splicing to mTOR/S6K1-mediated enhanced translation efficiency of spliced mRNAs. Cell. 2008;133(2):303-13.

56. Richardson CJ, Broenstrup M, Fingar DC, Julich K, Ballif BA, Gygi S, et al. SKAR is a specific target of S6 kinase 1 in cell growth control. Current biology : CB. 2004;14(17):1540-9.

57. Yang HS, Jansen AP, Komar AA, Zheng X, Merrick WC, Costes S, et al. The transformation suppressor Pdcd4 is a novel eukaryotic translation initiation factor 4A binding protein that inhibits translation. Molecular and cellular biology. 2003;23(1):26-37.

58. Dorrello NV, Peschiaroli A, Guardavaccaro D, Colburn NH, Sherman NE, Pagano M. S6K1- and betaTRCP-mediated degradation of PDCD4 promotes protein translation and cell growth. Science. 2006;314(5798):467-71.

59. Raught B, Peiretti F, Gingras AC, Livingstone M, Shahbazian D, Mayeur GL, et al. Phosphorylation of eucaryotic translation initiation factor 4B Ser422 is modulated by S6 kinases. The EMBO journal. 2004;23(8):1761-9.

60. Ganley IG, Lam du H, Wang J, Ding X, Chen S, Jiang X. ULK1.ATG13.FIP200 complex mediates mTOR signaling and is essential for autophagy. The Journal of biological chemistry. 2009;284(18):12297-305.

61. Hosokawa N, Hara T, Kaizuka T, Kishi C, Takamura A, Miura Y, et al. Nutrient-dependent mTORC1 association with the ULK1-Atg13-FIP200 complex required for autophagy. Molecular biology of the cell. 2009;20(7):1981-91.

62. Chan EY. mTORC1 phosphorylates the ULK1-mAtg13-FIP200 autophagy regulatory complex. Science signaling. 2009;2(84):pe51.

63. Egan DF, Shackelford DB, Mihaylova MM, Gelino S, Kohnz RA, Mair W, et al. Phosphorylation of ULK1 (hATG1) by AMP-activated protein kinase connects energy sensing to mitophagy. Science. 2011;331(6016):456-61. Epub 2011/01/06.

64. Zhao M, Klionsky DJ. AMPK-dependent phosphorylation of ULK1 induces autophagy. Cell metabolism. 2011;13(2):119-20. Epub 2011/02/03.

65. Kim J, Kundu M, Viollet B, Guan KL. AMPK and mTOR regulate autophagy through direct phosphorylation of Ulk1. Nature cell biology. 2011;13(2):132-41. Epub 2011/01/25.

66. Qu X, Yu J, Bhagat G, Furuya N, Hibshoosh H, Troxel A, et al. Promotion of tumorigenesis by heterozygous disruption of the beclin 1 autophagy gene. The Journal of clinical investigation. 2003;112(12):1809-20.

67. Komatsu M, Waguri S, Chiba T, Murata S, Iwata J, Tanida I, et al. Loss of autophagy in the central nervous system causes neurodegeneration in mice. Nature. 2006;441(7095):880-4.

68. Levine B, Kroemer G. Autophagy in the pathogenesis of disease. Cell. 2008;132(1):27-42.

69. Hoang B, Benavides A, Shi Y, Frost P, Lichtenstein A. Effect of autophagy on multiple myeloma cell viability. Molecular cancer therapeutics. 2009;8(7):1974-84.

70. Porstmann T, Santos CR, Griffiths B, Cully M, Wu M, Leevers S, et al. SREBP activity is regulated by mTORC1 and contributes to Akt-dependent cell growth. Cell metabolism. 2008;8(3):224-36.

71. Brown NF, Stefanovic-Racic M, Sipula IJ, Perdomo G. The mammalian target of rapamycin regulates lipid metabolism in primary cultures of rat hepatocytes. Metabolism: clinical and experimental. 2007;56(11):1500-7.

72. Peng T, Golub TR, Sabatini DM. The immunosuppressant rapamycin mimics a starvation-like signal distinct from amino acid and glucose deprivation. Molecular and cellular biology. 2002;22(15):5575-84.

73. Laplante M, Sabatini DM. An emerging role of mTOR in lipid biosynthesis. Current biology : CB. 2009;19(22):R1046-52.

74. Huffman TA, Mothe-Satney I, Lawrence JC, Jr. Insulin-stimulated phosphorylation of lipin mediated by the mammalian target of rapamycin. Proceedings of the National Academy of Sciences of the United States of America. 2002;99(2):1047-52.

75. Jones JR, Barrick C, Kim KA, Lindner J, Blondeau B, Fujimoto Y, et al. Deletion of PPARgamma in adipose tissues of mice protects against high fat diet-induced obesity and insulin resistance. Proceedings of the National Academy of Sciences of the United States of America. 2005;102(17):6207-12. Epub 2005/04/19.

76. Cunningham JT, Rodgers JT, Arlow DH, Vazquez F, Mootha VK, Puigserver P. mTOR controls mitochondrial oxidative function through a YY1-PGC-1alpha transcriptional complex. Nature. 2007;450(7170):736-40.

77. Topisirovic I, Ruiz-Gutierrez M, Borden KL. Phosphorylation of the eukaryotic translation initiation factor eIF4E contributes to its transformation and mRNA transport activities. Cancer research. 2004;64(23):8639-42.

78. Short JD, Houston KD, Dere R, Cai SL, Kim J, Johnson CL, et al. AMP-activated protein kinase signaling results in cytoplasmic sequestration of p27. Cancer research. 2008;68(16):6496-506.

79. Hong F, Larrea MD, Doughty C, Kwiatkowski DJ, Squillace R, Slingerland JM. mTOR-raptor binds and activates SGK1 to regulate p27 phosphorylation. Molecular cell. 2008;30(6):701-11.

80. Li R, Wheeler TM, Dai H, Sayeeduddin M, Scardino PT, Frolov A, et al. Biological correlates of p27 compartmental expression in prostate cancer. The Journal of urology. 2006;175(2):528-32.

81. Alkarain A, Slingerland J. Deregulation of p27 by oncogenic signaling and its prognostic significance in breast cancer. Breast Cancer Res. 2004;6(1):13-21.

82. Armstrong AJ, Netto GJ, Rudek MA, Halabi S, Wood DP, Creel PA, et al. A pharmacodynamic study of rapamycin in men with intermediate- to high-risk localized prostate cancer. Clinical cancer research : an official journal of the American Association for Cancer Research.16(11):3057-66.

83. Plas DR, Thomas G. Tubers and tumors: rapamycin therapy for benign and malignant tumors. Current opinion in cell biology. 2009;21(2):230-6.

84. Guertin DA, Stevens DM, Saitoh M, Kinkel S, Crosby K, Sheen JH, et al. mTOR complex 2 is required for the development of prostate cancer induced by Pten loss in mice. Cancer cell. 2009;15(2):148-59.

85. Hudes G, Carducci M, Tomczak P, Dutcher J, Figlin R, Kapoor A, et al. Temsirolimus, interferon alfa, or both for advanced renal-cell carcinoma. The New England journal of medicine. 2007;356(22):2271-81.

86. Thoreen CC, Kang SA, Chang JW, Liu Q, Zhang J, Gao Y, et al. An ATP-competitive mammalian target of rapamycin inhibitor reveals rapamycin-resistant functions of mTORC1. The Journal of biological chemistry. 2009;284(12):8023-32. Epub 2009/01/20.

87. Choo AY, Yoon SO, Kim SG, Roux PP, Blenis J. Rapamycin differentially inhibits S6Ks and 4E-BP1 to mediate cell-type-specific repression of mRNA translation. Proceedings of the National Academy of Sciences of the United States of America. 2008;105(45):17414-9. Epub 2008/10/29.

88. Efeyan A, Sabatini DM. mTOR and cancer: many loops in one pathway. Current opinion in cell biology. 2009.

89. Yu K, Toral-Barza L, Shi C, Zhang WG, Lucas J, Shor B, et al. Biochemical, cellular, and in vivo activity of novel ATP-competitive and selective inhibitors of the mammalian target of rapamycin. Cancer research. 2009;69(15):6232-40.

90. Feldman ME, Apsel B, Uotila A, Loewith R, Knight ZA, Ruggero D, et al. Active-site inhibitors of mTOR target rapamycin-resistant outputs of mTORC1 and mTORC2. PLoS biology. 2009;7(2):e38.

91. Workman P, Clarke PA, Raynaud FI, van Montfort RL. Drugging the PI3 kinome: from chemical tools to drugs in the clinic. Cancer research.70(6):2146-57.

92. Aspuria PJ, Tamanoi F. The Rheb family of GTP-binding proteins. Cellular signalling. 2004;16(10):1105-12.

93. Takahashi K, Nakagawa M, Young SG, Yamanaka S. Differential membrane localization of ERas and Rheb, two Ras-related proteins involved in the phosphatidylinositol 3-kinase/mTOR pathway. The Journal of biological chemistry. 2005;280(38):32768-74.

94. Basso AD, Mirza A, Liu G, Long BJ, Bishop WR, Kirschmeier P. The farnesyl transferase inhibitor (FTI) SCH66336 (lonafarnib) inhibits Rheb farnesylation and mTOR signaling. Role in FTI enhancement of taxane and tamoxifen anti-tumor activity. The Journal of biological chemistry. 2005;280(35):31101-8.

95. Mavrakis KJ, Zhu H, Silva RL, Mills JR, Teruya-Feldstein J, Lowe SW, et al. Tumorigenic activity and therapeutic inhibition of Rheb GTPase. Genes & development. 2008;22(16):2178-88.

96. Hanker AB, Mitin N, Wilder RS, Henske EP, Tamanoi F, Cox AD, et al. Differential requirement of CAAX-mediated posttranslational processing for Rheb localization and signaling. Oncogene.29(3):380-91.

97. Karbowniczek M, Spittle CS, Morrison T, Wu H, Henske EP. mTOR is activated in the majority of malignant melanomas. The Journal of investigative dermatology. 2008;128(4):980-7.

98. Basso AD, Kirschmeier P, Bishop WR. Lipid posttranslational modifications. Farnesyl transferase inhibitors. Journal of lipid research. 2006;47(1):15-31.

99. Finlay GA, Malhowski AJ, Liu Y, Fanburg BL, Kwiatkowski DJ, Toksoz D. Selective inhibition of growth of tuberous sclerosis complex 2 null cells by atorvastatin is associated with impaired Rheb and Rho GTPase function and reduced mTOR/S6 kinase activity. Cancer research. 2007;67(20):9878-86.

100. Finlay GA, Malhowski AJ, Polizzi K, Malinowska-Kolodziej I, Kwiatkowski DJ. Renal and liver tumors in Tsc2(+/-) mice, a model of tuberous sclerosis complex, do not respond to treatment with atorvastatin, a 3-hydroxy-3-methylglutaryl coenzyme A reductase inhibitor. Molecular cancer therapeutics. 2009;8(7):1799-807.

101. Lee N, Woodrum CL, Nobil AM, Rauktys AE, Messina MP, Dabora SL. Rapamycin weekly maintenance dosing and the potential efficacy of combination sorafenib plus rapamycin but not atorvastatin or doxycycline in tuberous sclerosis preclinical models. BMC pharmacology. 2009;9:8.

102. Ozcan U, Ozcan L, Yilmaz E, Duvel K, Sahin M, Manning BD, et al. Loss of the tuberous sclerosis complex tumor suppressors triggers the unfolded protein response to regulate insulin signaling and apoptosis. Molecular cell. 2008;29(5):541-51. Epub 2008/03/18.

103. Zhou X, Ikenoue T, Chen X, Li L, Inoki K, Guan KL. Rheb controls misfolded protein metabolism by inhibiting aggresome formation and autophagy. Proceedings of the National Academy of Sciences of the United States of America. 2009;106(22):8923-8.

104. Woodrum C, Nobil A, Dabora SL. Comparison of three rapamycin dosing schedules in A/J Tsc2+/- mice and improved survival with angiogenesis inhibitor or asparaginase treatment in mice with subcutaneous tuberous sclerosis related tumors. Journal of translational medicine.8:14.

105. Lee CH, Inoki K, Karbowniczek M, Petroulakis E, Sonenberg N, Henske EP, et al. Constitutive mTOR activation in TSC mutants sensitizes cells to energy starvation and genomic damage via p53. The EMBO journal. 2007;26(23):4812-23.

106. Manning BD, Cantley LC. AKT/PKB signaling: navigating downstream. Cell. 2007;129(7):1261-74.

107. Demidenko ZN, Blagosklonny MV. Growth stimulation leads to cellular senescence when the cell cycle is blocked. Cell cycle (Georgetown, Tex. 2008;7(21):3355-61.

108. Bunpo P, Dudley A, Cundiff JK, Cavener DR, Wek RC, Anthony TG. GCN2 protein kinase is required to activate amino acid deprivation responses in mice treated with the anti-cancer agent L-asparaginase. The Journal of biological chemistry. 2009;284(47):32742-9.

109. Hotamisligil GS. Endoplasmic reticulum stress and the inflammatory basis of metabolic disease. Cell.140(6):900-17.

110. Patil C, Walter P. Intracellular signaling from the endoplasmic reticulum to the nucleus: the unfolded protein response in yeast and mammals. Current opinion in cell biology. 2001;13(3):349-55.

111. Di Nardo A, Kramvis I, Cho N, Sadowski A, Meikle L, Kwiatkowski DJ, et al. Tuberous sclerosis complex activity is required to control neuronal stress responses in an mTOR-dependent manner. The Journal of neuroscience : the official journal of the Society for Neuroscience. 2009;29(18):5926-37. Epub 2009/05/08.

112. Ilic N, Utermark T, Widlund HR, Roberts TM. PI3K-targeted therapy can be evaded by gene amplification along the MYC-eukaryotic translation initiation factor 4E (eIF4E) axis. Proceedings of the National Academy of Sciences of the United States of America. 2011;108(37):E699-708. Epub 2011/08/31.

113. Balakumaran BS, Porrello A, Hsu DS, Glover W, Foye A, Leung JY, et al. MYC activity mitigates response to rapamycin in prostate cancer through eukaryotic initiation factor 4E-binding protein 1-mediated inhibition of autophagy. Cancer research. 2009;69(19):7803-10. Epub 2009/09/24.

114. Shi Y, Sharma A, Wu H, Lichtenstein A, Gera J. Cyclin D1 and c-myc internal ribosome entry site (IRES)-dependent translation is regulated by AKT activity and enhanced by rapamycin through a p38 MAPK- and ERK-dependent pathway. The Journal of biological chemistry. 2005;280(12):10964-73. Epub 2005/01/07.

115. Eilers M, Eisenman RN. Myc's broad reach. Genes & development. 2008;22(20):2755-66. Epub 2008/10/17.

116. Meyer N, Penn LZ. Reflecting on 25 years with MYC. Nature reviews Cancer. 2008;8(12):976-90. Epub 2008/11/26.

117. Larsson LG, Henriksson MA. The Yin and Yang functions of the Myc oncoprotein in cancer development and as targets for therapy. Experimental cell research. 2010;316(8):1429-37. Epub 2010/04/13.

118. Cotter TG. Apoptosis and cancer: the genesis of a research field. Nature reviews Cancer. 2009;9(7):501-7. Epub 2009/06/25.

119. Nilsson JA, Cleveland JL. Myc pathways provoking cell suicide and cancer. Oncogene. 2003;22(56):9007-21. Epub 2003/12/10.

120. Seoane J, Le HV, Massague J. Myc suppression of the p21(Cip1) Cdk inhibitor influences the outcome of the p53 response to DNA damage. Nature. 2002;419(6908):729-34. Epub 2002/10/18.

121. Wu S, Cetinkaya C, Munoz-Alonso MJ, von der Lehr N, Bahram F, Beuger V, et al. Myc represses differentiation-induced p21CIP1 expression via Miz-1-dependent interaction with the p21 core promoter. Oncogene. 2003;22(3):351-60. Epub 2003/01/25.

122. Nikiforov MA, Riblett M, Tang WH, Gratchouck V, Zhuang D, Fernandez Y, et al. Tumor cell-selective regulation of NOXA by c-MYC in response to proteasome inhibition. Proceedings of the National Academy of Sciences of the United States of America. 2007;104(49):19488-93. Epub 2007/11/29.

123. Eischen CM, Woo D, Roussel MF, Cleveland JL. Apoptosis triggered by Myc-induced suppression of Bcl-X(L) or Bcl-2 is bypassed during lymphomagenesis. Molecular and cellular biology. 2001;21(15):5063-70. Epub 2001/07/05.

124. Egle A, Harris AW, Bouillet P, Cory S. Bim is a suppressor of Myc-induced mouse B cell leukemia. Proceedings of the National Academy of Sciences of the United States of America. 2004;101(16):6164-9. Epub 2004/04/14.

125. Eischen CM, Roussel MF, Korsmeyer SJ, Cleveland JL. Bax loss impairs Myc-induced apoptosis and circumvents the selection of p53 mutations during Myc-mediated lymphomagenesis. Molecular and cellular biology. 2001;21(22):7653-62. Epub 2001/10/18.

126. Eischen CM, Weber JD, Roussel MF, Sherr CJ, Cleveland JL. Disruption of the ARF-Mdm2-p53 tumor suppressor pathway in Myc-induced lymphomagenesis. Genes & development. 1999;13(20):2658-69. Epub 1999/10/29.

127. Hemann MT, Bric A, Teruya-Feldstein J, Herbst A, Nilsson JA, Cordon-Cardo C, et al. Evasion of the p53 tumour surveillance network by tumour-derived MYC mutants. Nature. 2005;436(7052):807-11. Epub 2005/08/12.

128. Walker C, Ginsler J. Development of a quantitative in vitro transformation assay for kidney epithelial cells. Carcinogenesis. 1992;13(1):25-32. Epub 1992/01/01.

129. Kane RC, Bross PF, Farrell AT, Pazdur R. Velcade: U.S. FDA approval for the treatment of multiple myeloma progressing on prior therapy. The oncologist. 2003;8(6):508-13. Epub 2003/12/06.

130. Kang YJ, Lu MK, Guan KL. The TSC1 and TSC2 tumor suppressors are required for proper ER stress response and protect cells from ER stress-induced apoptosis. Cell death and differentiation. 2011;18(1):133-44. Epub 2010/07/10.

131. Zhang Y, Gao X, Saucedo LJ, Ru B, Edgar BA, Pan D. Rheb is a direct target of the tuberous sclerosis tumour suppressor proteins. Nature cell biology. 2003;5(6):578-81. Epub 2003/05/29.

132. Marciniak SJ, Ron D. Endoplasmic reticulum stress signaling in disease. Physiological reviews. 2006;86(4):1133-49. Epub 2006/10/04.

133. Schroder M, Kaufman RJ. The mammalian unfolded protein response. Annual review of biochemistry. 2005;74:739-89. Epub 2005/06/15.

134. Nishitoh H, Matsuzawa A, Tobiume K, Saegusa K, Takeda K, Inoue K, et al. ASK1 is essential for endoplasmic reticulum stress-induced neuronal cell death triggered by expanded polyglutamine repeats. Genes & development. 2002;16(11):1345-55. Epub 2002/06/07.

135. Zimmermann J, Erdmann D, Lalande I, Grossenbacher R, Noorani M, Furst P. Proteasome inhibitor induced gene expression profiles reveal overexpression of transcriptional regulators ATF3, GADD153 and MAD1. Oncogene. 2000;19(25):2913-20. Epub 2000/06/29.

136. Harding HP, Zhang Y, Bertolotti A, Zeng H, Ron D. Perk is essential for translational regulation and cell survival during the unfolded protein response. Molecular cell. 2000;5(5):897-904. Epub 2000/07/06.

137. Harding HP, Novoa I, Zhang Y, Zeng H, Wek R, Schapira M, et al. Regulated translation initiation controls stress-induced gene expression in mammalian cells. Molecular cell. 2000;6(5):1099-108. Epub 2000/12/07.

138. Palam LR, Baird TD, Wek RC. Phosphorylation of eIF2 facilitates ribosomal bypass of an inhibitory upstream ORF to enhance CHOP translation. The Journal of biological chemistry. 2011;286(13):10939-49. Epub 2011/02/03.

139. Vattem KM, Wek RC. Reinitiation involving upstream ORFs regulates ATF4 mRNA translation in mammalian cells. Proceedings of the National Academy of Sciences of the United States of America. 2004;101(31):11269-74. Epub 2004/07/28.

140. Dey S, Baird TD, Zhou D, Palam LR, Spandau DF, Wek RC. Both transcriptional regulation and translational control of ATF4 are central to the integrated stress response. The Journal of biological chemistry. 2010;285(43):33165-74. Epub 2010/08/25.

141. Armstrong JL, Flockhart R, Veal GJ, Lovat PE, Redfern CP. Regulation of endoplasmic reticulum stress-induced cell death by ATF4 in neuroectodermal tumor cells. The Journal of biological chemistry. 2010;285(9):6091-100. Epub 2009/12/22.

142. Jiang HY, Wek RC. Phosphorylation of the alpha-subunit of the eukaryotic initiation factor-2 (eIF2alpha) reduces protein synthesis and enhances apoptosis in response to proteasome inhibition. The Journal of biological chemistry. 2005;280(14):14189-202. Epub 2005/02/03.

143. Teske BF, Wek SA, Bunpo P, Cundiff JK, McClintick JN, Anthony TG, et al. The eIF2 kinase PERK and the integrated stress response facilitate activation of ATF6 during endoplasmic reticulum stress. Molecular biology of the cell. 2011;22(22):4390-405. Epub 2011/09/16.

144. Duvel K, Yecies JL, Menon S, Raman P, Lipovsky AI, Souza AL, et al. Activation of a metabolic gene regulatory network downstream of mTOR complex 1. Molecular cell. 2010;39(2):171-83. Epub 2010/07/31.

145. Hosoi H, Dilling MB, Liu LN, Danks MK, Shikata T, Sekulic A, et al. Studies on the mechanism of resistance to rapamycin in human cancer cells. Molecular pharmacology. 1998;54(5):815-24. Epub 1998/11/06.

146. Chen S, Blank JL, Peters T, Liu XJ, Rappoli DM, Pickard MD, et al. Genome-wide siRNA screen for modulators of cell death induced by proteasome inhibitor bortezomib. Cancer research. 2010;70(11):4318-26. Epub 2010/05/13.

147. Nawrocki ST, Carew JS, Maclean KH, Courage JF, Huang P, Houghton JA, et al. Myc regulates aggresome formation, the induction of Noxa, and apoptosis in response to the combination of bortezomib and SAHA. Blood. 2008;112(7):2917-26. Epub 2008/07/22.

148. Yin X, Giap C, Lazo JS, Prochownik EV. Low molecular weight inhibitors of Myc-Max interaction and function. Oncogene. 2003;22(40):6151-9. Epub 2003/09/19.

149. Wang D, Wengrod J, Gardner LB. Overexpression of the c-myc oncogene inhibits nonsense-mediated RNA decay in B lymphocytes. The Journal of biological chemistry. 2011;286(46):40038-43. Epub 2011/10/05.

150. Woo CW, Cui D, Arellano J, Dorweiler B, Harding H, Fitzgerald KA, et al. Adaptive suppression of the ATF4-CHOP branch of the unfolded protein response by toll-like receptor signalling. Nature cell biology. 2009;11(12):1473-80. Epub 2009/10/27.

151. Liang SH, Zhang W, McGrath BC, Zhang P, Cavener DR. PERK (eIF2alpha kinase) is required to activate the stress-activated MAPKs and induce the expression of immediate-early genes upon disruption of ER calcium homoeostasis. The Biochemical journal. 2006;393(Pt 1):201-9. Epub 2005/08/30.

152. Zeller KI, Zhao X, Lee CW, Chiu KP, Yao F, Yustein JT, et al. Global mapping of c-Myc binding sites and target gene networks in human B cells. Proceedings of the National Academy of Sciences of the United States of America. 2006;103(47):17834-9. Epub 2006/11/10.

153. Li Z, Van Calcar S, Qu C, Cavenee WK, Zhang MQ, Ren B. A global transcriptional regulatory role for c-Myc in Burkitt's lymphoma cells. Proceedings of the National Academy of Sciences of the United States of America. 2003;100(14):8164-9. Epub 2003/06/17.

154. Wang Q, Mora-Jensen H, Weniger MA, Perez-Galan P, Wolford C, Hai T, et al. ERAD inhibitors integrate ER stress with an epigenetic mechanism to activate BH3-only protein NOXA in cancer cells. Proceedings of the National Academy of Sciences of the United States of America. 2009;106(7):2200-5. Epub 2009/01/24.

155. Kim J, Klionsky DJ. Autophagy, cytoplasm-to-vacuole targeting pathway, and pexophagy in yeast and mammalian cells. Annual review of biochemistry. 2000;69:303-42. Epub 2000/08/31.

156. Suzuki K. Selective autophagy in budding yeast. Cell death and differentiation. 2012. Epub 2012/06/19.

157. Wong AS, Cheung ZH, Ip NY. Molecular machinery of macroautophagy and its deregulation in diseases. Biochimica et biophysica acta. 2011;1812(11):1490-7. Epub 2011/07/27.

158. Ogata M, Hino S, Saito A, Morikawa K, Kondo S, Kanemoto S, et al. Autophagy is activated for cell survival after endoplasmic reticulum stress. Molecular and cellular biology. 2006;26(24):9220-31. Epub 2006/10/13.

159. Rzymski T, Milani M, Singleton DC, Harris AL. Role of ATF4 in regulation of autophagy and resistance to drugs and hypoxia. Cell cycle (Georgetown, Tex. 2009;8(23):3838-47. Epub 2009/11/06.

160. Kouroku Y, Fujita E, Tanida I, Ueno T, Isoai A, Kumagai H, et al. ER stress (PERK/eIF2alpha phosphorylation) mediates the polyglutamine-induced LC3 conversion, an essential step for autophagy formation. Cell death and differentiation. 2007;14(2):230-9. Epub 2006/06/24.

161. Palam LR, Baird TD, Wek RC. Phosphorylation of eIF2 facilitates ribosomal bypass of an inhibitory upstream ORF to enhance CHOP translation. The Journal of biological chemistry.286(13):10939-49.

162. Kisselev AF, van der Linden WA, Overkleeft HS. Proteasome inhibitors: an expanding army attacking a unique target. Chemistry & biology. 2012;19(1):99-115. Epub 2012/01/31.

164. Schuck S, Prinz WA, Thorn KS, Voss C, Walter P. Membrane expansion alleviates endoplasmic reticulum stress independently of the unfolded protein response. The Journal of cell biology. 2009;187(4):525-36. Epub 2009/12/02.

165. Bernales S, McDonald KL, Walter P. Autophagy counterbalances endoplasmic reticulum expansion during the unfolded protein response. PLoS biology. 2006;4(12):e423. Epub 2006/11/30.

166. Siroky BJ, Yin H, Babcock JT, Lu L, Hellmann AR, Dixon BP, et al. Human TSC-associated renal angiomyolipoma cells are hypersensitive to ER stress. American journal of physiology Renal physiology. 2012;303(6):F831-44. Epub 2012/07/14.

167. Simonsen A, Stenmark H. Self-eating from an ER-associated cup. The Journal of cell biology. 2008;182(4):621-2. Epub 2008/08/30.

168. Axe EL, Walker SA, Manifava M, Chandra P, Roderick HL, Habermann A, et al. Autophagosome formation from membrane compartments enriched in phosphatidylinositol 3-phosphate and dynamically connected to the endoplasmic reticulum. The Journal of cell biology. 2008;182(4):685-701. Epub 2008/08/30.

169. Urano F, Wang X, Bertolotti A, Zhang Y, Chung P, Harding HP, et al. Coupling of stress in the ER to activation of JNK protein kinases by transmembrane protein kinase IRE1. Science. 2000;287(5453):664-6. Epub 2000/01/29.

170. Johnson GL, Nakamura K. The c-jun kinase/stress-activated pathway: regulation, function and role in human disease. Biochimica et biophysica acta. 2007;1773(8):1341-8. Epub 2007/02/20.

171. Huang S, Shu L, Dilling MB, Easton J, Harwood FC, Ichijo H, et al. Sustained activation of the JNK cascade and rapamycin-induced apoptosis are suppressed by p53/p21(Cip1). Molecular cell. 2003;11(6):1491-501. Epub 2003/06/25.

172. Kanki T, Wang K, Cao Y, Baba M, Klionsky DJ. Atg32 is a mitochondrial protein that confers selectivity during mitophagy. Developmental cell. 2009;17(1):98-109. Epub 2009/07/22.

173. Okamoto K, Kondo-Okamoto N, Ohsumi Y. Mitochondria-anchored receptor Atg32 mediates degradation of mitochondria via selective autophagy. Developmental cell. 2009;17(1):87-97. Epub 2009/07/22.

174. Komatsu M, Ichimura Y. Selective autophagy regulates various cellular functions. Genes Cells. 2010;15(9):923-33. Epub 2010/07/31.

175. Anelli T, Sitia R. Protein quality control in the early secretory pathway. The EMBO journal. 2008;27(2):315-27. Epub 2008/01/25.

176. Maiuri MC, Le Toumelin G, Criollo A, Rain JC, Gautier F, Juin P, et al. Functional and physical interaction between Bcl-X(L) and a BH3-like domain in Beclin-1. The EMBO journal. 2007;26(10):2527-39. Epub 2007/04/21.

177. Teckman JH, Perlmutter DH. Retention of mutant alpha(1)-antitrypsin Z in endoplasmic reticulum is associated with an autophagic response. American journal of physiology Gastrointestinal and liver physiology. 2000;279(5):G961-74. Epub 2000/10/29.

178. Kaul A, Overmeyer JH, Maltese WA. Activated Ras induces cytoplasmic vacuolation and non-apoptotic death in glioblastoma cells via novel effector pathways. Cellular signalling. 2007;19(5):1034-43. Epub 2007/01/11.

179. Duennwald ML, Lindquist S. Impaired ERAD and ER stress are early and specific events in polyglutamine toxicity. Genes & development. 2008;22(23):3308-19. Epub 2008/11/19.

180. Doyle KM, Kennedy D, Gorman AM, Gupta S, Healy SJ, Samali A. Unfolded proteins and endoplasmic reticulum stress in neurodegenerative disorders. Journal of cellular and molecular medicine. 2011;15(10):2025-39. Epub 2011/07/05.

181. Goto J, Talos DM, Klein P, Qin W, Chekaluk YI, Anderl S, et al. Regulable neural progenitor-specific Tsc1 loss yields giant cells with organellar dysfunction in a model of tuberous sclerosis complex. Proceedings of the National Academy of Sciences of the United States of America. 2011;108(45):E1070-9. Epub 2011/10/26.

CURRICULUM VITAE

Justin Thomas Babcock

EDUCATION

Indiana University, Indianapolis, IN
Ph.D., Biochemistry and Molecular Biology
Dissertation Title: “mTORC1 contributes to ER stress induced cell death”
December 2012

Purdue University, West Lafayette, IN
B.S., Biochemistry with Research and Academic Honors
August 2005

PROFESSIONAL EXPERIENCE

Indiana University School of Medicine-Indianapolis, IN (2005-2012)
Biochemistry Ph.D. Graduate Student

- Trained graduate students and technicians
- Participated in grant application and renewal process
- Reviewed and evaluated scientific papers
- Developed new avenues of investigation
- Wrote scientific literature
- Presented work at internal and external meetings

American Legion Emblem Sales-Indianapolis, IN (2001-2004)
Part-Time Warehouse Worker

- Picked and pack orders
- Inventory tracking and ordering

Climb Time Inc.-Indianapolis, IN (1999-2001)
Rock climbing instructor and Outdoor gear sales

- Taught private and group lessons regarding proper rock climbing safety and climbing techniques
- Sold rock climbing gear and clothing

FELLOWSHIPS

Howard Hughes Medical Institute Summer Fellowship, 2002, 2003, 2004, 2005
Studied the role of small physiologically-relevant electrical currents generated during wound healing, and the role they play in cell migration through the activation of voltage-gated Ca^{+2} channels. For this line of research, I used zebra fish keratinocytes as a model system and applied many microscopy techniques including immunofluorescence and Fura-2 calcium measurements. This fellowship allowed me to continue the undergraduate research I conducted during the school years at Purdue into the summers.

DeVault Gift Estate Graduate Fellowship, 2007-2008, 2008-2009, 2009-2010
During my Graduate studies at IU school of Medicine, I received this fellowship as part of a larger NIH program to train cancer researchers. This fellowship required me to take part in monthly meetings and once a year poster session. My thesis project during this time involved the study of Rheb/mTORC1 and its involvement in two different diseases: PTEN-null glioblastoma and lymphangioleiomyomatosis. For this line of research, I used tissue culture and mouse xenograft model systems. The techniques I used to carryout this research involved lentiviral delivery of shRNA and exogenous proteins, screening drug combinations, microscopy, RT-PCR, Chromatin Immunoprecipitation (ChIP), and many other molecular biology methods.

AWARDS

2ND Place Poster- Basic Science by Graduate Student
IU Simon Cancer Center, Annual Cancer Research Day
Indianapolis, Indiana
May 5, 2010

MEETING ABSTRACTS

Babcock, J.T., Fan, L., and Quilliam, L.A. Rheb1/mTOR inhibit migration of PTEN-null glioblastoma cells. *FASEB Summer Research Conference, "Regulation & Function of Small GTPases"* Vermont Academy, Saxtons River, VT, July 13-18, 2008.

Babcock, J.T., He, Y., Palam, L.R., Wek, R.C., and Quilliam, L.A. 4-Phenylbutyric acid: An AMPK agonist and mTORC1 inhibitor. *2009 Lymphangioleiomyomatosis (LAM) International Research Conference*, Cincinnati, OH, April 17-19, 2009.

Babcock, J.T., He, Y., and Quilliam, L.A. 4-Phenylbutyric acid: An AMPK agonist and mTORC1 inhibitor. *International Tuberous Sclerosis Conference: From DNA to Human Therapies*. Chicago, IL, September 23-26, 2009.

Babcock, J.T., He, Y., Wek, R.C., and Quilliam, L.A. Targeting mTOR-induced endoplasmic reticulum stress: a rational treatment for sporadic AML/LAM? *2010 Lymphangioleiomyomatosis (LAM) International Research Conference*, Cincinnati, OH, April 9-11, 2010. Oral presentation.

Babcock, J.T., He, Y., and Quilliam, L.A. mTOR activation accentuates a transcription-dependent stress response in bortezomib-treated TSC cells. *2011 Lymphangioleiomyomatosis (LAM) International Research Conference*, Cincinnati, OH, April 8-10, 2011.

Babcock, J.T., He, Y., Wek, R.C., and Quilliam, L.A. mTORC1 activity sensitizes cells to endoplasmic reticulum stress through a c-MYC-dependent mechanism. *Tuberous Sclerosis Complex: From DNA to Human Therapies*. Washington D.C., July 8-10, 2011.

Babcock, J.T., Nguyen, H.B., He, Y., Wek, R.C., and Quilliam, L.A. mTORC1 enhances bortezomib-induced TSC-null cell death through c-MYC-dependent up-regulation of the unfolded protein response. *Keystone Symposium X4: Tumor metabolism*. Keystone, CO, February 24-March 1, 2013.

PLATFORM PRESENTATIONS

Babcock, J.T., He, Y., Wek, R.C., and Quilliam, L.A. Targeting mTOR-induced endoplasmic reticulum stress: a rational treatment for sporadic AML/LAM? *2010 Lymphangioleiomyomatosis (LAM) International Research Conference*, Cincinnati, OH, April 9-11, 2010.

PUBLICATIONS

Babcock, J.T., and Quilliam, L.A. 2011. Rheb/mTOR activation and regulation in cancer: novel treatment strategies beyond rapamycin. Curr Drug Targets 12:1223-31.

Castro, A.F., Campos, T., **Babcock, J.T.**, Armijo, M.E., Martinez-Conde, A., Pincheira, R., and Quilliam, L.A. 2012. M-Ras induces Ral and JNK activation to regulate MEK/ERK-independent gene expression in MCF-7 breast cancer cells. J Cell Biochem.

Siroky, B.J., Yin, H.**, Babcock, J.T.**, Lu, L., Hellmann, A.R., Dixon, B.P., Quilliam, L.A., and Bissler JJ. 2012. Human TSC-associated renal angiomyolipoma cells are hypersensitive to ER stress. Am J Physiol Renal Physiol.

Nguyen, H.B., **Babcock, J.T.**, Wells, C.D., and Quilliam, L.A. 2012. LKB1 tumor suppressor regulates AMP kinase/mTOR-independent cell growth and proliferation via the phosphorylation of Yap. Oncogene.